Proceedings of Annual Eurolas Meeting
Munich. March 1995

Satellite signature effects on SLR
Properties of avalanche photo diode detectors for SLR

Compiled and edited by
A.T. Sinclair
Royal Greenwich Observatory
Cambridge, England

Royal Greenwich Observatory
Madingley Road
Cambridge CB3 0EZ
England
July 1995

Table of Contents

EUROLAS MEETING

1995 March 20, 21

Meetings of EUROLAS are held approximately annually, and are usually arranged as splinter sessions at some other scientific meeting. On this occasion a self-contained meeting was arranged, as there were several urgent technical matters that required fairly detailed discussion. The meeting was hosted by the EUROLAS Data Centre at DGFI in Munich. There were 38 participants, including 3 from NASA and 2 from the US Naval Research Laboratories. John Luck had hoped to be present to represent the Western Pacific Laser Tracking Network, but unfortunately was not able to be so. Three of our colleagues from Russia had planned to attend but unfortunately were not able to do so due to a hold up in obtaining visas.

The meeting covered four main items:

1. Formal session, including reports from the data centre and quick-look analysis centre, and reports and discussion on topical matters.

2. Satellite signatures and centre-of-mass corrections, particularly for systems operating at single photon return levels, and the effects of data processing methods.

3. Time-walk effects in avalanche photo-diode detectors depending on receive energy-level and laser pulse width.

4. The revision of the format for station-formed normal points.

The main purpose of this report is to give an account of the work presented and the discussions, conclusions and recommendations on items 2 and 3. Brief accounts of items 1 and 4 are also included. Item 4 continued the discussion of a proposal presented by NASA at the Laser Ranging Instrumentation Workshop in Canberra. A concensus viewpoint was reached in this continued discussion, and a draft of the revised format based on this concensus has been prepared for examination by WPLTN and NASA, and eventual consideration by CSTG.

Acknowledgements

We are grateful to ESA for providing some funding to EUROLAS for the support of its activities, which enabled six of our colleagues to participate in this meeting who would not otherwise have been able to do so, and also permitted the production and distribution of this report on the meeting. We are also grateful to the Lord Major and the city of Munich for providing an excellent evening reception.

H. Drewes
Director
Deutsches Geodaetisches Forschungsinstitut

W. Seemueller,
EUROLAS Data Centre
DGFI

A.T. Sinclair
President of EUROLAS
Royal Greenwich Observatory

A. Novotny
Secretary of EUROLAS
Czech Technical University

EUROLAS

Eurolas was formed in 1989 as a consortium of organisations that are involved in Satellite Laser Ranging (SLR). Initially Eurolas consisted of organisations in Western European countries, but has since been extended to include Eastern Europe and countries of the Former Soviet Union. The countries now involved and their laser ranging stations are:

Austria	Graz
Czech Republic	Helwan (in Egypt)
Finland	Metsahovi
France	Grasse
Germany	Wettzell and MTLRS-1
Germany	Potsdam and Santiago de Cuba
Greece	Dionysos
Latvia	Riga
Italy	Matera
Italy	Cagliari
The Netherlands	Kootwijk and MTLRS-2
Spain	San Fernando
Switzerland	Zimmerwald
Poland	Borowiec
Russia	Balkhash and Komsomolsk
UK	Herstmonceux
Ukraine	Katzively, Simeiz and Evpatoria
Uzbekistan	Maidanak I and II

The main objectives of Eurolas are:

1. to promote cooperation among the members
2. to provide representation of European SLR groups with respect to other international agencies involved in SLR
3. to coordinate and promote European participation in international SLR related programmes
4. to coordinate the assignment of priorities and scheduling of European SLR operations
5. to promote standardisation of operational procedures
6. to promote task sharing between member groups and sharing of software development and information on technical innovations.

On behalf of Eurolas the Deutsches Geodätisches Forschungsinstitut at Munich operate the Eurolas Data Centre, and The Technical University at Delft operate a Quick-Look Data Analysis Centre.

Summary of the conclusions and recommendations of the meeting.

Session on satellite signatures and centre of mass corrections.

1. We should try to determine what all single photon systems are doing at present and what they have been doing from 1990 (when on-site normal points were introduced), to cover:
   - laser pulse width
   - typical return level
   - data processing method

2. In future, from some date to be decided:
   Determine **mean** and RMS using iterated 2.5×RMS rejection.
   Determine skewness and kurtosis from this retained data set.
   Form normal points from this data set, forming simple arithmetic mean within each bin.

3. Determine the **peak** of the distribution of the whole pass or calibration run.

4. Subtract the correction (**mean–peak**) from each normal point and from the calibration value.

Session on the use of avalanche photo diode detectors

Systems that detect the first photo-electron should :

- determine the return rate at which the time walk begins to occur (typically about 30%)
- determine the jitter characteristics over this range
- adopt a maximum return rate to be used operationally for both satellite ranging and calibrations which is below the rate at which time walk occurs, and that gives tolerable jitter
- endeavour to use the full second half of the laser pulse train, in order to give a better overall return rate.

Meanwhile, development of techniques for the automatic compensation of detector time walk should be continued.

Summary of technical session on "Satellite Signatures and Centre-of-Mass Corrections"

1. Introduction

It is now recognised that the reflected pulse from spherical geodetic satellites such as Lageos is non-symmetrical due to the reflecting properties and distribution of the retro-reflectors, and is skewed towards longer ranges. Over the years several stations have suspected that they have detected this effect in their data, but in some cases it was later shown to be due to a feature of the system performance, and so it became somewhat disreputable to talk about satellite signature effects, as this might just be explaining away what were really system problems. However the precision of current SLR systems is such that this effect is now of real significance, and papers presented at the Annapolis Laser Ranging Instrumentation Workshop in 1992 by Appleby and by Kirchner demonstrated this effect beyond doubt. The effect can be detected easily by systems which operate at single-photon return levels, as during the course of a satellite pass these systems obtain returns which come from retroreflectors distributed over the whole of the effective reflecting area. Systems that operate at a multi-photon return level using an MCP detector see rather less of the effect. The output pulse from the MCP from each shot maps to some extent the return distribution from the satellite, but this is seldom examined. Instead it is passed through a discriminator. This can operate in various ways, but in general it reacts to some characteristic of the leading part of the MCP output pulse (e.g. leading edge half maximum), rather than to its whole distribution.

The standard centre-of-mass corrections for the two Lageos satellites were obtained by ground measurements using multi-photon, and no ground measurements were made at single photon return levels using detectors that respond to the first photon received. For all the years that satellite signature effects were not recognised, and anyway were fairly insignificant relative to the precision of the current data, the same centre of mass correction has been used for multi-photon systems and for systems operating at single photon return levels. (However some analysts solve for range biases for individual SLR systems, and these will absorb effects due to the use of a centre-of-mass correction which might be inappropriate for some systems.) At the Laser Ranging Instrumentation Workshop in Canberra in November 1994 Reinhart Neubert presented a paper giving a theoretical calculation of the centre-of-mass correction values that are appropriate for single photon systems for several satellites. In the case of Lageos he obtained a value about 8 mm less than the standard value; i.e., the effective mean reflection point is about 8 mm further in to the satellite than that for MCP systems. Over the following months the consequences of this result were analysed, and were reported and discussed for the first time at this Eurolas meeting.

Two other factors have to be taken into account in discussing the effects of satellite signature, and these were explored thoroughly at the Eurolas meeting. The first is the effect of using a high return rate for a system that detects the first returning photon. This moves the mean reflection point nearer the face of the satellite. The second is due to the use of avalanche photo diode detectors. It seems to be intrinsic to the physics of these devices that they introduce a skewness of the range measurements, which becomes convolved with the skewness of the satellite signature, and a suitable data processing method is needed to eliminate any biases from this effect.

The speakers at the meeting addressed all these topics, and papers describing their work are included in this report. This summary attempts to take an over-view of the whole problem, referring to the individual contributions by Reinhart Neubert, Graham Appleby, Van Husson, and Andrew Sinclair where they are relevant.

2. Satellite signature

For simplicity we consider the case of Lageos, although in their papers Neubert and Appleby have applied the same methods to other satellites. The radius of Lageos is 298 mm, and the part of the satellite over which the corner cubes are oriented such that they can reflect light back to the SLR station is at a distance of 200 to 260 mm from the centre of the satellite. (The reason why this does not extend to the near edge at 298 mm is because the apex of each corner cube is recessed into the body, and the refractive index of the solid cubes further increases the effective depth.) Neubert has calculated theoretically the reflecting power (or optical transfer or response function) of the satellite over this region, and obtains a sharply spiked curve as shown in figure 3a of his paper. An SLR station will see the result of this response function convolved with the shape of its laser pulse, and also with the response characteristics of its detector (we refer to these as the system distribution). We first consider the convolution of a symmetrical system distribution with the Lageos response function. An example is shown in Neubert's figure 3b for a system distribution with a gaussian profile and FWHM of 35 ps. The result is to round off the sharp spike, and to spread the range measures over a greater span, but still leave a highly skew distribution. For wider system distributions the profile of the laser pulse will begin to dominate the resulting distribution, increasing its width and reducing the skewness, as is shown in Figure 1 below, where the vertical scale of the successive plots is arbitrary, and is chosen to separate the curves.

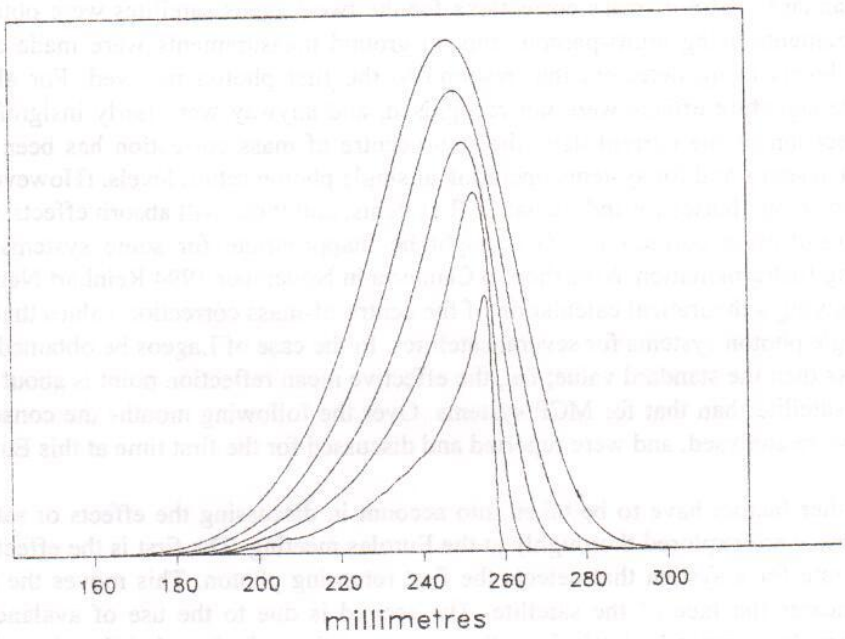

Figure 1. Lageos response function convolved with gaussian system distribution.
The inner curve is the Lageos response function. The outer curves are the response function convolved with gaussian system distributions of widths :

sigma		FWHM
3.2 mm (1-way)	=	50 ps (2-way)
6.4 mm	=	100 ps
9.6 mm	=	150 ps
12.7 mm	=	200 ps

Note that these plots are for illustrative purposes, and use an approximate digitisation of the satellite response curve given by Neubert. The various centre-of-mass values deduced from these curves illustrate the typical variation to be expected from these values, but cannot be taken as definitive values. These profiles represent **on average** the profile of the returning reflected pulse. As Neubert points out individual pulses will vary due to coherent interference.

Neubert's impulse response function for Lageos differs significanltly from that derived in the report of the Lageos-II pre-launch tests. This is discussed in a paper by Sinclair, Neubert and Appleby which is included in these proceedings. It is important to note that Neubert's figure 3a showing the response function gives both the shape of the response function and its location relative to the centre of mass of the satellite, and so the horizontal axis is the distance from the centre of mass in millimetres. However his plot 3b and the curves plotted above give just the shape of the laser pulse after it has been reflected by the satellite, and further consideration is needed of the reference point to be adopted in the data distribution both from the satellite and from calibration ranging in order to relate it to the centre of mass of the satellite. In fact these figures give the location relative to the centre of mass in the special case of a symmetrical laser pulse and system response, with the mean adopted as reference point.

3. The response of the detector to the received pulse for systems at multi-photon level

For a system operating at multi-photon return levels a pulse of photons of the shape in Figure 1 above enters the detector on each shot (the pulse shape may be poorly defined if the number of photons is not large, but statistically it will have the shape as in the figure). These systems typically use an MCP detector, and this will convert the pulse of photons to an electrical pulse which perhaps might preserve some of the shape of the input pulse. However these output pulses are not usually examined; instead they are passed into a discriminator, which triggers on some part of the pulse, usually the leading edge or peak. Clearly there will be a big difference in the raw range value obtained between, for example, triggering on the peak or leading-edge-half-max of one of these curves, which could be 10 mm or so. However the system would use the same triggering technique for its terrestrial calibrations, and so these would also differ by a similar amount depending on the technique used, and so the calibrated range measurement to the satellite would be much the same whichever triggering technique was used, but not precisely the same. The satellite signature causes the data from the satellite to have a slightly different distribution from that from a target board, and so there are slight differences to the calibrated satellite range measurements depending on the triggering technique of the discriminator, and hence there is a small difference in the appropriate centre-of-mass correction for the satellite depending on the discriminator technique. The plot shown in Figure 2 below is taken from the Lageos-II pre-launch tests results given by Varghese (Proc. of Annapolis Laser Ranging Instrumentation Workshop, p.6-45). It shows that there could be a variation of the centre-of-mass correction over about 5 mm depending on the discriminator method and the laser pulse width. This dependence on laser pulse width is also shown from theoretical calculations in figure 6 of Neubert's paper for the case of constant fraction discrimination (where on his horizontal axis an RMS width of 12.7 mm corresponds to a laser pulse full-width-half-max of 200 ps). Note that Varghese's plot, as is described in more detail in the report of the Lageos-II ground tests, is actually the plot of a mathematical model, based on theory but with parameters chosen to give a good fit to experimental results, particularly those from CW FFDP measurements. Experiments using a pulsed laser and MCP or streak camera detectors gave rather more disparate results. The MCP measurements used constant fraction detection, and these are marked by triangular points in Varghese's plot. For short pulse lengths these have centre of mass correction values several mm smaller than the standard value. In practice most MCP systems have fairly large laser pulse

widths, and so for Lageos I and II the appropriate centre-of-mass correction differs little from the standard value of 251 mm, and the level of precision of SLR systems is not yet such that this is of significant concern (but is approaching that point).

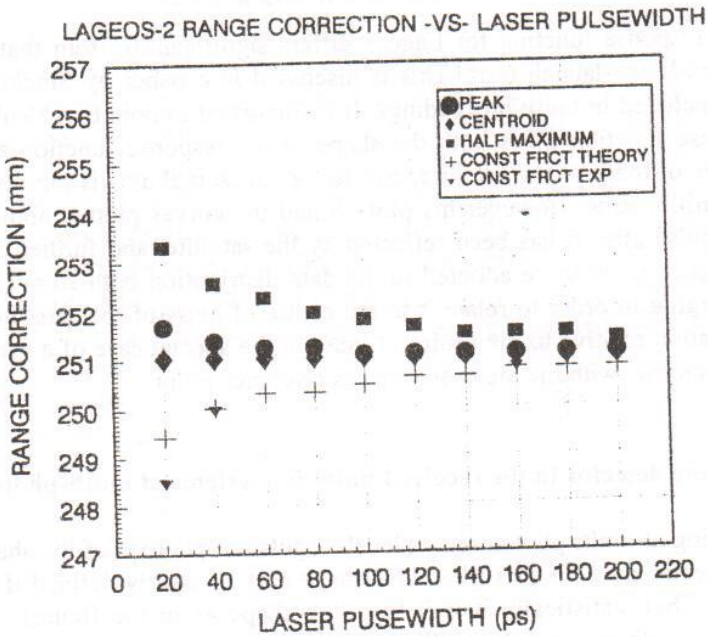

Figure 2. Variation of centre of mass correction with laser pulse width and discriminator method (from Varghese, 1992)

4. Systems operating at single photon return levels

For a system operating at single photon return levels, at most only a single photon from the reflected pulse survives to reach the detector on each shot, and this can come from anywhere in the returning pulse, with a probability proportional to the density profile of the reflected pulse. Thus if the detector was perfect then over the course of a pass the distribution of the range residuals for the individual photons would reproduce the density profile of the reflected pulse. However all detectors add some scatter to the measurements, which increases the broadening of the data distribution, and avalanche photo diode detectors in particular also add a skew tail which increases the skewness arising from the satellite signature for satellites such as Lageos. In his paper included in this report Appleby (figure 3) gives plots of typical distributions of data obtained from various satellites at Herstmonceux, and in particular gives detailed plots for Lageos and Etalon. He also constructs the theoretically expected data distribution for these satellites from the known construction of the satellites and the known characteristics of the Herstmonceux system when ranging to a target board, and finds that the theoretical and observed data distributions agree well.

Since no ground-test measurements of the Lageos and other satellites have been made at single photon return levels it is necessary to calculate the centre-of-mass corrections theoretically. Neubert (figure 3a) gives the response function for Lageos, calculated theoretically. He considers the shape that this takes when convolved with the laser pulse width, and this process can be

extended as has been done by Appleby to include the further spreading and skewness caused by the detector. This gives the shape of the distribution of the resulting range measurements, as shown in Neubert's figure 3(b) for Lageos and in Appleby's figure 5 for Lageos and Etalon. It is seen that the data distributions are non-symmetrical, with a skewness towards long ranges. At the Herstmonceux Laser Ranging Instrumentation workshop in 1984 a recommendation was made for the formation of on-site normal points, and this involves taking the mean of the data distribution as the reference point, using an iterated 3.0×RMS rejection. This was before the effects of satellite and system signature were fully recognised. It is now appropriate to question whether this recommendation needs revision, and in fact most stations operating at the single photon level have already appreciated that the effect of the skew tail of the data needs to be removed, and mostly they achieve this by using a tighter clipping of the data than 3.0×RMS. We now consider this point in a slightly different form; whether some other reference point in the data distribution should be used instead of the mean. The obvious alternative is the peak of the distribution, and we also consider the leading edge half maximum (LEHM). This software choice of reference point is analogous to what is done in hardware in multi-photon systems. These systems have a hardware setting of the discriminator which determines which reference point in the pulse shape it triggers from.

If it is decided to use the peak or LEHM of the data from the satellite as the reference point then the same reference point should be used for calibration data obtained from a terrestrial target. Also the reference point used must be taken into account in the theoretical calculation of the centre of mass correction for a satellite. For example, if the LEHM is selected, then the mathematical process is to convolve the satellite response function about the LEHM of the system response distribution.

4.1 The mean (or centroid)

The use of the mean (or centroid) of the data distribution as the refernce point has the advantages that it is reasonably easy to calculate, and provided that the laser pulse width and the response of the detector do not introduce any skewness to the data then the centre of mass correction for a satellite is independent of the width of the system distribution. For example, the centroids of the Lageos response function and the 4 distribution curves given in Figure 1 above are all at 242.7 mm, and this gives the approriate centre of mass correction value. The disadvantage is that this value is some 8 mm different from the standard value. Also in practice the system response of single photon systems is not symmetrical, and in order to reduce the effect of the skew tail a tighter clipping than 3.0×RMS is usually used. In these circumstances the invariance of the mean does not hold, and the appropriate centre of mass correction does depend on the width of the system distribution, and thus the case for using the mean is weakened.

4.2 Peak and other reflection points

Provided the system response is symmetrical, the distribution curves in Figure 1 above can also be used to give the centre of mass correction that is appropriate when using the peak as the reference point. If the peak is used as the reference point then the location of the peak gives the appropriate value to use for the centre of mass correction, and this varies with the width of the system distribution. It is seen from Figure 1 that the peaks move to the left (reflection point deeper into the satellite) as the width of the system distribution is increased, moving from 253 to 247 mm for system distribution widths from 50 to 200 ps.

While still assuming a symmetrical system distribution we consider one other possible reference point, the leading edge half maximum. This does not coincide with the mean and peak of the symmetrical system distribution, and so we cannot use Figure 1 to give the centre of mass corrections, as this took the mean as zero point when convolving the system distribution with the satellite response. Instead we must take the leading-edge-half-maximum of the calibration ranging distribution as the zero point when convolving with the satellite response function. We then obtain the curves shown in Figure 3 below. These have the same shape as in Figure 1 above, but they have been shifted. The locations of the leading-edge-half-maximum of these curves give the centre of mass correction values, and these vary from 254.5 to 249.7 mm for system distribution widths from 50 to 200 ps, and in fact over the range of widths of 100 to 200 ps the variation of the leading edge half maximum is only 2.9 mm.

Appleby extends these theoretical calculations to consider the actual distribution of data from a station using an avalanche photo diode detector, and convolves this with the Lageos response (and also Etalon). For a system with a typical 12 mm single shot precision on calibration targets this gives a centre-of-mass correction for Lageos of 246 mm using the peak as the reference point, and 250 mm if using the leading-edge-half-max.

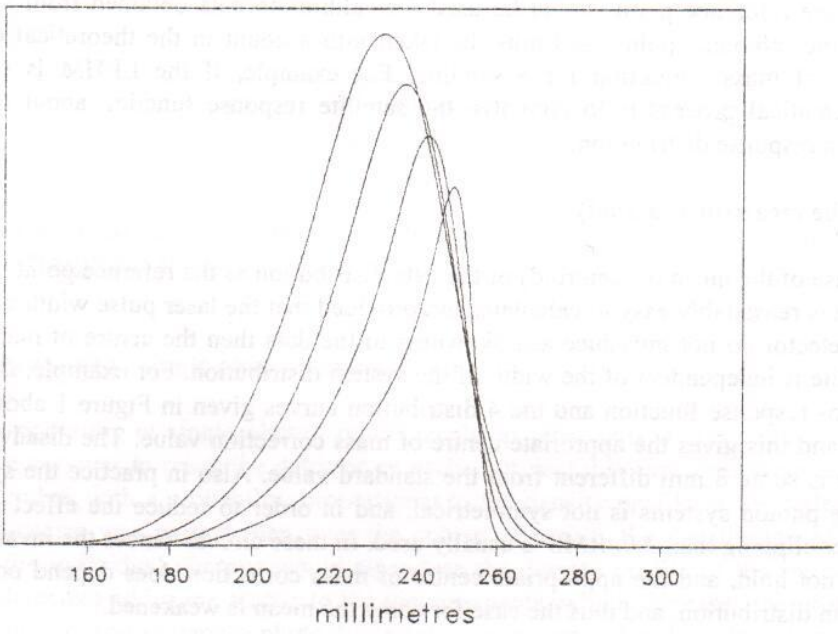

Figure 3. The Lageos response function convolved with the same gaussian system distributions as in Figure 1, but with the leading edge half max taken as the zero point.

4.3 Use of mean and a tight clipping of the data

Neubert (figure 5 of his paper) shows the different values obtained for the centre-of-mass correction of Lageos using an iterated 2.5σ and 2.0σ clipping, and obtains values of about 247 and 249 mm respectively. Thus tighter clipping moves the centre-of-mass value closer to the standard value of 251 mm, and in fact the computation of the mean using tight clipping is actually a way of achieving a measure of the location of the peak of the distribution. (Note that

the use of the term σ (sigma) is very common - it is used in the Herstmonceux recommendation - but is strictly only applicable when referring to a gaussian distribution of data. However in practice it just means the same as the RMS of the data from some mean value). Neubert's figure 5 shows that the determination of a mean value using a tight clipping can be slow to converge, and this is because both the value of σ and the current estimate of the mean are varying at each iteration. In fact in some cases this procedure can fail to converge, or can converge on a different point according to whether the first guess was a high or low value. Also the final value obtained for σ is always smaller than would be obtained using a 3.0σ clipping, and can give an artificially good impression of the single-shot precision of the system. These matters, with some recommendations, are discussed in the paper by Sinclair. In brief, it is better first to determine the RMS (or σ) of the data using a wide clipping, and then keep this value fixed when making a subsequent determination of the mean using a much tighter clipping.

4.4 Summary

The use of a tight clipping in order to determine the mean has two important properties. First, it diminishes the unwanted contribution from the long skew tail of the data distribution that arises from the characteristics of avalanche photo diode detectors, and also to some extent from the satellite signature (this is quite a large contribution for the Etalon satellites, as shown by figure 5 of Appleby's paper). Second, it gives a reference point for which the centre-of-mass correction is fairly close to the standard value of 251 mm. In effect the use of a tight clipping gives an estimate of the peak of the distribution instead of the mean, and it was decided by the meeting that the peak is the appropriate reference point to use. The paper by Sinclair describes two methods of determining the peak of the distribution.

The results in Appleby's paper suggest that the leading-edge-half-maximum would be an even better reference point to use. It effectively removes the influence of the skew tail, and it gives a centre-of-mass value very close to the standard value. However the implementation of this appears to be a little to hard conceptually to be accepted at this time.

Using the peak the centre-of-mass correction for Lageos is about 3-5 mm deeper into the satellite than the standard value. In these discussions it must be borne in mind that all of the values quoted for centre of mass corrections (both ground measurements and theoretical calculations) have uncertainties of several mm Hence at the present level of data precision most analysts will probably be content to use the standard value. Sufficient extra information will be given in the data format so that the appropriate centre of mass correction can be calculated, although the intention is that operational and data processing procedures should be adopted such that the corrections are small enough to be neglected.

5. The effect of return rate on the cente-of-mass correction

The various values of the centre of mass correction quoted in Section 4 apply for single photon return level, which in effect means that the detected events statistically sample the whole of the reflecting region of the satellite. Clearly if several photons are received each shot then a detector operating at the single photon level will be more likely to trigger on an early photon which will have been reflected from the near face of the satellite, and hence the mean reflection point will move further out from the centre of the satellite, giving a bigger value for the centre of mass correction. Figure 4 in Neubert's paper gives a plot of the theoretically calculated variation of the mean reflection point for different return levels. This shows that from very low to very high

return rates the shift of the mean reflection point is about 16 mm. He expresses the return rate in terms of the average number of photo-electrons generated within the detector, and this is a convenient measure for theoretical work. Other measures that are used in other contexts are the average number of photons entering the detector, and the average return rate. These are related by:

Number of photons entering the detector	N
Number of photo-electrons	qN
Average return rate (per cent)	$(1 - e^{-qN})\times 100$

where q is the quantum efficiency of the detector.

Taking q = 0.2 gives the following:

qN	N	Rate(%)
0.125	0.625	11.7
0.25	1.25	22.1
0.5	2.5	39.3
1	5	63.2
2	10	86.4
4	20	98.1
8	40	99.9
16	80	100.0
32	160	100.0

So it is seen from Neubert's figure that for return rates from 11% to 86 % there is a centre of mass shift for Lageos of about 6 mm. The use of such higher return rates would have the advantage that the appropriate centre of mass correction would be closer to the standard value. However, as discussed in the session on avalanche photo diode detectors, if the return rate approaches 100% it is difficult to measure the actual energy that is being received, and so it is difficult to determine the appropriate value that should be used for the centre of mass correction, and also to calibrate the time walk effect that occurs in the detector at higher receive energy and the effect of the migration of the detection point towards the leading edge of the laser pulse. Thus at the present state of the technology it was concluded that it is best to keep to low return rates, say less than 30%, so that the total shift of the centre of mass for a return rate between zero and 30% is only 2 mm.

6. Observational results demonstrating satellite signature

The paper by Husson, Su and Conklin presents a brief summary of some of the results from the collocation at GSFC of SALRO (operating at low return rates and using an avalanche photo diode detector) and MOBLAS 7 (using an MCP detector). They make comparisons of the MOBLAS-7 data with itself using various editing levels, and find no significant difference. This is to be expected; the comments made earlier in this report explain why MCP systems see little of the satellite signature effect. The SALRO ranges shorten by 5 to 7 mm as the editing level is changed from 3.0 to 2.0 sigma, which is about what would be expected from satellite signature. No information about the difference of the absolute values of the centre of mass corrections for single photon and MCP systems can be drawn from the paper, as this would require careful consideration of the return rate and editing level used for the calibration ranging. The two figures in the paper show that the relative differences betwen the three editing levels remain fairly constant during a pass, but the absolute value of the difference from the MOBLAS-7 ranges

varies quite considerably. The authors comment that there was a strong correlation between the return rate and the bias, and so these plots are probably showing the effects discussed in the session on avalanche photo diodes of time walk and migration towards the leading edge of the laser pulse. We comment that as the effects of varying return level have only recently been recognised by the community it is no criticism of SALRO that in its test phase it is demonstrating these effects.

Further evidence for the size of the satellite signature effect can be seen in the table of data below which gives for many passes tracked at Herstmonceux the average of the differences of two estimates of the peak of the distribution from the mean of the distribution. The mean was formed using a 3.0×RMS rejection. One of the estimates of the peak is by making a second detemination of the mean, but using a very tight rejection of 1.0×RMS, where the RMS is held fixed at the value obtained in the 3.0×RMS iteration. (This is probably about equivalent to using a 2.0×RMS where the RMS is allowed to vary through the iterations.). The 'Gauss fit' method of determining the peak is a good but rather complicated method, which involves forming a histogram of the data distribution and then fitting a Gaussian profile to the histogram.

Satellite	No. of passes	Average of 'Mean minus Peak'	
		Gauss fit	1×RMS
		mm	mm
Terrestrial	4092	2.2	2.7
Starlette	634	2.3	2.7
Stella	371	2.7	3.0
Meteor-3	294	2.7	2.8
ERS-1	620	2.2	2.4
Lageos-I	957	6.0	6.9
Lageos-II	691	5.8	6.6
Ajisai	301	19.2	21.6
Topex	1391	23.7	21.9
Etalon-I	73	13.4	17.7
Etalon-II	75	14.2	17.8

Note that the 'mean minus peak' for terrestrial ranging to a calibration target is about 2-3 mm, and so the values of about this amount for Starlette, Stella, Meteor-3 and ERS-1 are probably due to a large extent to the system rather than to the satellite. For the others the effect of satellite signature is clearly seen.

7. Conclusions

The conclusions of the meeting concerning the handling of the satellite signature effect by stations operating detectors that trigger on the first photo-electron were :

1. We should try to determine what all single photon systems are doing at present and what they have been doing from 1990 (when on-site normal points were introduced), to cover:
   - laser pulse width
   - typical return level
   - data processing method

2. In future, from some date to be decided:
   Determine **mean** and RMS using iterated 2.5×RMS rejection.
   Determine skewness and kurtosis from this retained data set.
   Form normal points from this data set, forming simple arithmetic mean within each bin.

3. Determine the **peak** of the distribution of the whole pass or calibration run. (Methods are discussed in paper by Sinclair).

4. Subtract the correction (**mean–peak**) from each normal point and from the calibration value.

Satellite Signature Model: Application to LAGEOS and TOPEX

Reinhart Neubert
GeoForschungsZentrum Potsdam, Dept. Recent Kinematics and Dynamics of the Earth
Telegrafenberg A17, D-14473 Potsdam, Germany
Tel.: (49)-331-288-1153, Fax: (49)-331-288-1111, Internet: neub@gfz-potsdam.de

EUROLAS Annual Meeting, Munich, March 20-21 , 1995

Background:

The basic assumptions of the signature model [1] are:

- the surface of the reflector array is uniformly covered with many cube corners
- the orientation of the satellite is regarded to be random

The second assumption justifies the incoherent superposition of the contributions of the individual cube corner reflectors to the signal at the photodetector using the basic relations derived by Arnold [2],[3]. In this way the average light intensity corresponding to a given fictive reflection plane can be derived. The resulting optical transfer function of the reflector array is then convoluted with the laser pulse shape and the result interpreted as the probability density function for the emission of a photoelectron. Although the real signal shape at the detector is strongly fluctuating because of coherent interference, the distribution computed by incoherent superposition may be regarded as a representation of the average signal. Therefore we call it in a simplifying manner: signal shape. The probability distribution for the emission of the first photoelectron is then derived using Poisson statistics [4]. This distribution depends on the average number of photoelectrons per shot and describes the expected distribution of range residuals.

Summary of Results:

The standard method to compute normal points is based on the mean of the range residuals. Therefore the investigation is focused on the dependence of the mean on signal level and data editing. The Centre of Mass Corrections (CoM) for all spherical satellites are estimated at zero level as well as for the conditions of a typical single photon detecting station.
In the case of LAGEOS, iterative 2.5-sigma editing (eventually followed by a single 1-sigma clipping) leads to a CoM of about 248 mm. For a single photon detector with 50 ps overall resolution, the peak of the distribution is very near to the standard value of 251 mm.
The model is extended to include ring- shaped arays as used on the TOPEX satellite. It is used to derive the dependence of the signal shape from the elevation angle. An observed residual histogram at about 45° elevation agrees reasonably well with the model.

References:

[1] R.Neubert: An Analytical Model of Satellite Signature Effects
Internat. Workshop on laser Ranging Instr., Canberra 1995, to be published
[2] D.A.Arnold: Optical and Infrared Transfer Function of the LAGEOS Retroreflector Array
Final Report, Grant NGR 09-015-002, Suppl. No.57, (May 1978)
[3] D.A.Arnold: Method of Calculating Retroreflector-Array Transfer Functions
SAO Special Report 382
[4] B.Saleh: Photoelectron Statistics, Berlin: Springer (1978)

LAGEOS Signature

Centre of Mass Correction, RMS

- Analytical Model
  - Averaging over all orientations, incoherent
  - gaussian laser pulse 35ps FWHM
  - gaussian jitter of ranging electronics 50 ps rms
  - "ideal" single photon detector
- Results
  - CoM, RMS versus signal level
  - Com, RMS versus clipping iterations
  - CoM for multi-pe PMT detection versus rise time

1. LAGEOS Signature Model: Basic Assumptions

Systematic Ranging Errors

- Signature Effects
  - Lageos: 1.....6 mm
  - Topex: 10....30 mm
- Meteo Data
  - pressure 0.2 mb - 0.5....2 mm
  - humidity 1 mm
- Calibration path

  1.....10 mm

2. Systematic Ranging Errors: Comparison of signature effects with other, e.g. meteo data errors

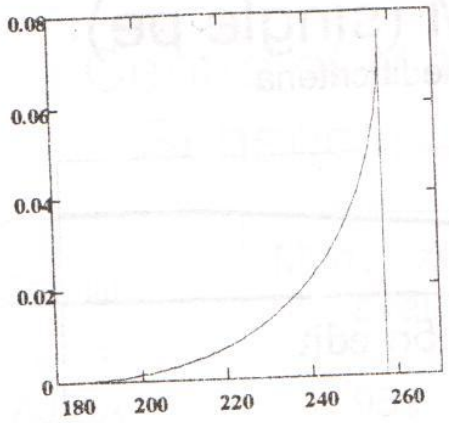

Figure 3(a). Lageos optical response function.

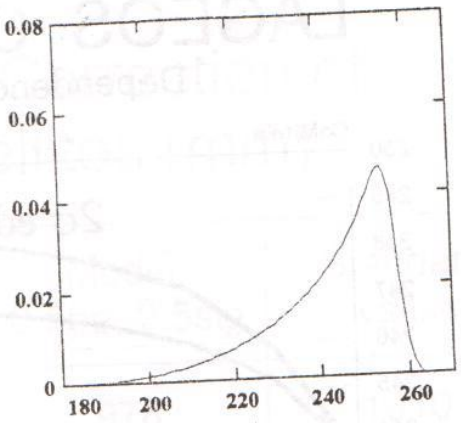

Figure 3(b). Lageos signal shape for 35 ps FWHM laser pulse.

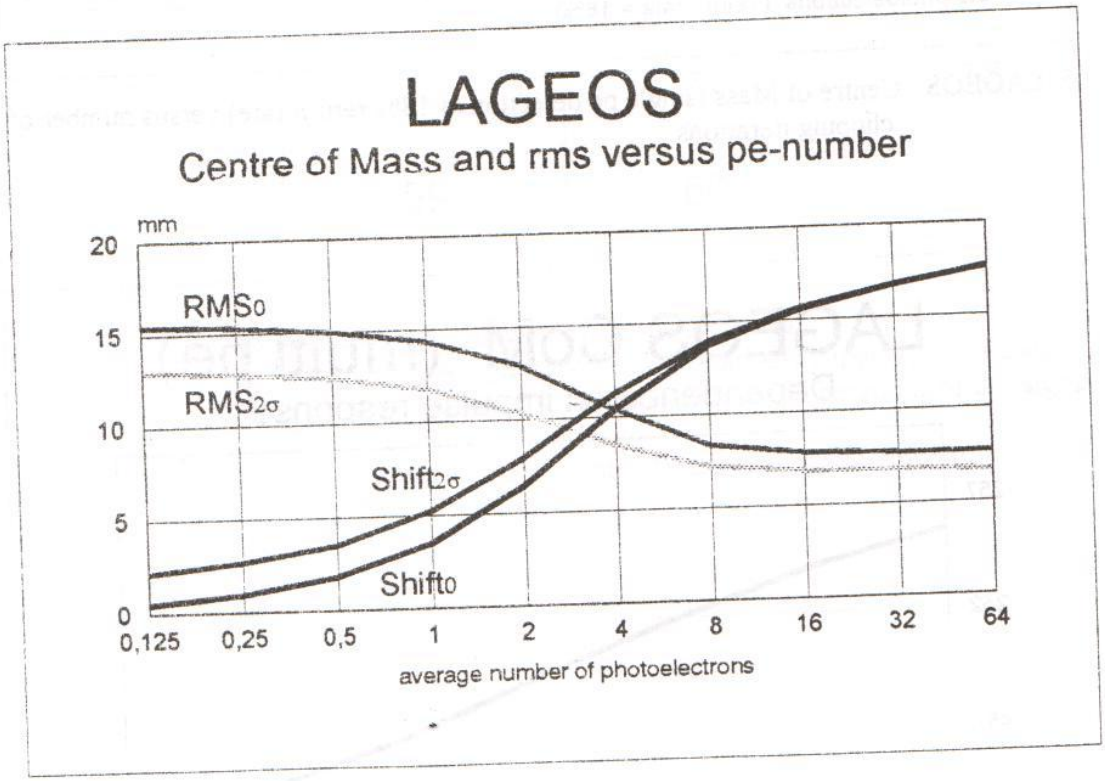

4. LAGEOS: Centre of Mass and RMS versus average photoelectron number. Curves are given for 2-sigma edition (1 iteration) as well as without any clipping.

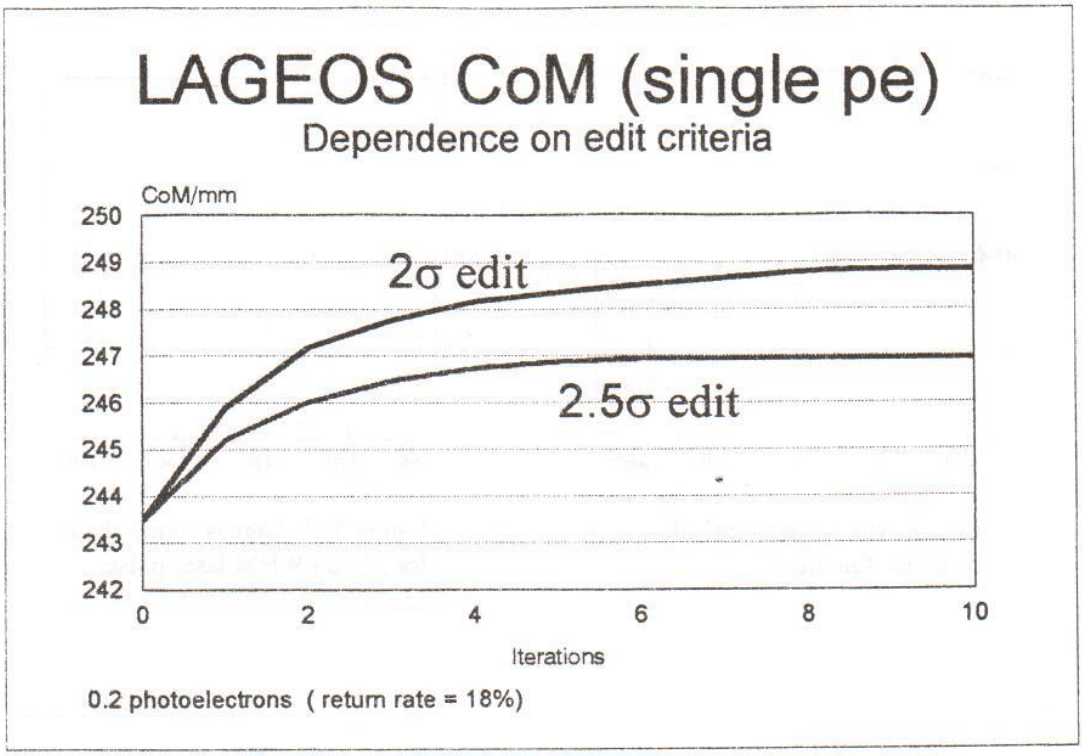

5. LAGEOS: Centre of Mass (single pe detection at 18% return rate) versus number of clipping iterations.

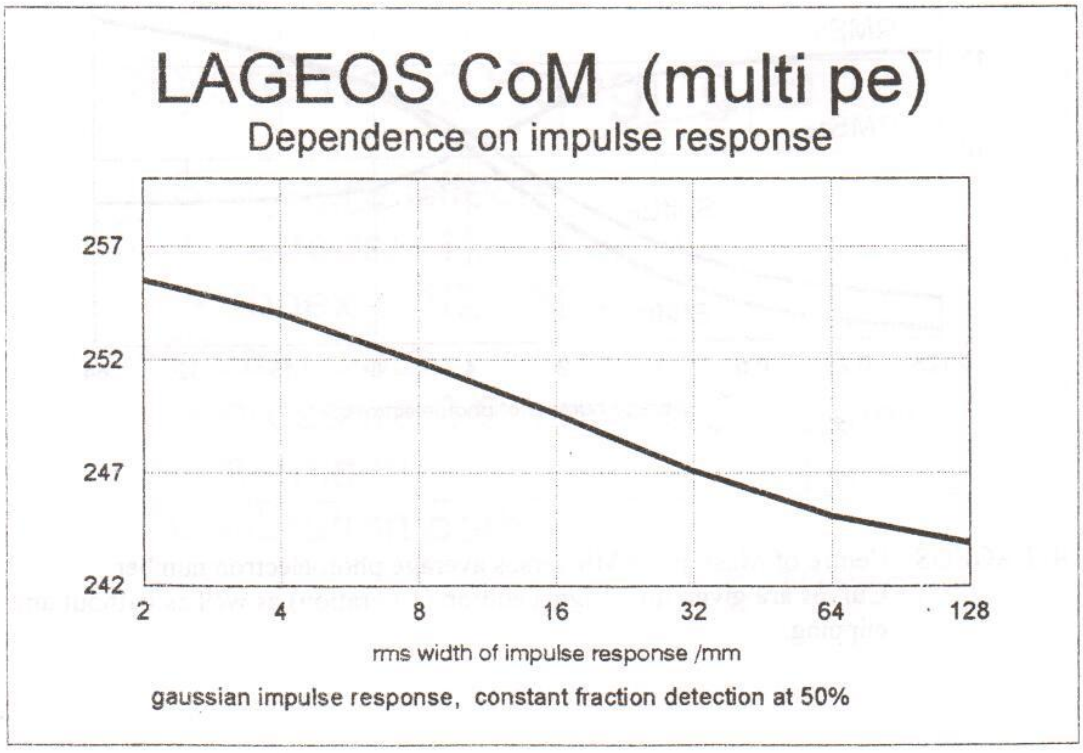

6. LAGEOS: Centre of Mass (multi pe) versus bandwidth of the detection system. This graph is obtained by convoluting the optical transfer function with gaussians of different width and taking the leading edge at half maximum.

Centre of Mass Correction of Spherical Satellites (mm)

Satellite	Model, zero level	Model, 0.5pe, 2.5sig	Standard value
AJISAI	959	978	1010
ETALON	579	590	558
LAGEOS	243	248	251
STARL	75	77	75
GFZ-1	59	60	

7. Table: Centre of Mass Corrections of Spherical Satellites
column 1: very low signal level and without any clipping of the data
column 2: mean signal of 0.5 photoelectrons, 10 iterations of 2.5-sigma clipping
column 3: standard value adopted by the analysts community

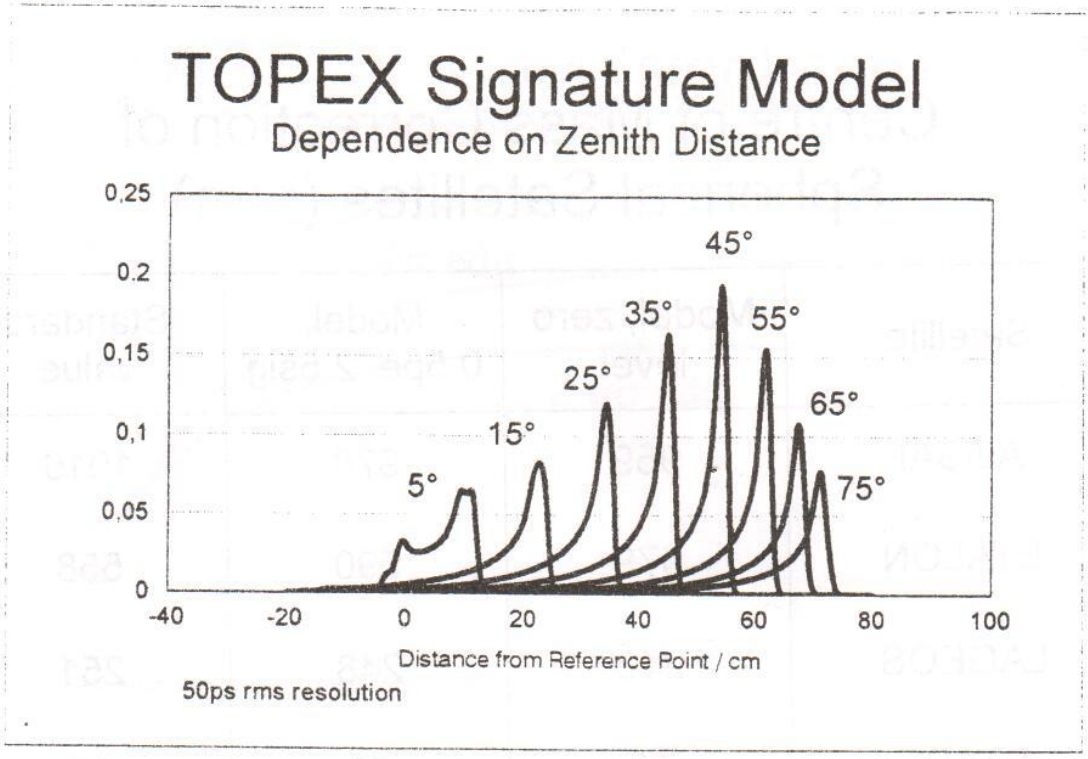

8. TOPEX Signature Model: Signal shape for different elevation angles.

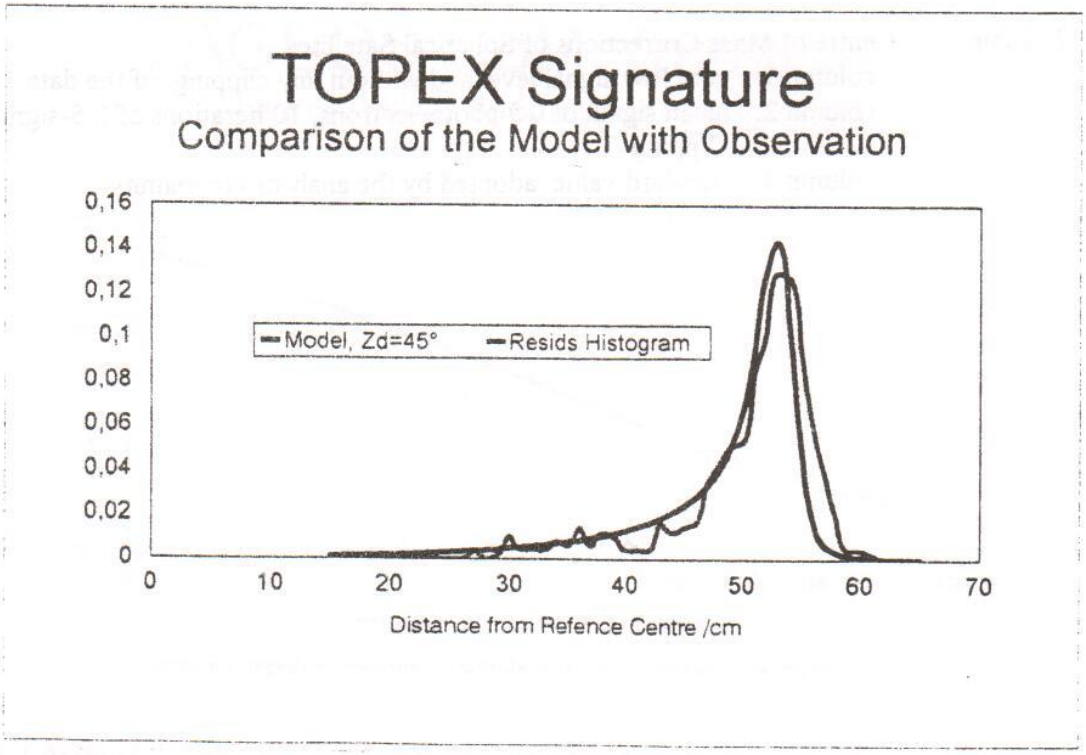

9. TOPEX: Comparison of an experimental residual histogram with the theory. Measurements were taken at 50% return rate and points between 40° and 50° elevation have been selected. For the theoretical curve a fixed elevation of 45° is assumed.

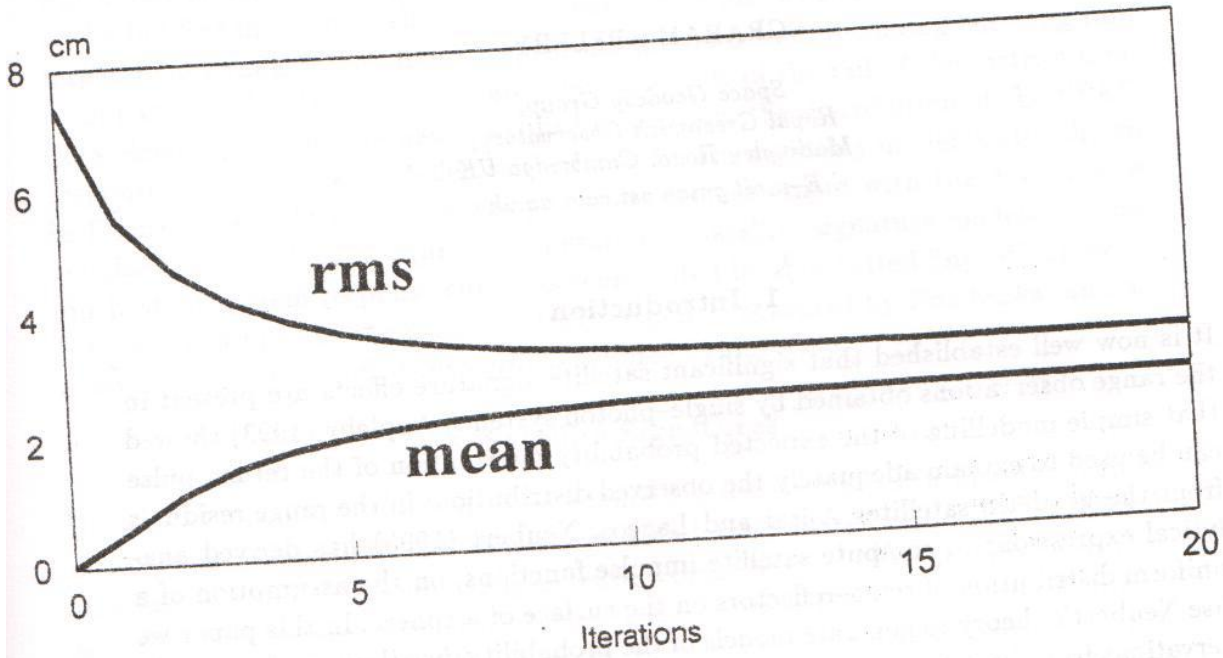

10. TOPEX: Mean and RMS versus clipping iterations.

CENTRE OF MASS CORRECTIONS FOR LAGEOS AND ETALON FOR SINGLE–PHOTON RANGING SYSTEMS

GRAHAM APPLEBY

Space Geodesy Group,
Royal Greenwich Observatory,
Madingley Road, Cambridge UK.
E–mail gma@ast.cam.ac.uk

1. Introduction

It is now well established that significant satellite signature effects are present in the range observations obtained by single–photon systems. Appleby (1993) showed that simple modelling of the expected probability distribution of the return pulse can be used to explain adequately the observed distributions in the range residuals from the geodetic satellites Ajisai and Lageos. Neubert (1995) has derived analytical expressions to compute satellite impulse functions, on the assumption of a uniform distribution of retro–reflectors on the surface of a sphere. In this paper we use Neubert's theory to generate models of the probability distribution of range observations from Lageos and Etalon, and use the models to compute centre–of–mass corrections appropriate to different methods of treatment of the observations. We show that the models fit very closely the observations made at Herstmonceux, and we extend them to represent other single–photon systems having different characteristics.

2. Ranging–System Response

A ranging system response is represented by the observed distribution of range measurements to a flat target–board, provided that a single–photon return level is maintained. A typical set of results from the Herstmonceux system is shown in histogram form in Figure 1, where a large number of observations was obtained during a ranging session of some 20 minutes. The range measurements have been converted to one–way range in mm, and expressed with respect to an arbitrary origin. The derived single– shot precision is 11mm, and the distribution is seen to be significantly skewed towards long ranges, with significant numbers of observations at distances up to 200mm from the distribution peak.

We develop a model of the system signature represented by these observations by estimating the probability distributions for the components of the system. We use a digitised version of the response curve of the RGO SPAD provided by Prochazka (1993), and to approximate the laser pulse a near–gaussian distribution of FWHM 120ps, taken from a streak camera image of a mode–locked Yag laser pulse (Wilson

and Hawkes, 1987). We assume gaussian responses of FWHM 47ps and 64ps for the Stanford interval timer and start diode respectively. We numerically convolve these distributions to form a model of the expected whole–system single–photon response, which may be directly compared to the observed distribution. This model is plotted as the full line in figure 1, shown as an envelope about the observed distribution of target–board ranges. The model represents the data well, including the long tail, except that it clearly over– estimates the amplitude of the tail of the distribution. To address this point, we have modified empirically the distribution of the SPAD response to reduce the modelled tail amplitude. The resulting model is also shown in Figure 1, as a dotted line envelope, where the agreement with the data is now satisfactory. For the subsequent computation of satellite signature models, we use our best–fit system response curve, as represented by this dotted line. We show in Figure 2 as a full line the original SPAD response measured by Prochazka, and as a dotted line the modified response as implied by our data.

3. Satellite Signatures

By way of introduction, we show in Figure 3 a series of plots in histogram form of range residuals from the target board and from most of the spherical laser satellites (+ Topex/Poseidon), in increasing order of size. The curves in each plot are best–fit Gaussian distributions, used in the data filtering process. There is a clear broadening of the distributions with increasing satellite size, such that the single–shot precision decreases from about 10mm for target board and ERS–1 ranging, through 17mm for Lageos, to 45mm for Etalon. Decreasing precision is accompanied by poorer fit to the Gaussian distributions, with the Etalon data being particularly badly approximated.

We now use the system response model and the satellite impulse functions of Neubert (1995) to generate theoretical probability distributions of range measurements of Lageos and Etalon. The satellite impulse functions computed from Neubert's expressions are shown in Figure 4, where the x–axis gives increasing distance in mm from the front surface of the satellite. The y axis is an arbitrary amplitude. The corner cube cutoff angles Φ_c were taken as 0.75 radians for the uncoated quartz glass of Lageos (Arnold, 1987) and 1.00 radians for the aluminium back–coated cubes of Etalon (Mironov *etal*, 1992). For this comparison with real observations, we choose to take the mean value of the system response as the zero–point of our system, and convolved the system about the satellite impulses with respect to that origin. We compare in Figure 5 the resulting distributions with those of typical sets of range residuals, where the x–axis represents true distance from the satellite surface, for mean–value data processing. The distributions have been fitted together in a least–squares sense by adjusting the vertical scale of the model, and shifting the range residuals from their original mean value of near–zero. The models are seen to represent the data very closely, and emphasize in particular the long tail in the distribution of ranges from Etalon, which might have appeared to be system

noise. It is interesting to note that this long tail relative to that of Lageos is due mainly to the larger value of Φ_c for the Etalon reflectors.

3. 1. CENTRE OF MASS CORRECTIONS.

We now use our models of the single–photon signatures of Lageos and Etalon to derive appropriate centres–of–mass (CoM) corrections for 3 different methods of range estimation, and for laser systems with different levels of precision. We take our system response curve and use the smoothing algorithm derived by Sinclair (1993) to estimate the peak, the mean and the leading–edge, half–maximum (LEHM) of the distribution. For each of these three estimates of the origin of the system response, we convolve it with the satellite impulse functions to form models of the expected distributions of satellite range observations. We again use the smoothing algorithm to estimate for Lageos and Etalon the CoM corrections for mean, peak and LEHM detection.

The whole process is repeated for hypothetical systems with single–shot calibration precision 6 mm and 20 mm respectively, by altering the width of our model of the laser pulse. Shown in Tables I and II are the deduced CoM corrections for Lageos and for Etalon for each of the three systems, including the Herstmonceux results (11mm precision), for each of the processing methods.

References

Appleby, G.M. : 1993, "Satellite Signatures in SLR Observations". In *Proc. Eighth Int. Workshop on Laser Ranging Instrumentation*, Annapolis, MD.

Arnold, D.A. : 1987, "Optical and Infrared Transfer Function of the LAGEOS Retroreflector Array, Final Report", Grant NGR 09-015-022, Suppl. No 57.

Mironov, N.T. and A.I. Emetz : 1993, "Etalon–1, –2 Centre of Mass Correction and Array Reflectivity" .In *Proc. Eighth Int. Workshop on Laser Ranging Instrumentation*, Annapolis, MD

Neubert, R. : 1995, "An Analytical Model of Satellite Signature Effects", In press in *Proc. Ninth Int. Workshop on Laser Ranging Instrumentation*, Canberra.

Prochazka, I. : 1993. "Single Photon Avalanche Diode Detector Package; Upgrade kit for RGO", July 1993.

Sinclair, A.T. : 1993, "SLR Data Screening; Location of Peak of Data Distribution". In *Proc. Eighth Int. Workshop on Laser Ranging Instrumentation*, Annapolis, MD

Wilson, J and J.F.B. Hawkes, 1987. "Lasers. Principles and Applications", Prentice Hall International Series in Optoelectronics.

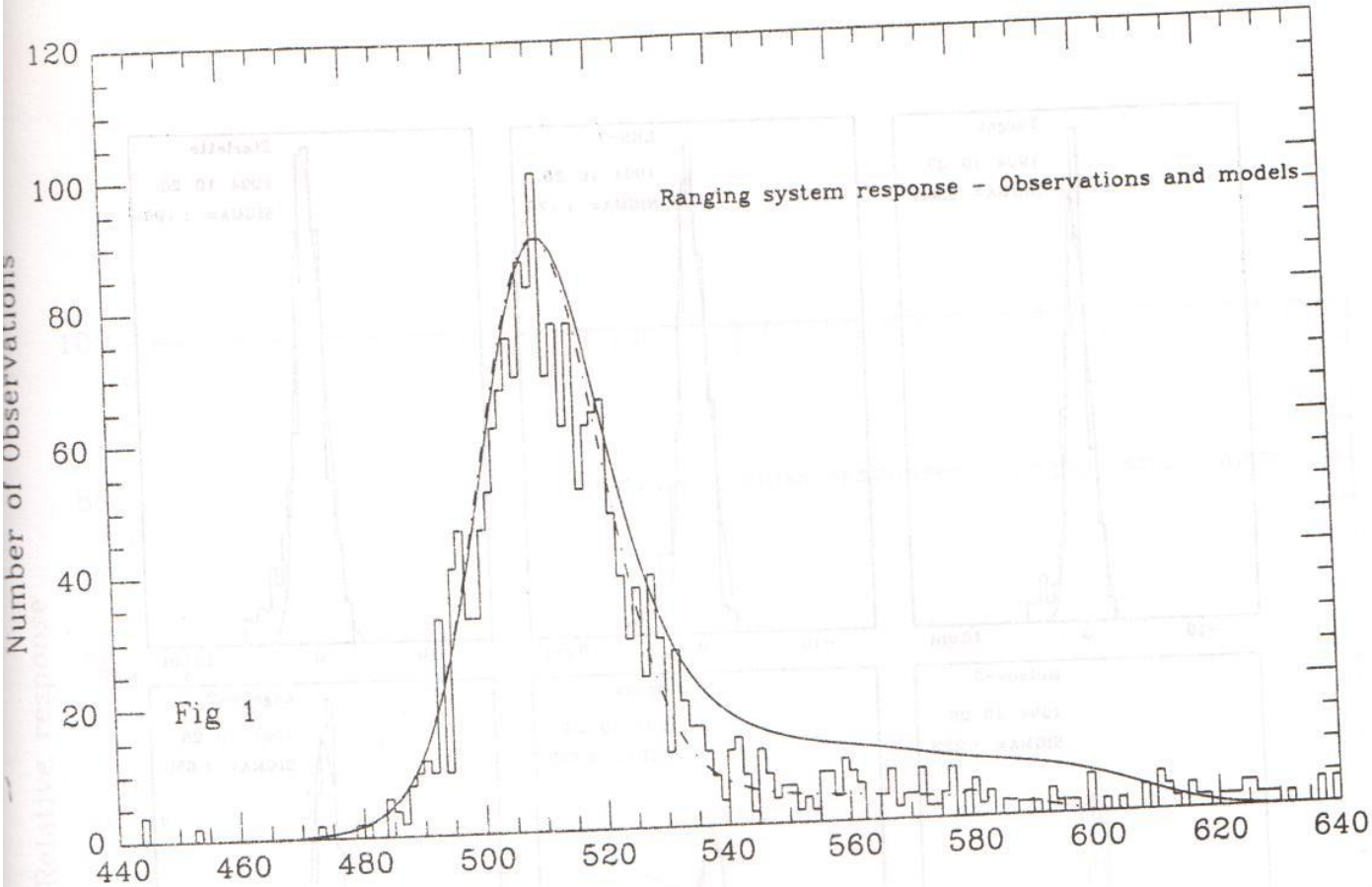
Ranging system response – Observations and models
Number of Observations
0
20
40
60
80
100
120
440
460
480
500
520
540
560
580
600
620
640

Fig 1

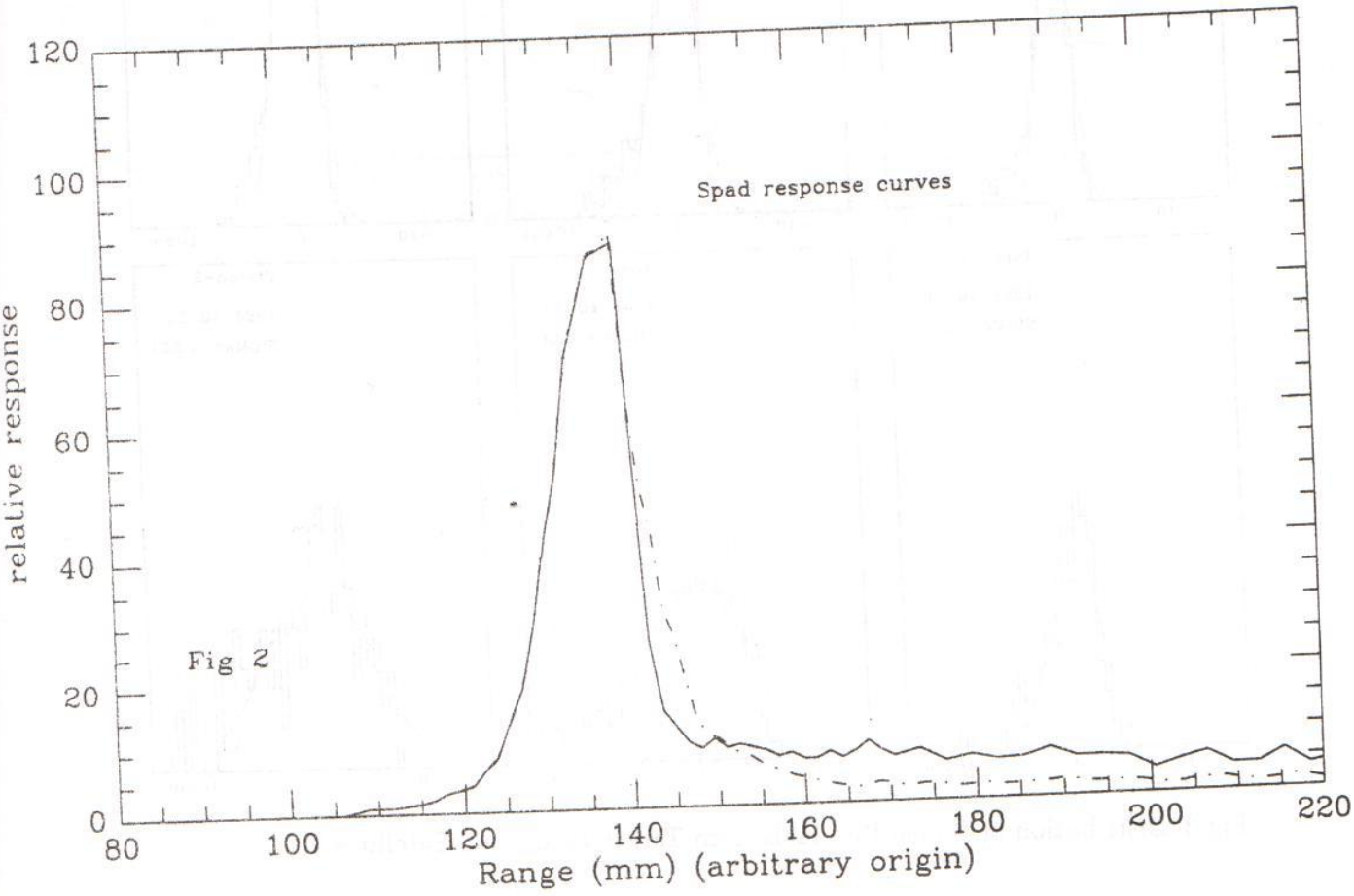
Spad response curves
relative response
0
20
40
60
80
100
120
80
100
120
140
160
180
200
220
Range (mm) (arbitrary origin)

Fig 2

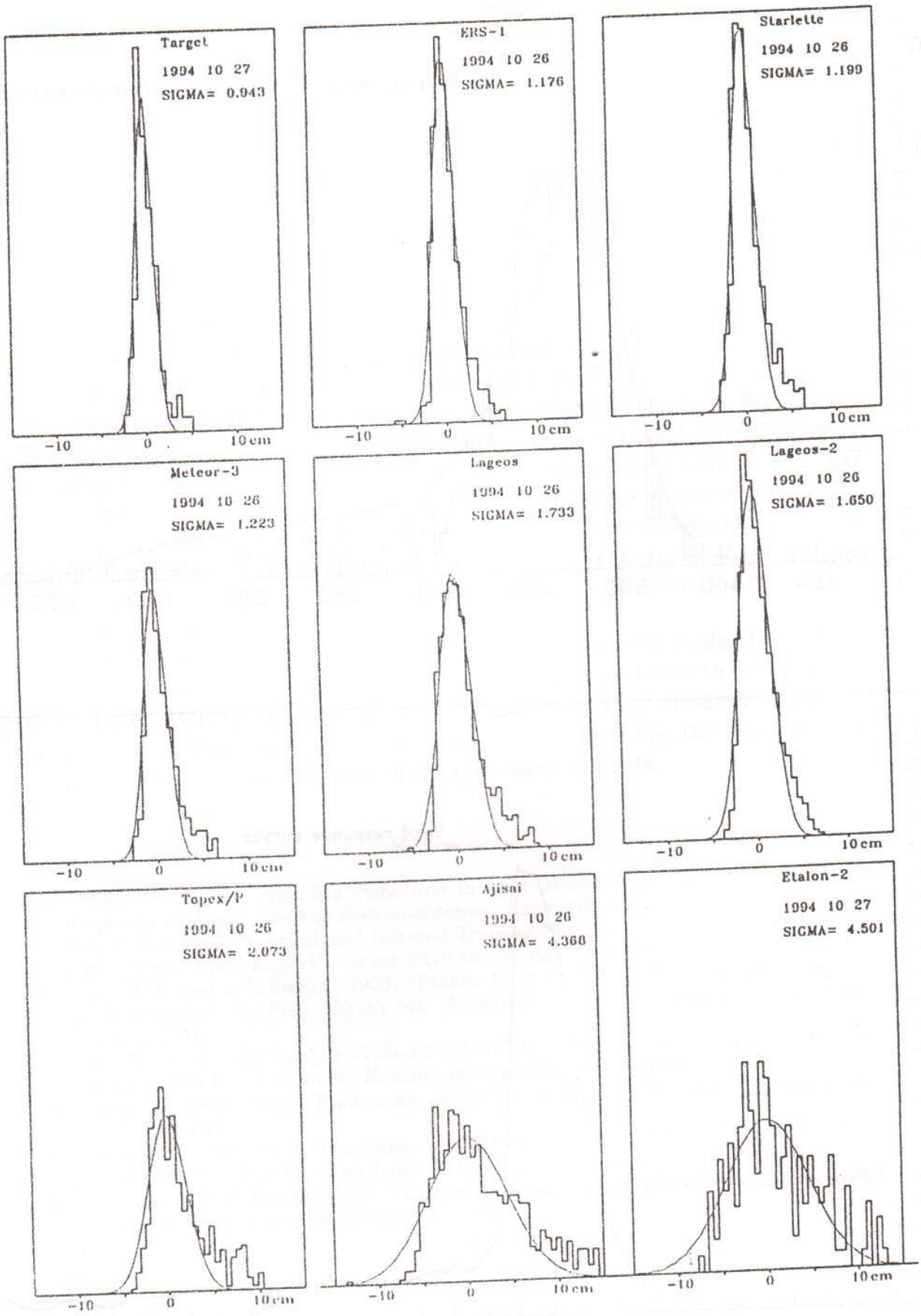

Fig 3 Distribution of Range Residuals from Target Board and Satellites.

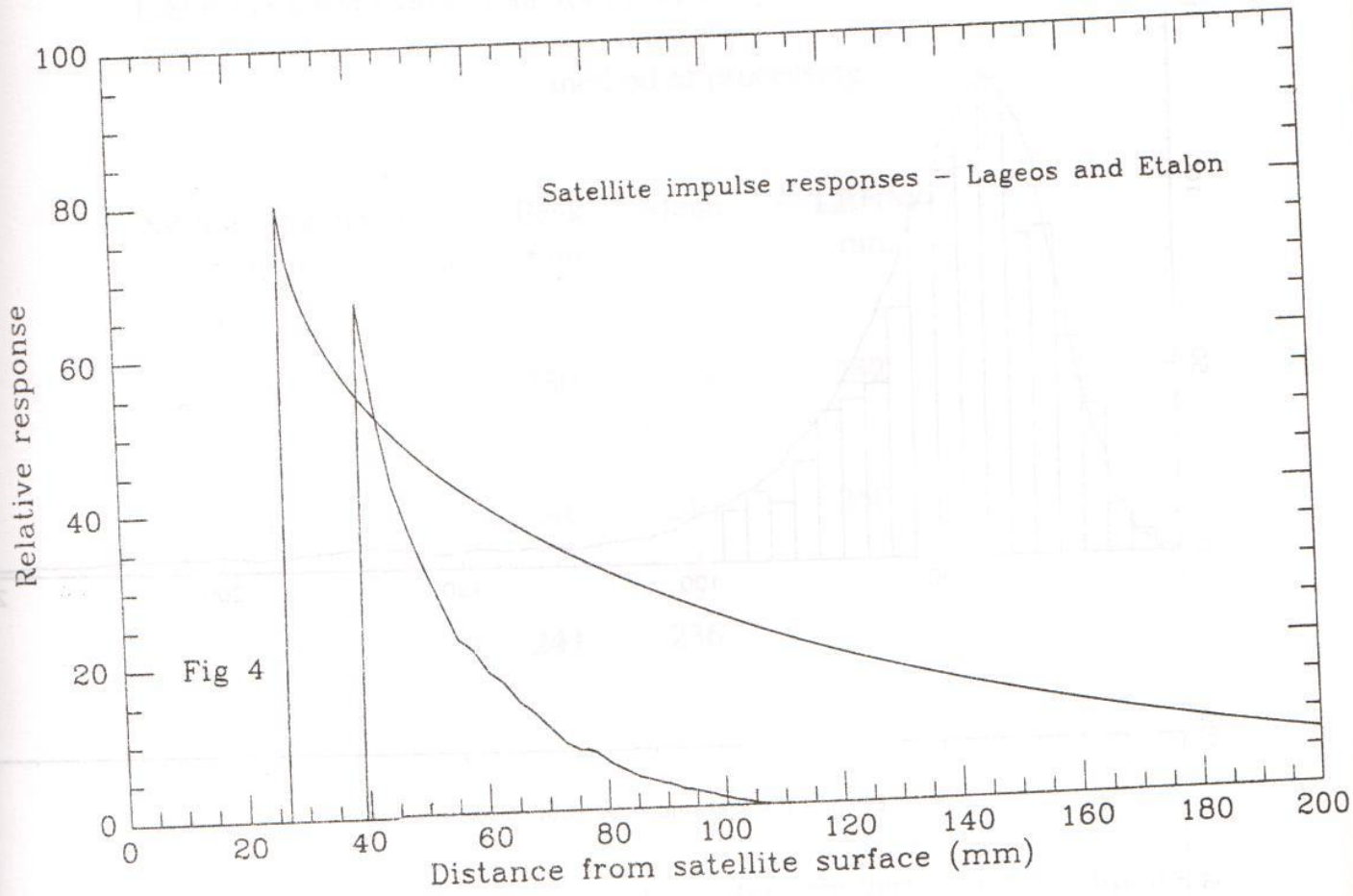
Satellite impulse responses – Lageos and Etalon
Relative response
Distance from satellite surface (mm)
0
20
40
60
80
100
120
140
160
180
200

Fig 4

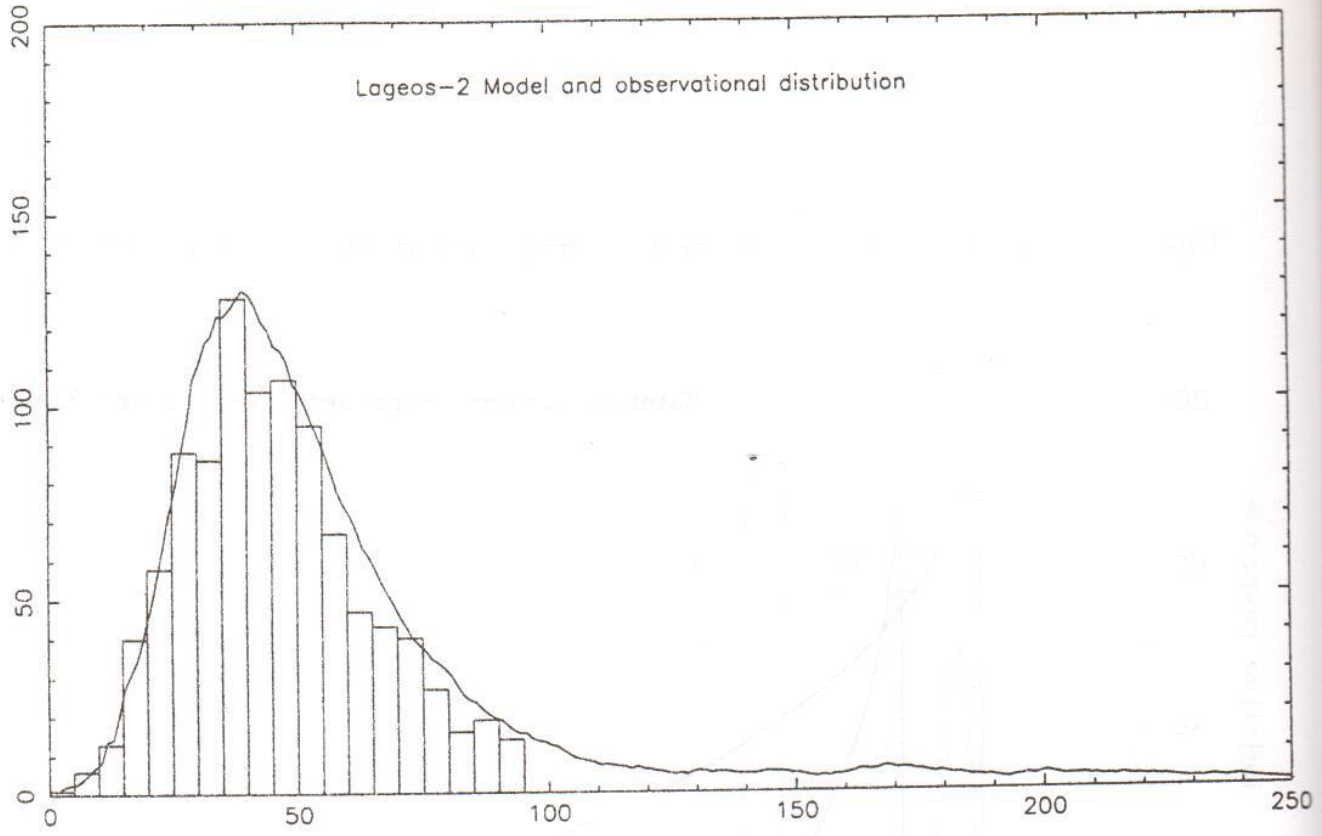
Lageos−2 Model and observational distribution
0
50
100
150
200
250

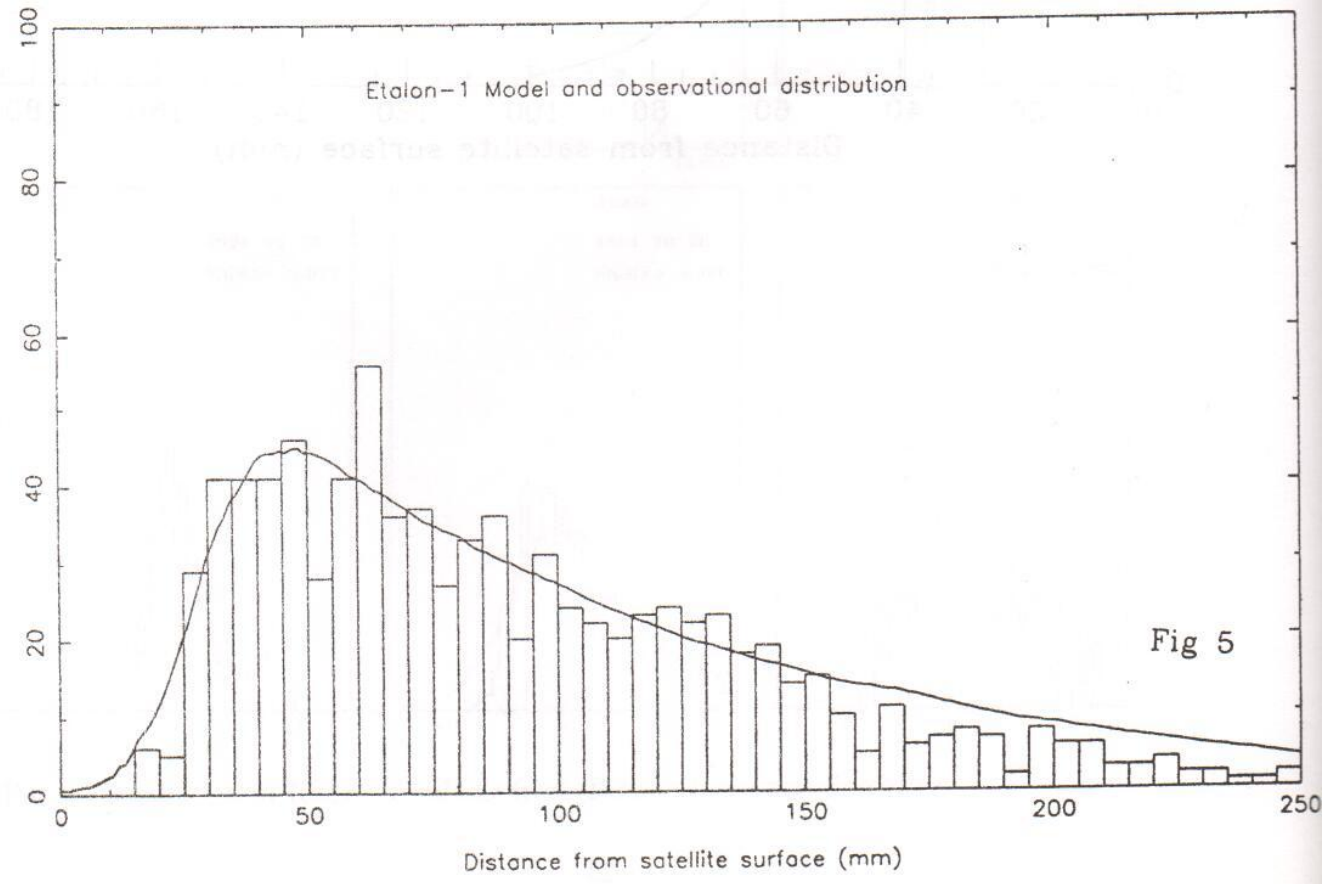
Etalon−1 Model and observational distribution
0
20
40
60
80
100
0
50
100
150
200
250
Distance from satellite surface (mm)

Fig 5

TABLE 1.

LAGEOS CoM Corrections for different system precision and method of processing.

System Precision (mm)	Peak mm	Mean mm	LEHM mm
6	250	248	252
12	246	240	250
20	241	236	247

Notes.

Mean is 3-sigma determination. The values are very dependent upon level of rejection.

If the system is represented by a Gaussian, the mean is not dependent on system precision, but the peak is.

TABLE 2.

ETALON CoM Corrections for different system precision and method of processing.

System Precision (mm)	Peak mm	Mean mm	LEHM mm
6	605	581	610
12	599	582	607
20	594	584	595

Notes.

Mean is 3-sigma determination. The values are very dependent upon level of rejection.

If the system is represented by a Gaussian, the mean is not dependent on system precision, but the peak is.

SALRO/MOBLAS 7 Collocation Analysis

Van S. Husson, Grace Su, Brion Conklin
AlliedSignal Technical Services Corporation
NASA SLR
7515 Mission Dr.
Lanham, Maryland, USA 20706

The SALRO/MOBLAS 7 collocation was a very new unique collocation. This was the first collocation of a Single-Photon Avalanche Diode detector system against a Micro-Channel Plate detector system. SALRO was the test system being evaluated and was built in Australia by Electro Optic Systems. MOBLAS 7 is the global satellite laser ranging standard.

Fullrate data provided by both systems was the primary data product used in the analysis. POLYQUICK, the NASA collocation analysis standard, was the primary data analytical tool. SALRO fullrate data pre-screened at the 2.0 sigma level was provided on each simultaneous pass. Two sigma editing was performed to eliminate data skewness caused by the satellite array coupled with single photon detection. Multiple versions of two passes (LAGEOS-1 on June 28, 1994 at 10:12 GMT and LAGEOS-2 on July 12, 1994 at 1:02 GMT) with different editing applied (3.0, 2.5, and 2.0) were provided for specialized analysis. Below in table 1 is the summary results of the POLYQUICK analysis of these 2 passes. All bias results are relative to MOBLAS-7. A positive bias indicates SALRO is measuring a longer range relative to MOBLAS-7, and conversely a negative bias indicates SALRO is measuring a shorter range than MOBLAS 7. In this analysis, no LAGEOS center of mass corrections were applied to either system.

Table 1. Salro Editing Analysis Summary

Date	Time	3.0 sigma bias(mm)	2.5 sigma bias(mm)	2.0 sigma bias(mm)
June 28, 1994	10:12	-0.8	-3.0	-7.9
July 12, 1994	1:02	0.1	-2.0	-4.8

The results indicate that SALRO ranges shorten by -5 to - 7 millimeters as the editing level is decreased from 3.0 to 2.0 sigma. The bias changes as a function of editing are also fairly consistently across a pass. Attachments 1&2 are the graphs of the June 28 LAGEOS-1 pass and the July 12 LAGEOS-2 pass, respectively, of the mean bias between SALRO and MOBLAS 7 per each two minute bin. The biases between each editing level are fairly constant throughout the pass.

This same type of editing analysis was applied to MOBLAS 7. The results of this analysis are summarized in Table 2. All bias results are relative to MOBLAS 7 with a conventional 3.0 sigma edit applied.

There was a correlation of the SALRO bias with the range of Lageos. The bias was near zero at the longer ranges (low elevation) where the return rates were lower, and more negative at the higher elevations were return rates were higher. SALRO does not measure signal strength, so return rate is the only estimate of signal strength. On the low satellites also there was strong correlation between return rate and the bias. The higher return rates again had more negative biases (shorter SALRO ranges). The return rates on low satellites and LAGEOS could reach 50% and 20%, respectively, at the higher elevations. So at times during a pass the return rate was certainly higher than single photon level, and so the data can be expected to show the effects of time walk in the avalanche photo diode detector, and also migration of the detection point towards the leading edge of the laser pulse at the higher return rates. It is probable that the overall variations shown in the figures are caused by these effects.

Table 2. MOBLAS 7 Editing Analysis Summary

Date	Time	3.0 sigma bias(mm)	2.5 sigma bias(mm)	2.0 sigma bias(mm)
June 28, 1994	10:12	0.0	0.0	0.0
July 12, 1994	1:02	0.0	0.0	0.0

The results indicate that MOBLAS 7 ranges remain the same regardless what editing level was applied to the data.

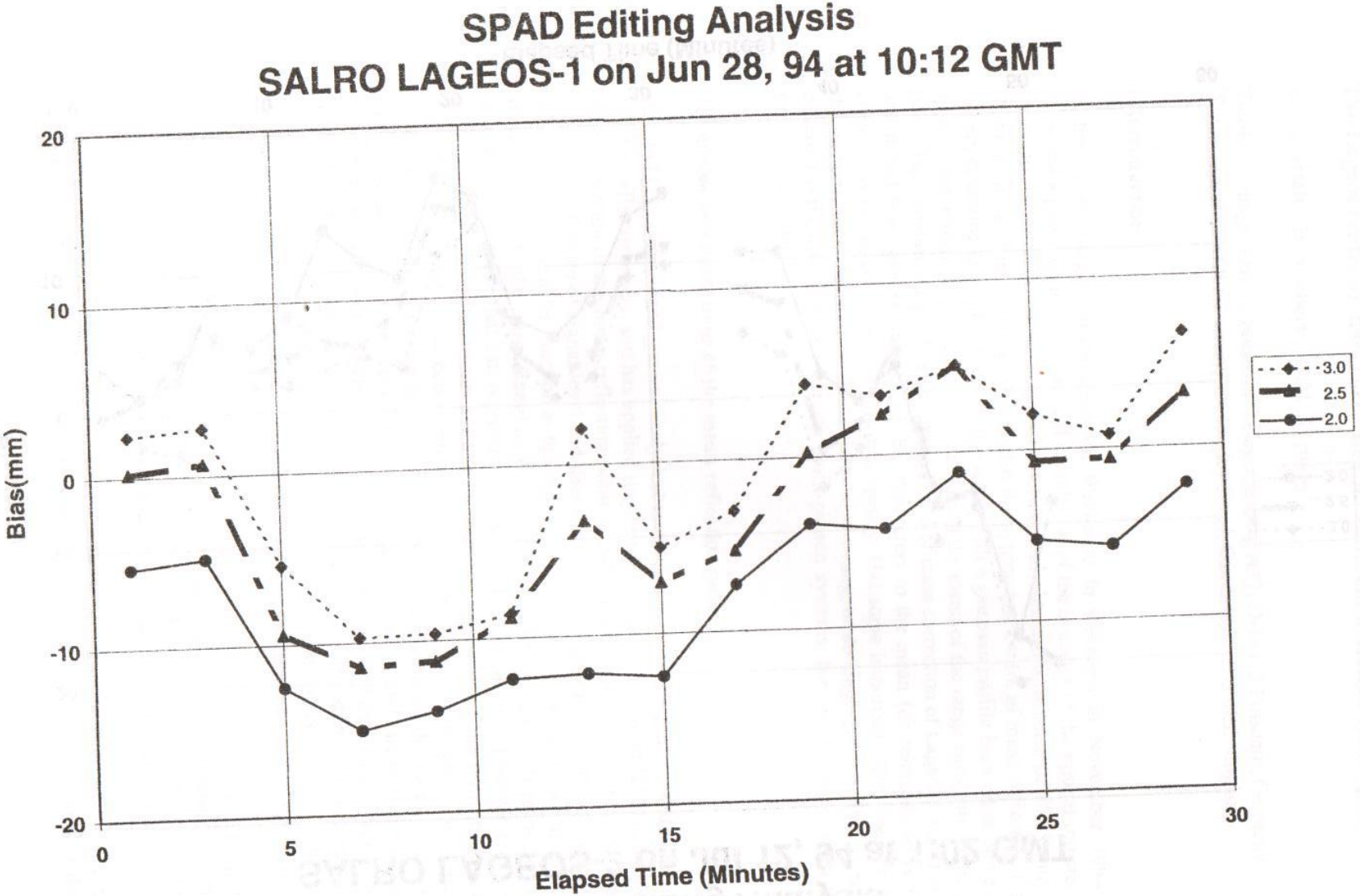

Attachment 1

SPAD Editing Analysis
SALRO LAGEOS-2 on Jul 12, 94 at 1:02 GMT

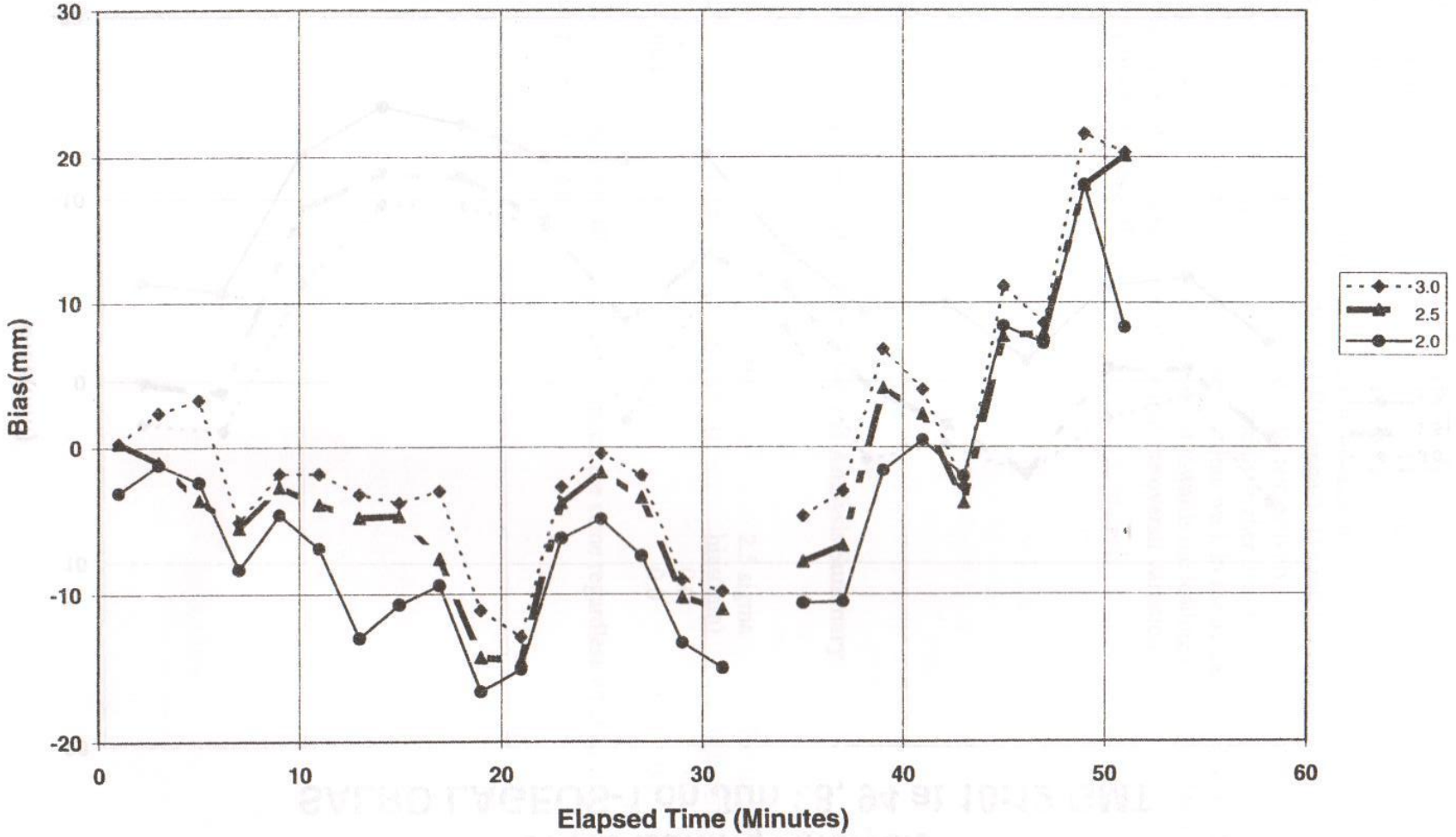

Attachment 2

The Lageos centre of mass correction for different detection techniques

A.T. Sinclair[†], R. Neubert[§], G.M. Appleby[†]

[§]GeoForschungsZentrum Potsdam, Telegrafenberg A17, D-14473 Potsdam, Germany.
[†]Royal Greenwich Observatory, Madingley Road, Cambridge CB3 0EZ. England

1. Introduction

At the Laser Ranging Instrumentation Workshop in Canberra in November 1994 Neubert presented a paper giving a theoretical calculation of the centroid of the optical transfer function (or response function) of the Lageos I satellite, and obtained a distance of 242.7 mm from the centre of mass of the satellite. This is also the appropriate centre of mass correction for an SLR system operating at single photon return level, with a gaussian profile laser pulse and a detection system that introduces no asymmetry, and using the mean of the range residuals as the reference point. The standard adopted value for the centre of mass correction of Lageos I and II is 251 mm, and it had been generally assumed that this refers to the mean (or centroid) reflection point. Hence it is necessary to resolve this discrepancy. Has some important effect been omitted from the theoretical calculation; is the standard value wrong, or do single photon systems actually see different reflection characteristics to multi-photon systems, for which the standard value was primarily derived ?

2. Various determinations of the mean reflection point

Arnold [1] has developed general analytical methods for calculating the optical transfer function of retro-reflector arrays, and has applied the theory to Lageos in Arnold [2], and obtains a value for the location of the mean reflection point of 242.5 mm. Neubert's [3] main objective was to model the influence of signal level and data filtering on ranging results, and in doing so he used Arnold's optical transfer function as the input, and obtained a value for the mean reflection point of 242.7 mm. At the Laser Ranging Workshop in Canberra Degnan [4] presented an elegant analytical expression that can represent the transfer function of any spherical satellite. Degnan [5] applied this theory to the satellite Lageos, but obtained results rather far from Arnold's value. Later Neubert traced this as being primarily due to a slip in one of the parameter values adopted by Degnan, who used a value of 1.905 cm for the dimension from the face to the vertex of the corner cubes, whereas the actual value is 2.784 cm. With this and one or two other minor slips corrected Degnan's work would give the same as Neubert, 242.7 mm. Egger [6] has developed a computer simulation model of the processes involved in SLR : start detection, reflection at the satellite, and detection of the return pulse. His model is in the process of revision, but gives for the optical centroid of Lageos-II the value 242.0 mm (1995, private communication).

The report on the pre-launch optical testing of Lageos-I [7] gives a value of 251 mm for leading edge half maximum detection, and 249 mm for peak detection, with standard deviations of 1.3 and 1.7 mm respectively. The standard error quoted for centroid detection is 11.5 mm, and no results for the centroid location are given, presumably due to this large uncertainty.

The report on the pre-launch testing of Lageos-II [8] describes the results of very extensive and meticulous experimental measurements using several techniques. In Section 6 of the report all

the results are assessed, and a model is produced for the optical transfer function that best represents the experimental measurements. This model uses theoretical considerations to decide the mathematical form of the expression, and adopts parameter values for the model that give a good fit to the experimental measurements. The model fits their results from CW FFDP best, and has disparities of several mm from results using a pulsed laser and streak tube detector. The location of the centroid of their transfer function model is at 251.0 mm.

So, in summary, the various values for the location of the centroid of the transfer function are

Arnold	242.5
Neubert	242.7
Degnan	242.7
Egger	242.0
Lageos-II test report	251.0

The uncertainty of any of these values is about 2 mm, and so there are no sigificant differences among the first 4 values, which are all theoretical. The theoretical models all assume incoherent superposition of the laser pulses reflected from the individual reflectors (i.e. the phases are sufficiently randomised that interference can be neglected). Work by Egger ([6] and his PhD thesis) suggests that variations of up to 4 mm can occur due to coherency effects. The Lageos-II measurements were averaged over sufficient individual measurement that the coherency effects should average out. An important factor in the theoretical calculations is the expression adopted for the functional dependence of the reflectivity of an individual corner cube on the angle of incidence. Among other factors this depends on the location of the observer within the reflected pulse, and this is off-centre due to velocity aberration. This effect is included in Arnold's work, and has been adopted in Neubert's work, and it is found that the effect will not explain the difference of about 8 mm between the theoretical results and the Lageos-II test report.

3. Comparison of impulse response functions

The Lageos-II test report (p. 6-10) gives a plot of the impulse response function that has been constructed to represent the experimental measurements, and on p. 6-3 it gives the mathematical expressions for the leading and trailing edges of this function. We have plotted the function from these expressions, and it is shown in Figure 1, together with Neubert's impulse response function. It is seen that there is a small difference in the location of the leading edge and the peak, but the major difference is in the trailing edge; the trailing edge of the Lageos-II report is very sharply cut off compared with that of Neubert.

The Lageos-II report started with experimental measurements of centre of mass correction for a range of laser pulse widths and detection methods, and from it constructed an impulse response function that would explain the measurements. The report then used this function to compute model values of the centre of mass correction for a range of laser pulse widths. These in effect are smoothed versions of the experimental measurements. These values are given on p. 6-16 of the Lageos-II report, and are plotted in Figure 2 of this paper, marked by the solid points. The Lageos-II report shows that these points agree very well with the measurements from the CW FFDP experiments, but not too well with the pulsed laser/streak tube measurements, and these are plotted as unfilled points in Figure 2.

From Neubert's theoretical impulse response function we have computed theoretical values of the centre of mass correction for the same range of laser pulse widths and for the same three detection methods. A gaussian laser profile is assumed, and no other source of jitter or skewness is included in the model. These values are plotted in Figure 3, marked by the solid points, and the same experimental pulsed laser/streak tube points as in Figure 2 are plotted as unfilled points.

The major difference of Figures 2 and 3 is that the theoretical values of the centre of mass correction using centroid detection are significantly lower than those from the Lageos-II report, which is a direct consequence of the difference of the centroid values of the theoretical and experimental impulse response functions discussed above. Also the theoretical curves for leading edge half maximum and peak detection show a greater slope than those in the Lageos-II report. The theoretical curves actually agree quite well with the pulsed laser/streak tube measurements using leading edge half maximum or peak detection, but not particularly well with the centroid values.

4. Observational results from single photon systems

We have shown that the theoretical calculations do not agree with the experimental measurements from the Lageos-II testing. The experimental testing was all done at multi-photon return levels, where a pulse of several hundred photons would enter the detector, and this incoming pulse would have the signature of the impulse response function convolved with the laser pulse. The critical factor is how much of that signature remains in the output pulse from the detector, and how much this remaining signature will affect the different discriminator techniques used. For a system operating at single photon level only a single photon enters the detector on each shot. Ideally the characteristics of the detector are not important, and usually no discriminator is used. A large number of such measurements will show a data distribution which, for an ideal detector, will show the same distribution as the average of the pulses that entered the detector. The concept of mean, peak or leading edge half maximum detection applies to the software processing of this data distribution in order to select a particular reference point.

Appleby [9] has used Neubert's response function for Lageos and also a model for the laser and SPAD detector at Herstmonceux, derived from laboratory and target board measurements, in order to model the data distribution that would be obtained from single photon ranging, and compared this with the actual data distribution obtained at Herstmonceux from Lageos ranging, and they agree very well. They certainly would not agree if the response function from the Lageos-II report was used. Applying the same theoretical methods to the Etalon satellites Appleby again gets good agreement between theory and observation, giving further confidence that the theory is correct. Also at Herstmonceux the mean and the peak of the distribution of each pass are routinely calculated and archived. The average values of the differences of the mean and peak are 6.9 mm for Lageos-I from 957 passes, and 6.6 mm for Lageos-II from 691 passes. The average difference between mean and peak when ranging to a flat target board is 2.7 mm, and hence the additional amount for the Lageos satellites is about 4 mm. The single shot precision of the system (a combination of laser pulse width and detector jitter) is about 11 mm RMS = 170 ps FWHM. We see that the difference of 4 mm agrees very well with the difference between the centroid and peak curves in Figure 3 for a pulse width of 170 ps, and does not agree at all with the corresponding difference in Figure 2. Husson, Su and Conklin [10] have processed the data from the collocation of SALRO and MOBLAS-7, and find changes in the bias of SALRO data from Lageos of between 5 and 7 mm using the mean of the data calculated with wide and narrow

clipping of the data, and this again is essentially a measure of the difference between the mean and the peak, and is in good agreement with the Herstmonceux value.

5. Conclusions and discussion

We have shown that there is a significant difference between the theoretical impulse response function for Lageos and the modelled function chosen to best represent the experimental measurements made at multi-photon return levels. The observational data from single photon ranging are consistent with the theoretical model. It would seem that the experimental measurements at multi photon return levels are not seeing the tail of the Lageos response function. We can speculate that perhaps the tail of the pulse that enters the detector is lost from the pulse that emerges from the detector, but this is just speculation. Provided the experimental set-up for the Lageos ground test simulates accurately the actual bahaviour of the real ranging systems that use pulsed lasers, multi-photon return levels and MCP detectors then the centre of mass correction derived from these ground tests is the correct value to use for the MCP systems. The standard adopted centre of mass correction is 251 mm, which agrees well with all 3 curves in Figure 2 for pulse lengths longer than about 100 ps. The experimental results quoted in the Lageos-II report for pulsed lasers/MCP detectors using constant fraction discrimination gave a centre of mass correction of about 248.5 mm for very short laser pulses, but rising close to 251 mm for longer pulses. Hence in practice the value of 251 mm is reasonably appropriate for the actual operational MCP systems.

Clearly the standard value of 251 mm is not appropriate for single photon systems using centroid detection. However in practice most such systems have been using the centroid of the data edited with a fairly tight clipping, and this moves the reference point towards the peak. It has now been recognised that the peak is the more appropriate reference point to use, in order to reduce the unwanted effects of the skew tail of the data that is typical of avalanche photo diode systems, and this has the additional advantage that the centre of mass correction is closer to the standard value.

Consideration of the various papers in these proceedings and the curve plotted in Figure 3 suggests that for a typical single photon system of single shot precision to a target board of 140 ps (= 9 mm), using the peak as reference point, the value 249 mm would be appropriate for the centre of mass correction if the system distribution had a gaussiam profile, and 248 mm if the system had a slightly skew distribution as is typical when using a photo diode detector. So we consider that the correction 248 mm will be appropriate for typical single photon systems when they use the peak as the reference point.

References

[1] D.A. Arnold. Method of calculating retroreflector-array transfer functions. SAO Special Report 382. 1979.

[2] D.A. Arnold. Optical and infrared transfer function of the Lageos retroreflector array, Final Report, Grant NGR 09-015-002, Suppl.No.57, May 1978.

[3] R. Neubert. An analytical model of satellite signature effects. Proc Int Laser Ranging Workshop, Canberra 1994 (in production).

[4] J.J. Degnan. Effects of detection threshold and signal strength on Lageos range bias. Proc.Int.Laser Ranging Workshop, Canberra 1994 (in production)
[5] J.J. Degnan, Millimeter accuracy satellites for two color ranging. Proc.Int.Laser Ranging Workshop, Annapolis 1992, pp.7-36 to 7-51.
[6] D. Egger. Systems analysis and computer simulation studies of the laser ranging measurement process. Proc. ESA Workshop on Space Laser Applications. ESA SP-202. 1984.
[7] M.W. Fitzmaurice et al. Prelaunch testing of the laser geodynamic satellite (LAGEOS). NASA Technical Paper 1062. 1977.
[8] P.O. Minott et al. Prelaunch optical characterization of the laser geodynamic satellite (LAGEOS 2). NASA Technical Paper 3400. 1993.
[9] G.M. Appleby. Centre of mass corrections for Lageos and Etalon for single-photon ranging systems. (In these Proceedings).
[10] V.S. Husson, G. Su, B. Conklin. SALRO/MOBLAS 7 collocation analysis. (In these Proceedings).

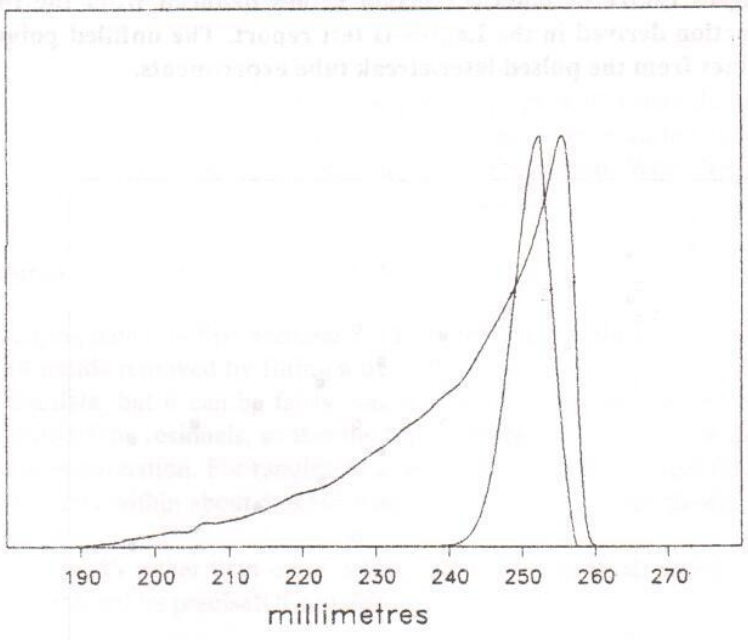

Figure 1. Comparison of Lageos impulse response functions, from Lageos-II test report (inner curve), and the theoretical curve from Neubert.

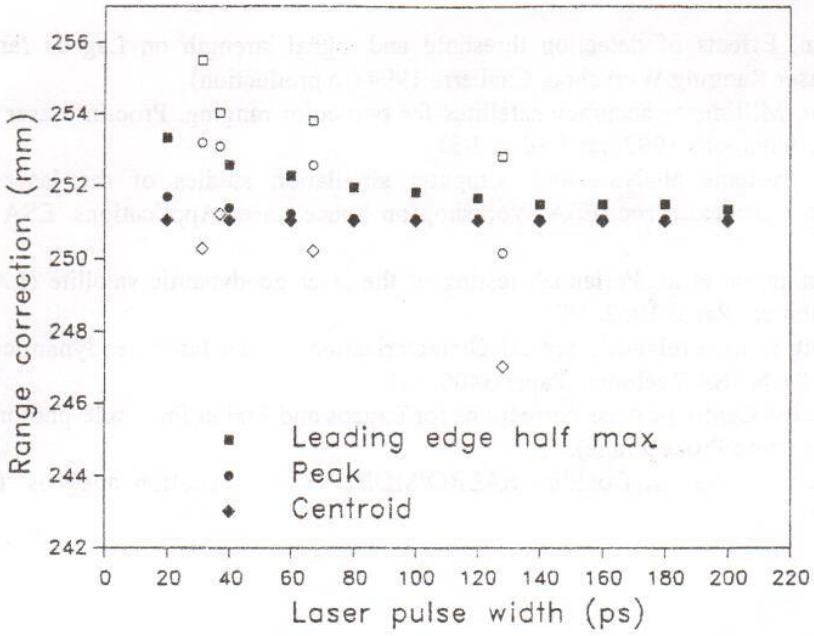

Figure 2. Lageos centre of mass correction values deduced from the impulse response function derived in the Lageos-II test report. The unfilled points are measured values from the pulsed laser/streak tube experiments.

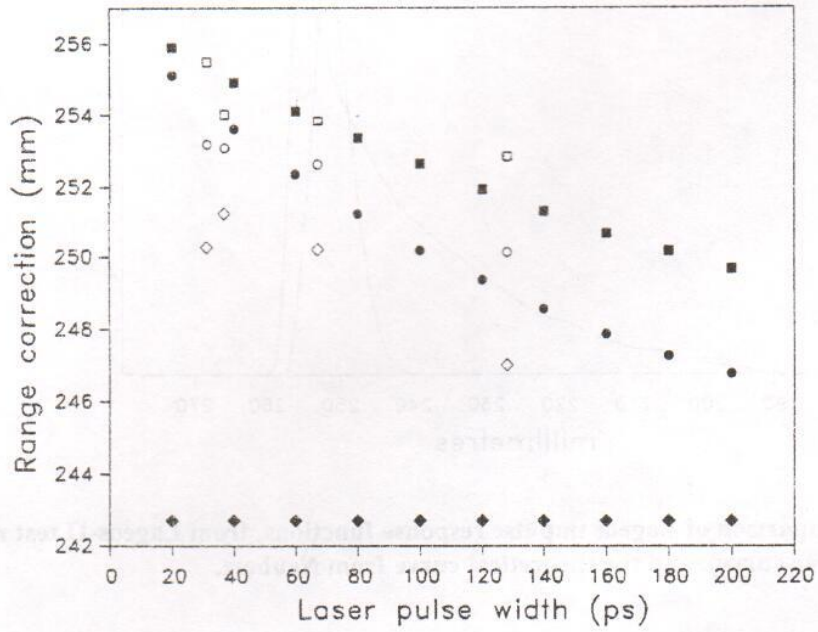

Figure 3. Lageos centre of mass correction values deduced from Neubert's theoretical impulse response function. The symbols are the same as in Figure 2, and the unfilled points reprsent the same streak tube measurements as in Figure 2.

Data screening and peak location

A.T. Sinclair
Royal Greenwich Observatory, Madingley Road, Cambridge CB3 0EZ. England.

1. Introduction

At the 5th Laser Ranging Instrumentation Workshop held at Herstmonceux in 1984 a procedure was recommended for the formation of normal points from full rate ranging data. This included the recommendations (quoted here only in outline) that the data should be screened using an iterated 3 σ rejection level, and that the retained data should be divided into normal point bins and the arithmetic mean should be taken. It is now recognised that for systems operating at the single photon return level the data are usually skewed towards long ranges, due to the characteristics of the pulse after reflection by the satellite, and in part due to the properties of the avalanche photo diode detectors that are now widely used by these systems (the satellite signature is not seen to the same extent by MCP systems due to the characteristics of the MCP and discriminator). In this situation it is more appropriate to use the peak of the distribution of the data rather than the mean to form the normal points, as these are then referred to the peak reflection point on the satellite, and for the Lageos satellites this is close to the reflection point as measured in ground testing. Also use of the peak has the advantageous effect of reducing any bias to the normal points from the skew tail of the data distribution caused by a photo diode detector.

In this note we describe two methods for determining the peak of a data distribution, and also consider the optimum level for screening of the data. The methods were earlier described in Sinclair (1992, Proceedings of the Annapolis Laser Ranging Instrumentation Workshop, p.2-34), and this note summarises some of that work, and includes further examples.

2. Data screening and determination of the mean

For satellite ranging data it is first necessary to form residuals of the observed range data from predicted ranges, with all trends removed by fitting a trend function. In this process it is necessary to make some screening of the data, but it can be fairly coarse, say about 5×RMS, where RMS is the (at this stage) approximate RMS of the residuals, so that the full characteristics of the data distribution are retained for the next stage of examination. For ranging to a terrestrial calibration target there is no need to fit a trend function, and the data within about 5×RMS from the mean range value should be retained.

Note that we use RMS rather than σ for setting the screening level, as this is more appropriate for a distribution that will not be precisely Gaussian.

The next stage is to make the main screening of the data and a determination of the mean value, using an iterated rejection level of $n\times$ (RMS from the mean), where all the data within the coarse screening are reconsidered at each iteration, and both RMS and the mean are varying through the iterations until convergence is obtained. The value of n is discussed later in this note, but it should be in the range 2.5 to 3.0.

The next stage is to find the peak of the distribution of the retained data, and also determine the quantities skewness and kurtosis for the retained data, which also describe properties of the data distribution.

2. Location of the peak

The usual way of examining the distribution of a set of measurements of some quantity is to plot a histogram. However histograms have several disadvantages. They do not work very well for sparse data. The shape of the histogram is somewhat dependent on the choice of bin size and on the bin boundaries. The resolution with which the peak can be determined is limited by the bin width. In order to overcome these limitations a method that has been used successfully at the Herstmonceux SLR for some time is to fit a gaussian profile to the histogram bin peaks. However this is a fairly complicated process, and so efforts have been made to find a simpler method.

A reasonably effective and simple method to locate the peak is to determine a second iterated mean value of the data, but this time using a very tight rejection level. A rejection level of 1.0×RMS has been found to be suitable, but it is important that during the iterations the value of the RMS is held fixed at the value obtained for the main screening of the data. Otherwise the process might not converge at all, or it might converge on some chance tight clustering of a few data points. Even so, the process can occasionally fail to converge if the data distribution is poor.

2.1 Smoothing method

We assume that we have a set of data points, all of which are measurements of some quantity, and we denote them by (x_i , i=1, n). Our objective is to determine and to plot in the y direction a quantity describing the distribution of the data. In the smoothing method each data point is regarded as the most probable value of that particular measurement, but the actual value is described by a probability distribution about the measured value. So we spread (or smooth) the effect of each data point around the measured value using a gaussian probability distribution. Then at any given location on the x-axis there will be contributions from the gaussian distributions of all of the data points, and these are summed to give the value of y at that particular value of x, which is in some sense a measure of the total probability that that particular value of x is the most likely value, and hence the value of x corresponding to the peak of y is the most likely value of the quantity implied by the whole data set. This process is described by the formula:

$$y = k \sum_{i=1}^{n} \exp\left[-\tfrac{1}{2}\,(x - x_i)^2 / \sigma^2\right]$$

where σ is the somewhat arbitrary standard deviation of the smoothing function, although it would seem reasonable to choose a value close to the single shot precision of the system. We regard the scale of y as arbitrary, and k is an arbitrary factor chosen to give some convenient maximum value of y. The procedure is to take a range of values of x spanning the actual data values, and at each x value evaluate the expression for y. So, for example, if the data are 2-way light time measurements in picosec, the values of x will probably be contained within a span of 2000 ps, and it would be suitable to evaluate y at steps in x of 10 ps (equivalent to a span of 300 mm of 1-way range with a step of 1.5 mm). So there would be 201 steps, and if there were 1000 data points then the exp function would be evaluated 201000 times.

It will be recognised that this process is simply a convolution of a gaussian distribution function with the original distribution of data values. In practice it is not necessary that the smoothing function should be the gaussian distribution function; any function of an approximately similar shape will work equally well, and may be advantageous in order to reduce the computation time if the computer used is rather slow.

The following function is similar in shape to the function $\exp(-\frac{1}{2}z^2)$, and gives very similar results for plots of the data distribution and location of the peak :

Put $$z = \frac{|x - x_i|}{\sigma}$$

Then, for $z < 2.558$, $$f = \frac{1 - 0.15275z^2}{1 + 0.41964z^2}$$

for $z > 2.558$, $$f = 0$$

This function is plotted in Figure 1 together with the function $\exp(-\frac{1}{2}z^2)$.

2.2 Choice of the smoothing parameter σ

Figure 2 shows a family of 4 smoothing curves for a pass of Lageos II taken at Herstmonceux. The pass contains 617 data points. The smoothing curves are for values of σ of 20, 40, 60 and 80 ps, and are drawn with different vertical scaling factors in order to separate them. The conventional histogram of the data is also drawn. (There is a mix of units of 2-way light time for the smoothing parameter, and 1-way range for the horizontal axis.) It is seen that the smoothing of 20 ps is too low to give a single peak, but smoothings of 40, 60 and 80 all give a single peak. However it is found that for passes with fewer data points a smoothing of 40 ps is often insufficient, but 60 ps will in most cases give a single peak. Figure 3 shows an example of this, for a pass of Lageos I containing 553 data points. The smoothing of 40 ps gives a single peak, but is rather biased. In both figures 2 and 3 it is seen that as the smoothing value is increased the skew tail has more influence, and pulls the peak in the direction of the skewness.

We need a compromise, of a smoothing parameter which will give a single peak in most cases, but is low enough so that the skew tail does not have an undue influence. We propose to adopt a value of $\sigma = 60$ ps. In the cases where this does not give a single peak, we fit a cubic polynomial to the subset of the (x, y) values for which y is greater than 40% of the greatest y value, and the peak of this cubic is taken as the peak of the data distribution.

Figure 4 shows a pass of Ajisai containing 547 data points. It is seen that the smoothing curve for $\sigma = 60$ ps fails to give a single peak, so superimposed on this curve is the fitted cubic polynomial, which gives a single peak, in what seems to be a realistic location of the peak of the data distribution.

All this may seen somewhat arbitrary, but it is no more arbitrary than the manual settings of discriminator levels in an MCP system. What is required is a robust, repeatable procedure, which is the software equivalent for single photon systems of the standard hardware settings used by MCP systems. Unfortunately there is no pre-launch measurement data at single photon levels on the geodetic satellites on which this procedure could be calibrated, but good progress is now being made with mathematical modelling of the reflection characteristics of the satellites, and these can be used to produce simulated data sets at single photon level which can be used to calibrate the procedure.

3. Formation of normal points

The procedures described in section 2 for determining the peak of a distribution of data (either the mean of the data using a tight rejection level, or the smoothing method) have been tested on simulated sparse passes with about 80 data points, and work well. However they are unlikely to work well on the few points that there might be in a normal point bin. Hence it is suggested that the location of the peak should only be determined for the whole of the data in a satellite pass, or for the whole of a typical terrestrial calibration run. The mean of the whole pass, or of the whole calibration run, should also be determined, and hence the quantity *"mean – peak"* should be determined. Within the normal point bins the mean of the data points should be formed, and from this the whole-pass quantity *"mean – peak"* should be subtracted, so that the normal points on average are referred to the peak of the whole pass rather than he mean. For a terrestrial calibration run the peak of the whole run is taken as the calibration value.

4. Data screening

The Herstmonceux algorithm recommends that the mean of the data should be used as the quantity that forms the normal points. Then, if the data have a skew tail, the level of screening adopted will have a significant effect on the mean value. However if the peak of the distribution is to be used as the reference point then the level of screening is less important, since in principle the peak is independent of the skew tail, and in our proposed methods for determining the peak we have attempted to minimise the effect of the skew tail. In figures 2, 3 and 4 the locations are marked where the data would be screened if the mean and RMS were determined using an iterated 2.5×RMS rejection, or using a 3.0×RMS rejection. It appears that nothing useful is lost if the data are screened at 2.5×RMS, and the data are probably improved by eliminating these outliers. In practice many SLR stations operating at the single photon level have come to this conclusion, and most use a tighter screening than the Herstmonceux recommendation. However we repeat that the choice of screening level is of lower importance once it is decided to use the peak as the reference point.

The tighter screening will, however, have an effect on the skewness and kurtosis values that are calculated from the retained data, giving a reduced value of the skewness, and a value of the kurtosis probably below 3 if 2.5×RMS screening is used, whereas the value would probably be greater than 3 for a single-photon system using 3.0×RMS screening.

4. A standard subroutine

A subroutine has been written in FORTRAN to carry out the functions described in this note, and is available from the Eurolas Data Centre. The descriptive header of the subroutine is duplicated below. The subroutine returns some arrays of quantities that can be plotted in order to see the distribution function, but the subroutine does not include any coding for plotting, as this is machine dependent. Note that the subroutine determines the location of the leading edge half maximum of the distribution, in addition to peak and mean. This is a possible alternative to the peak as choice of reference point.

```
      SUBROUTINE DISTRIB(RES,M,DMEAN,RMS,NUSE,SKEW,RKURT,QMEAN,NQ,
     1   PEAK,FWHM,NPEAK,LEHM,X,Y,XFIT,YFIT,IERR)
C
C  TO EXAMINE DISTRIBUTION OF SLR DATA, AND DETERMINE MEAN, PEAK and
C  LEADING EDGE HALF MAX. Also determines RMS, full-width-half-max,
C  skewness and kurtosis of the distribution.
C
C  WRITTEN BY A.T. SINCLAIR (RGO).
```

```
C  FOR A SATELLITE THE DATA ARE RESIDUALS OF THE MEASURED QUANTITY
C  FROM A SMOOTHING FUNCTION, SUCH THAT ALL TRENDS ARE REMOVED.
C  FOR A CALIBRATION TARGET THE RAW RANGE MEASURES CAN BE USED.
C
C  Same reference point must be used for calibration data as is used
C  for a satellite (ie. mean, peak or leading-edge-half-max).
C
C  A BAND OF DATA WIDER THAN +/- 3.0*RMS AROUND THE APPROX PEAK
C  OF THE DATA DISTRIBUTION SHOULD BE INPUT TO THE SUBROUTINE, SO
C  THAT NO CLIPPING OCCURS BEFORE ENTRY TO THIS ROUTINE.
C
C  The functions of the routine are:
C    1. Determine the mean and RMS-from-mean of the data, using an
C       iterated rejection level of n*RMS. The value of n is hard coded
C       at the start of the routine (parameter AN). A value of n=3.0
C       should normally be used, but for systems using first-photon
C       detection it may be considered that a tighter value might be
C       more suitable (but not less than 2.5). The data within this band
C       of n*RMS are used for calculating the skewness and kurtosis.
C
C    2. Determine the mean using a very tight rejection of 1.0*RMS, where
C       RMS is now held fixed at the value determined in (1). This gives
C       an estimate of the peak of the data distribution.
C
C    3. Use a "smoothing" method to derive a distribution function for
C       the data. This method regards each data point as being the centre
C       of a Gaussian distribution with sigma=60 ps, and sums the
C       contributions of all these Gaussians at 201 points spread over a
C       width of +/- 1000 ps (15 cm 1-way) about the mean. The peak of
C       this distribution function is located.
C
C    4. Fit a quartic polynomial to the peak of the data distribution
C       (actually to the part greater than 40% of the maximum). The reason
C       is that sometimes if the input data are sparse the smoothing method
C       may not give a single peak. Increasing the smoothing sigma will
C       usually fix this, but will also move the estimated location of the
C       peak towards the direction of skewness of the data. Instead the
C       peak of the fitted polynomial is used.
C
C  So the routine returns two estimates of the peak, from the 1.0*RMS
C  and from the smoothing/polynomial fit. These should be in close
C  agreement (except that if the data distribution is poor the 1.0*RMS
C  iteration can fail to converge).
C
C  UNITS: THE UNITS OF THE INPUT DATA ARE TWO-WAY LIGHT TIME IN PICOSEC.
C         THE UNITS OF OUTPUT QUANTITIES, RMS, MEAN, PEAK AND FWHM
C         ARE ALSO TWO-WAY LIGHT TIME IN PICOSEC.
C
C  ALL ARGUMENTS OF SUBROUTINE ARE DOUBLE PRECISION OR INTEGER.
C
C  INPUT:
C    RES(5000)     ARRAY CONTAINING THE DATA VALUES (UP TO 5000)
C    M             NUMBER OF DATA VALUES
C
```

```
C  OUTPUT:
C    DMEAN          ARITHMETIC MEAN VALUE OF DATA WITHIN n*RMS.
C    RMS            RMS OF DATA FROM THE MEAN USING ITERATED n*RMS REJECTION.
C    NUSE           NUMBER OF POINTS WITHIN n*RMS.
C    SKEW           SKEWNESS OF DATA WITHIN n*RMS (dimensionless).
C                   (NEGATIVE IF SKEWED TOWARDS SHORT RANGES)
C    RKURT          KURTOSIS OF DATA WITHIN n*RMS (dimensionless)
C
C                    (value of n is hard-coded at start of the subroutine =AN)
C
C    QMEAN          ARITHMETIC MEAN USING 1.0*RMS REJECTION.
C    NQ             NUMBER OF POINTS RETAINED IN FORMING ITERATED
C                     MEAN USING 1.0*RMS REJECTION (SAME RMS AS ABOVE).
C    PEAK           PEAK VALUE OF DISTRIBUTION FUNCTION OF DATA
C                     USING SMOOTHING METHOD.
C    FWHM           FULL-WIDTH HALF-MAXIMUM OF DISTRIBUTION
C                     (FOR GAUSSIAN DISTRIBUTION, FWHM = 2.355*SIGMA)
C    NPEAK          NUMBER OF PEAKS WITHIN FWHM.
C                     IF VALUE IS GREATER THAN 1 THEN THE PEAK OF THE
C                     FITTED POLYNOMIAL IS USED INSTEAD OF THE PEAK OF
C                     THE DISTRIBUTION FUNCTION.
C    LEHM           (DOUBLE PRECISION). LOCATION OF LEADING EDGE HALF
C                     MAXIMUM OF THE DISTRIBUTION. Note that the leading
C                     edge has shorter range measurement values than the
C                     trailing edge.
C    X(201)         ARRAY OF ORDINATE VALUES OF DISTRIBUTION, USING
C                     SMOOTHING METHOD.
C    Y(201)         ARRAY OF ABCISSA VALUES OF DISTRIBUTION, WITH PEAK
C                     VALUE SET ARBITRARILY TO 100.
C                     (PLOT Y AGAINST X TO SEE DISTRIBUTION OF DATA)
C    XFIT(201)      ARRAY OR ORDINATE VALUES OF POLYNOMIAL FITTED TO THE
C                     PEAK OF THE DATA DISTRIBUTION.
C    YFIT(201)      ARRAY OF ABCISSA VALUES OF THE FITTED POLYNOMIAL.
C    IERR           ERROR RETURN:
C                       IERR=0 : OK.
C                       IERR=1 : TOO MANY DATA POINTS INPUT.
C                       IERR=2 : DETERMINATION OF MEAN USING REJ=n*RMS
C                                  NOT CONVERGED.
C                       IERR=3 : DETERMINATION OF MEAN USING REJ=1*RMS
C                                  NOT CONVERGED.
C                       IERR=4 : FAILURE TO INVERT MATRIX IN POLYNOMIAL FIT.
C                       IERR=5 : LESS THAN 5 POINTS REMAINING IN POLYNOMIAL FIT.
C
C    Note. For errors IERR=1 or 2 the subroutine will return immediately
C          with no further computation.
C          For IERR=3 it will continue with calculation of other quantities,
C          but the value of the 1*RMS mean will be unreliable.
C          For IERR=4 or IERR=5 the polynomial fit to the distribution
C          function is not carried out, and the value of PEAK is not
C          replaced by the peak of the polynomial if there are more than
C          one peak to the distribution function.
C
```

```
      IMPLICIT DOUBLE PRECISION (A-H,O-Z)
      DOUBLE PRECISION RES(5000),DMEAN,RMS,SKEW,RKURT,QMEAN,
     1  PEAK,FWHM,LEHM,X(201),Y(201),XFIT(201),YFIT(201),C(5)
      INTEGER*4 M,NUSE,NPEAK,IERR
      REAL SX,F,FUNC
C
      IF(M.GT.5000) THEN
        IERR=1
        RETURN
        ENDIF
C
C  SET REJECTION LEVEL n FOR SCREENING OF DATA.
C  SHOULD BE 3.0 FOR SYSTEMS OPERATING MULTI=PHOTON DETECTION DEVICES
C  (EG MCPs), AND POSSIBLY 2.5 FOR SYSTEMS OPERATING SINGLE PHOTON DETECTION
C   DEVICES( EG PHOTO-DIODES).
C
      AN=2.5
C
C  SET OTHER PARAMETER VALUES (IN 2-WAY PICOSEC) :
C    SIG    :  THE SIGMA OF THE GAUSSIAN SMOOTHING FUNCTIONS.
C    WIDE   :  THE FULL WIDTH OVER WHICH THE DISTRIBUTION IS EVALUATED.
C    STEP   :  THE STEP AT WHICH THE DISTRIBUTION IS EVALUATED:
C
      SIG=60.D0
      WIDE=2000.D0
      STEP=10.D0
```

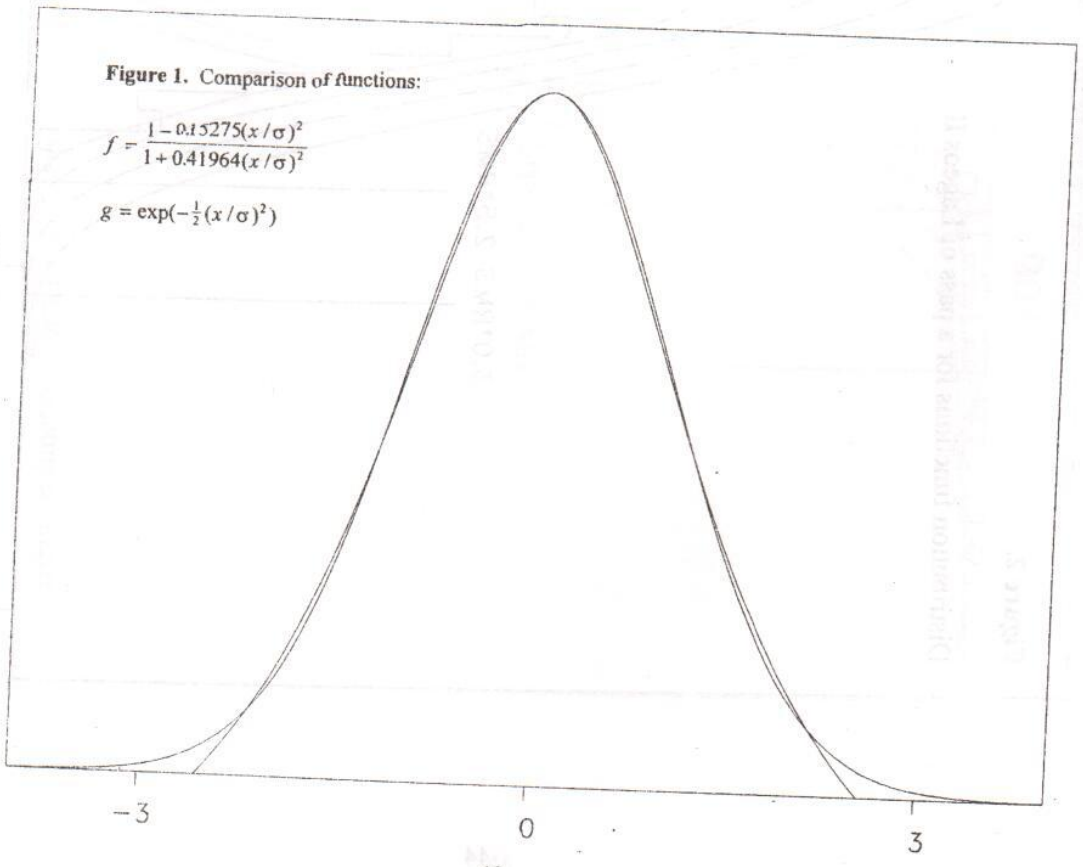

Figure 2.

Distribution functions for a pass of Lageos II

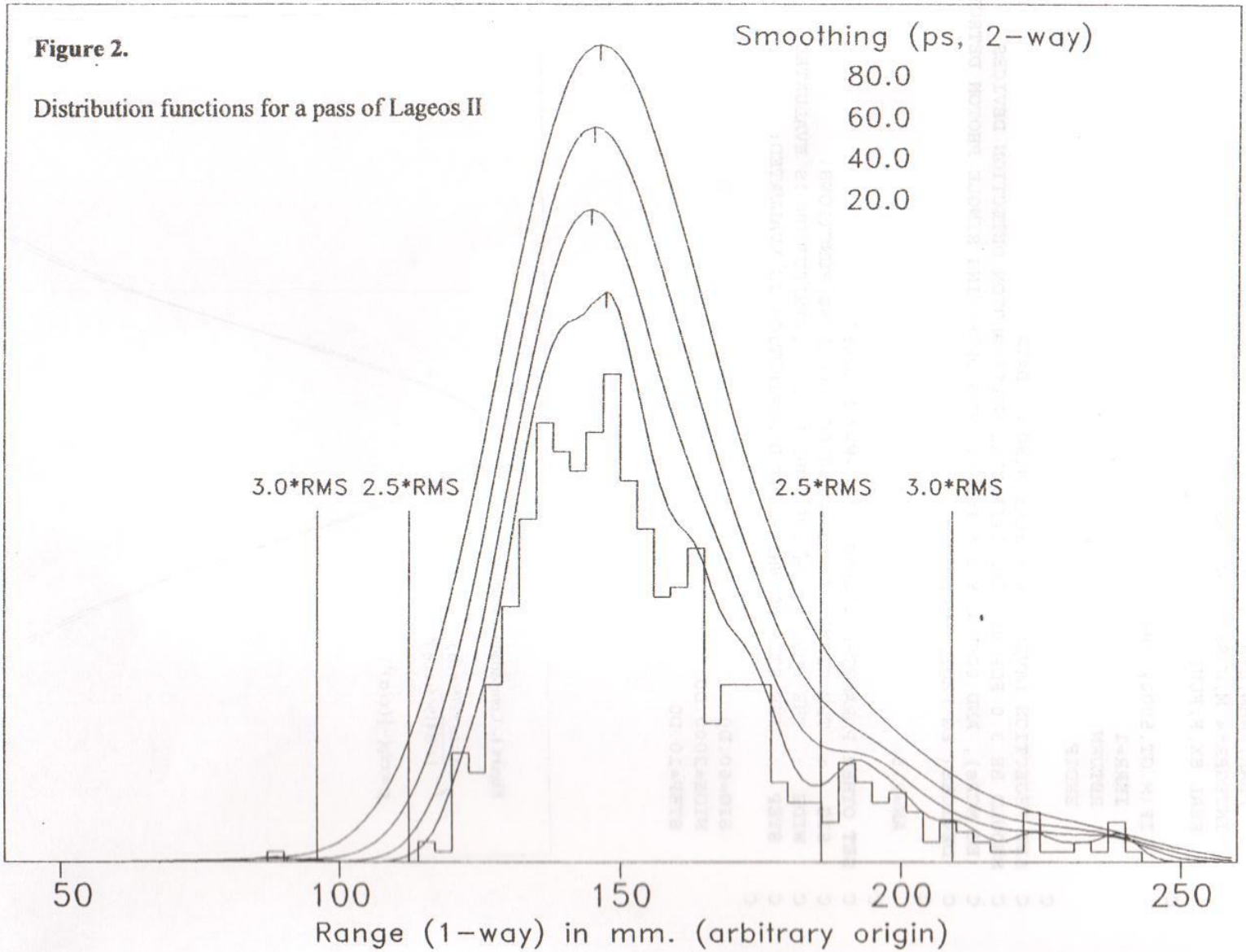

Figure 3.

Distribution functions for a pass of Lageos I

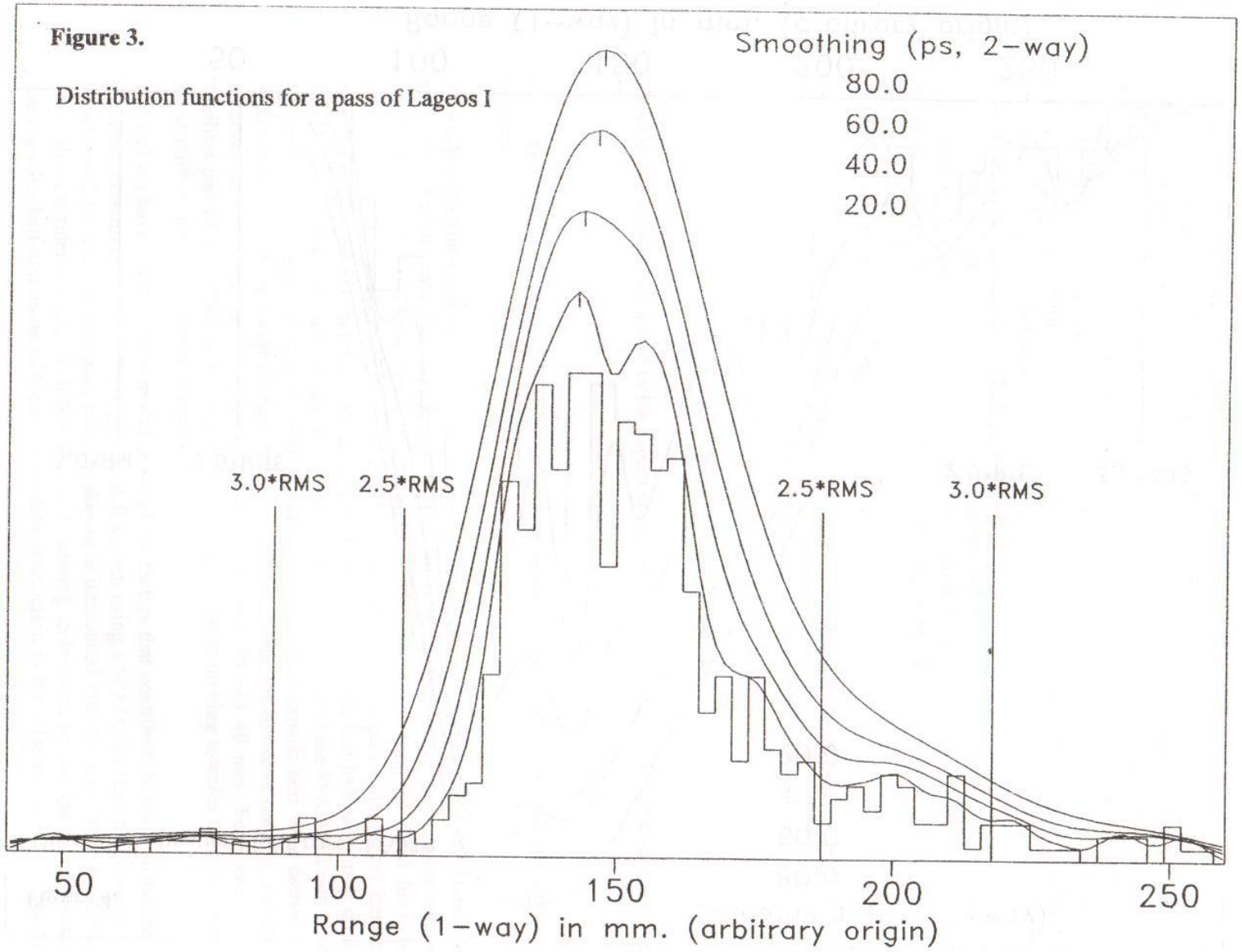

Figure 4.

Distribution finctions for a pass of Ajisai.

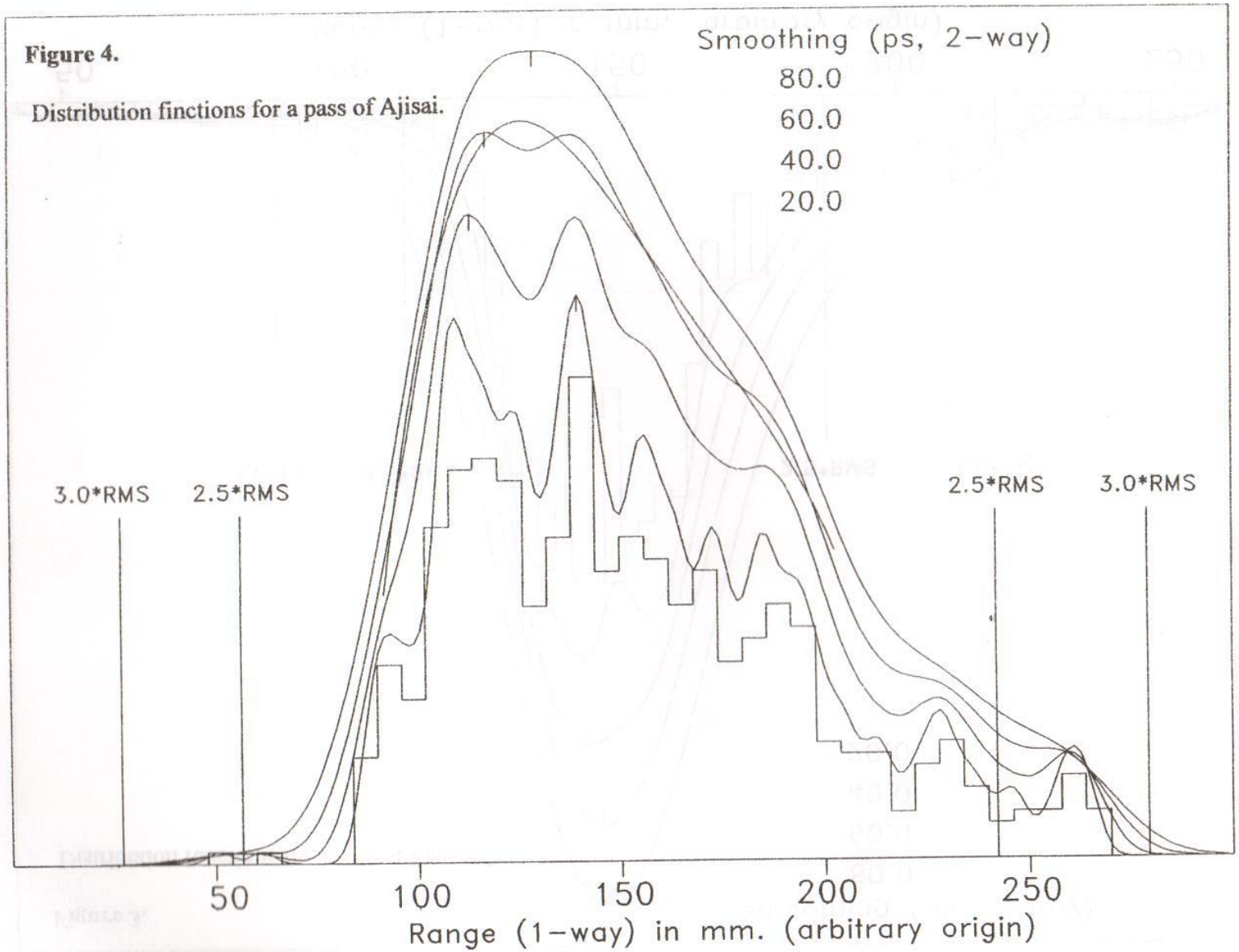

Summary of technical session on

"The use of avalanche photo diode detectors for SLR".

This technical session was the third in a sequence of meetings and discussions to understand the operation of avalanche photo diode (APD) detectors for satellite laser ranging, and the effects that they can have on the data. The first meeting was held at Graz in March 1994, and chaired by Dr Georg Kirchner, and took the form of a small workshop. Most of the potential problems were recognised at this meeting, and plans were made for carrying out measurements and experiments on SLR systems in order to quantify and understand the various effects. The results of these investigations were reported at the Laser Ranging Instrumentation Workshop at Canberra in November 1994, and there was a discussion of the operational procedures that should be adopted in order to minimise any biases to the data from the use of APDs. Finally in this session at the Eurolas meeting all this work was brought together, and the papers presented and reproduced in this report are a summary of the definitive conclusions from these earlier investigations, with recommended operating procedures that should be adopted by SLR stations using APD detectors.

The effects that have been identified are:

- a time walk depending on receive energy level due to the laser pulse width
- a time walk depending on receive energy due to the physics of the detector
- variation of the jitter of the detector depending on receive energy
- a data distribution that is skewed towards long ranges

These topics were all discussed in the papers presented at the meeting, and summaries are given below.

G.M. Appleby and P. Gibbs : Energy dependent range biases for single photon detection systems

This paper describes experiments of ranging to a calibration target board using a SPAD detector at a range of return rates from single photon to about 1000 photons, which gave a time walk of about 40 mm (270 ps). Part of this time walk can be explained by modelling the effect due to the laser pulse width, but about 25 mm remains. It is concluded that this part is due to the intrinsic properties of the SPAD, and this is in agreement with laboratory tests that had been made on the SPAD. The ranging experiments also showed an increase in the jitter of the SPAD at a return rate of about 20%, and again this agrees with laboratory tests. Further experiments were carried out on satellites, by making abrupt changes to the return level during the course of ranging, and these produced distinct steps in the range residuals of between 10 and 40 mm. For some of the satellites part of this effect is due to the mean reflection point moving towards the near face of the satellite as the return rate is increased.

The authors have constructed a model of all of the factors that contribute to the distribution of the range measurements made by a typical SLR system using a SPAD: the laser pulse width, the target board or satellite response, and the skewness introduced into the data from the SPAD. They also consider the use of different data processing techniques, to use the mean, peak or leading-edge-half-maximum of the resulting data distribution as the reference point. This model

is used to deduce the variation of the appropriate centre of mass correction for Lageos as the return rate is varied. They show that using the leading-edge-half-maximum as reference point gives very little variation of the COM correction with energy. Use of the peak gives rather more, and use of the mean gives the most variation of the COM correction

U. Schreiber, W. Maier, K.H. Haufe and B. Kriegel : Properties of Avalanche Photo Diodes

The paper by Ulrich Schreiber et al gives experimental results to show that a detector system consisting of an MCP detector plus discriminator has very little time walk with receive energy variation, whereas an APD detector has a considerable time walk above a certain return rate, but below this the time walk is negliglible. They consider the hypothesis that the time walk is due to laser pulse width. They model this process theoretically, and show how it could produce a range distribution with a sharp leading edge and a skew tail, similar to what is observed. However they dismiss this as being the sole cause of the time walk, as it cannot produce an effect of the observed magnitude. Further they show that experimental results from various APDs being used operationally in several SLR systems fall into two distinct families of time-walk behaviour, and this is without taking any account of the different laser pulse widths being used in the individual SLR systems. Hence the major factor appears to be a property of the APDs rather than a function of the laser pulse widths in use.

They discuss the physical processes that take place in the avalanche region, and describe several mechanisms whereby multiple photo-electons could speed up the avalance process, or even slow it due to the depleted electric field once a part-avalanche has occurred, thus causing the long ranges in the skew tail of the distribution. The multiplication factor of electrons in the avalanche growth process is a measure of the time taken for the avalanche to build up, and causes the response delay (of more than 1 ns) of the detector to an incoming signal. This factor has a very strong dependence on the structure of the semiconductor, and a very weak dependence on temperature, and also a noticeable dependence on the wavelength of the photon. They describe experimental results showing an increase of measured range of about 200 ps at 1.06 microns compared with 0.532 microns.

Ivan Procházka and Josef Blazej : Properties of SPAD detectors used for laser ranging

The authors have compared three different single photon detection systems, using a SPAD, an RCA APD and 8850-series PMT plus discriminator , and show that all of them give a non-symmetrical distribution of range measurments, with a skew tail towards long ranges. Hence it is concluded that the skewness is an intrinsic property of single photon detection systems.

They have made laboratory measurements of the time walk against return energy level of a SPAD detector, and they also find that there is negligible time walk up to a certain threshold return level, after which the time walk increases (in the direction of short ranges) by about 32 ps for each factor of 10 increase in return energy, most of which could not have been due to laser pulse width as they were using a very narrow pulse laser. They find an increase in the timing jitter for return levels in the region of 2-10 photons (equal to about 33% to 86% return rate), which they conclude is due to some effect in the avalanche build-up mechanism. They also find that as the return rate is increased, the skew tail of the data distribution is greatly diminished. This gives a further time-walk effect at low return rates, this time towards long ranges, if the data

are processed by taking the mean as the reference point, since the presence of the skew tail at low return rates biases the mean towards the direction of skewness, whereas at higher return rates the mean coincides closely with the peak. If the peak is used as the reference point then this effect disappears.

Georg Kirchner : Automatic compensation of SPAD time walk effects

SPADs introduce measurable timewalk effects if the input energy exceeds significantly the Single Photon Level. However, it seems that any change in this input energy also causes a slight change of the characteristic rise time of the avalanche breakdown. Some preliminary target measurement experiments using the Graz SLR system, and using the maximum range of received energy that can typically be obtained from satellites, showed rise time differences of up to 20 ps, with corresponding time walks of about 200 ps. Assuming a linear dependence between rise time and time walk, the authors have built a test discriminator circuit, which translates any change of the SPAD rise time into a tenfold shift of SPAD pulse detection epoch. Using this circuit, the timewalk effect was reduced from 200 ps to less than 20 ps, and further fine adjustment to give "zero" time walk should be possible. An improved circuit has been built, for easier adjustment, and to verify the preliminary results. This approach would allow fully automatic compensation of SPAD time walk effects, similar to the Constant Fraction Discriminators used for PMTs and MCPs.

A further development reported from Graz is the use of the whole of the second half of the laser pulse chain for ranging, so that multiple tracks of returns are obtained. Each track is kept below single photon return level, and the separation of the pulses in the comb is large enough that even if photo-electons are generated in the APD from several tracks the effect is still that of a single photo-electron. The advantages of this technique are to improve the overall return rate, and to give a means of measuring the return rate from the first track (as the other tracks will vanish if this is too high).

Stephan Riepl : Two colour ranging to Ajisai using a Streak Camera detector

This paper gave an indication of possible future lines of developments in detector technology, describing a successful attempt to track Ajisai in two colours simultaneously, using a Streak Camera at Wettzell.

Conclusions and recommended operating procedures for APD detectors

It was recognised that, for a system detecting the first photo-electron, one of the effects of increasing the receive energy above about a 30% return rate is to move the detection point on the satellite nearer to the near face of the satellite. For Lageos this has the advantageous result of bringing the appropriate centre-of-mass correction closer to the standard value of 251 mm, but has the disadvantage of causing a time-walk in the APD detector. However it is difficult to measure the receive energy, and thus difficult to quantify both the shift in the detection point on the satellite and the time walk of the detector. Hence it is recommended that these effects should be avoided by keeping the receive energy to low values, which should also be such as to keep below the level at which there is a peak in the timing jitter of the detector.

The recommended operating procedures at the present state of development of APDs are :

Systems that detect the first photo-electron should :

- determine the return rate at which the time walk begins to occur (typically about 30%)
- determine the jitter characteristics over this range
- adopt a maximum return rate to be used operationally for both satellite ranging and calibrations which is below the rate at which time walk occurs, and that gives tolerable jitter
- endeavour to use the full second half of the laser pulse train, in order to give a better overall return rate.

Meanwhile, development of techniques for the automatic compensation of detector time walk should be continued.

ENERGY DEPENDENT RANGE BIASES FOR SINGLE–PHOTON–DETECTION SYSTEMS.

GRAHAM APPLEBY AND PHILIP GIBBS

Royal Greenwich Observatory, Cambridge and Herstmonceux, UK

1. Introduction.

We have carried out experimental ranging to both target board and satellites in order to quantify potential energy–dependent range bias in the observations. We obtain biases relative to single–photon ranging of up to 40 mm for return levels of around 1000 photons. We use our models of the system response and of satellite signatures to compute the expected biases, and compare with the observations. We confirm the presence of an energy–dependent bias intrinsic to the SPAD detector.

2. High Energy Experiments.

2. 1. TARGET–BOARD RANGING.

We compute the return rate from ranging sessions by counting the number of laser shots in a given time interval, say 15 seconds. For each of these shots we check whether a noise event is detected, each of which reduces by one the effective number of laser shots. Given the number of true returns within the interval, we compute the true return rate as a percentage of the corrected number of laser shots. This information is displayed to the observer in near realtime. For a detector with quantum efficiency q, where $(0 < q < 1)$, we can relate the return rate to the number n of photons reaching the detector from

$$rate = (1 - e^{-(qn)}) \times 100$$

For the SPAD we have qe=0.2. For standard calibration ranging this rate is maintained at about 10-15% by attenuation of the outgoing laser beam, and by selection from a set of ND filters in the receive path, so that $n \leq 1$. For the duration of the ranging experiments the outgoing beam was attenuated such that the highest value ND filter was required to maintain single-photon returns. A series of calibration ranges was performed at different receive levels by selection of different ND filters, such that some 12 return levels of between 1 and 1000 photons were obtained. We note that for n above about 15, the observed return rate is close to 100%, so for rates $\geq$ 100%, n is estimated from the known relationships between the densities of the filters. The observations at each return level were used to form iterated mean

calibration values and single–shot rms precision, with rejection of outliers at 3 × rms. The calibration and precision values are shown in Figure 1 as functions of return energy level, where we plot data both from the full dynamic range of the experiment as a function of $Log(n)$, and as a function of return rate (0–100 %). For this latter sub-set it is seen that the calibration value changes by about 15 mm. The range precision changes little, with mean value about 9 mm, but with a temporary *decrease* to 13 mm at around 20%. This precision decrease has been noted consistently in the Herstmonceux data, and is also seen by Prochazka (1993) in laboratory tests of the SPAD. For the results over the full range of the experiment, we see that the calibration value changes by some 40 mm, and the single-shot precision increases to about 6mm.

2. 2. MODEL OF TARGET-BOARD RESULTS.

We have developed a model of the system response which closely represents the observed distribution of single–photon returns from the target board (Appleby, 1995, these proceedings). We now simulate our energy–dependent experiments by sampling from the model a given mean number n photons reaching the detector, as described in detail in Appleby (1993). We sample from the distribution a large number of times (> 500), finally forming from the simulated data the peak, the 3 × rms iterated mean, and the Leading–Edge, Half–Maximum (LEHM), using the procedure developed by Sinclair (1993).

We have plotted as the dotted line over the full zero-1000 photon return level these mean values, and also present in Table 1 the numerical values of change of calibration value as represented by the peak, the mean and LEHM. We see from comparing our model to the observations that the model under-estimates by some 25 mm the total change in calibration value, and that the model tends to 'flatten out' at high return level as 'photons' are sampled from close to the leading edge of the modelled distribution.

We now add to these model values an estimate of an energy-dependent timewalk intrinsic to the SPAD system by using the measurements of Prochazka (1993) over a dynamic range of between zero and 200 photons. The results of this complete model are shown as the full lines in Figure 1, where we plot the mean values.

We now find agreement between the observations and the model at most return levels, where the model agrees with the observed change at the 1-2 mm level, showing that the laser contributes only about 50% of the observed effect over the range of zero to 1000 photons. However, at the higher levels of return, the model over-estimates the total effect by some 4 mm, and does not fully model the observed increase in single-shot precision. Clearly, we have over-estimated the timewalk intrinsic to the SPAD, or our estimate of the laser pulse–width is too large. However, on the assumption that we have correctly estimated the pulse–width, the results from this experiment suggest that the timewalk for our device is some 15 mm, or 100 ps, over a dynamic range of from zero to 200 photons.

2. 3. SATELLITE RANGING.

We might expect that the bias effects measured from target-board ranging would also be present during satellite ranging if we depart from the single-photon regime. For this experiment, we observed nighttime passes of the satellites ERS-1, Meteor-3, Starlette, Stella, Lageos and Topex/Poseidon. At intervals throughout each pass the return levels were changed rapidly between single and multi–photons by removing or inserting ND filters in the receive path. For each pass the single–photon observations were reduced in the standard way, and then the deduced smoothing functions removed from the multi–photon data. The post solution residuals for all six passes are shown in Figure 2, where 'steps' of between 10 and 40 mm are clearly evident. For each pass we have computed separately the peak values and precision of the single and multi–photon sections of the data, and these values are displayed in Figure 3. From the known densities of the ND filters required to maintain single–photon levels we have estimated the numbers n of photons reaching the detector during the high-level return phases.

2. 4. MODELLING OF SATELLITE RESULTS.

Analogous to our model of the target-board results, we have modelled the satellite 'steps' as a function of the numbers of photons reaching the detector. We used for Lageos the model derived in Appleby (1995, these proceedings) from the satellite impulse function of Neubert (1995). We digitized the responses for ERS-1 from the curves derived by Degnan (1993), estimated the Starlette and Stella responses from the same source, and used the Topex/Poseidon responses of Varghese (Varghese and Pearlman, 1992). We do not currently have a model of the response of the small Meteor–3 LRA. We convolved these responses with our system response as characterized by the temporal distribution of the target-board ranges, and sampled from the resulting probability distributions in order to predict the range 'steps'. To these 'step' values we then added the intrinsic bias due to the SPAD, as deduced in the target board experiments. The results of the pass–averaged high and low–energy residual peak values and precision estimates, and the observed and predicted steps are shown in Table 2, along with the mean numbers of photons Np. In most cases as expected the multi-photon data has the greater single-shot precision, and the predicted 'steps' are in reasonable agreement with the observations, given the quoted observational precision values.

2. 5. LAGEOS COM VALUES

We have used the above simulations to model the changes to the Lageos CoM correction appropriate to a range of return energy levels. The results are given in Table 1 following the equivalent calibration values, and again are quoted as peak, 3 × rms iterated mean and LEHM. The CoM values have been calculated from the Lageos response model, followed by *subtraction* of the equivalent change of calibration value at each particular return energy level. We note that this correction

implies that calibration and satellite ranging are always carried out at the same energy level; if this is not true, much larger corrections to CoM may be appropriate, depending on the differences in energy. We see that the CoM correction for LEHM processing is little affected by return energy level, as may be anticipated from that statistic's lack of influence from the tail of the distribution. The peak value of CoM is less affected than that of the mean.

3. Conclusion.

We have shown that for our SPAD–based system, departure from the regime of single–photon return levels will result in range bias. We have experimentally examined the degree of bias as a function of return level, over a range of energy from single to 1000 photons. Simple statistical modelling of the system adequately explains the observational results, and implies that finite pulse-length accounts for about half the bias, and a plausible degree of energy-dependent time-walk within the SPAD system accounts for the remainder. For satellite ranging we find similar energy-dependent biases, which again are adequately explained by our models which include the effect of each satellite's response function. We conclude that if significant departures from single photons do occur during satellite passes, then the data should either be corrected using a measurement of the calibration dependence of the system on receive energy level, or sufficient information on the actual receive energy be included with each raw data point or normal point in order that analysts be able to compute appropriate CoM corrections. We finally note that provided calibration ranging and satellite ranging continue to be carried out at a strictly single–photon level, our normal practice, then range bias is minimal, at the expense of some loss of single–shot precision.

References

Appleby, G.M, 1993. Satellite Signatures in SLR Observations, NASA Conf. Proc 3214, Eighth International Workshop on Laser Ranging Instrumentation, Anapolis, MD, May 1992.

Degnan, J.J, 1993. Millimeter Accuracy Satellite Laser Ranging : A Review. Contributions of Space Geodesy to Geodynamics : Technology, Geodynamics 25, AGU.

Neubert, R. : 1995, "An Analytical Model of Satellite Signature Effects", In press in *Proc. Ninth Int. Workshop on Laser Ranging Instrumentation*, Canberra.

Prochazka, I, 1993. Single Photon Avalanche Diode Detector Package; Upgrade kit for RGO, July 1993.

Sinclair, A.T. : 1993, "SLR Data Screening; Location of Peak of Data Distribution". In *Proc. Eighth Int. Workshop on Laser Ranging Instrumentation*, Annapolis, MD

Varghese, T and M. Pearlman, 1992 September. SPAD Operations on the Topex/Poseidon Retroreflector Array, Private Communication.

Figure 1.

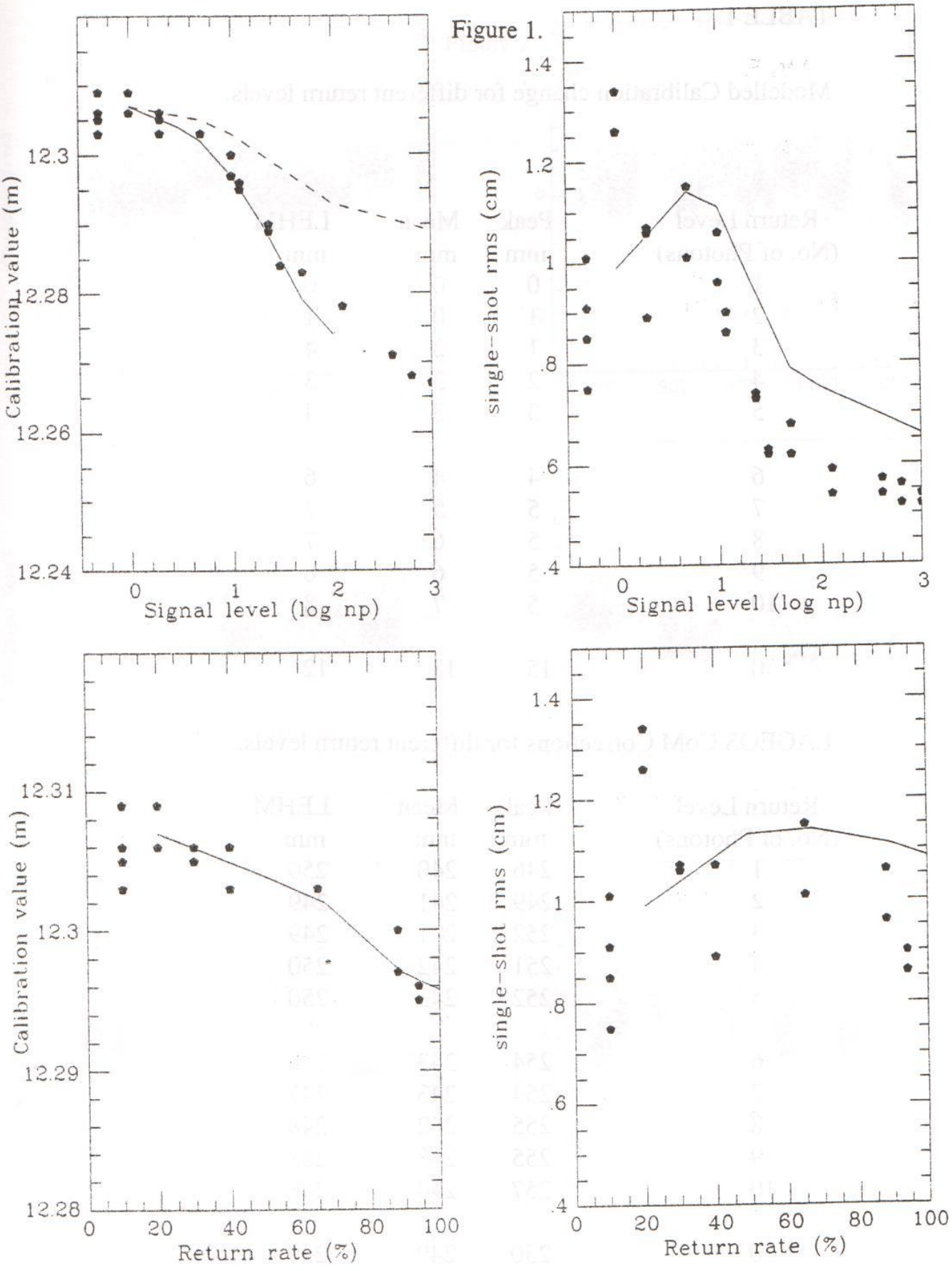
Calibration value (m)
12.3
12.28
12.26
12.24
0
1
2
3
Signal level (log np)
single-shot rms (cm)
1.4
1.2
1
.8
.6
.4
0
1
2
3
Signal level (log np)
Calibration value (m)
12.31
12.3
12.29
12.28
0
20
40
60
80
100
Return rate (%)
single-shot rms (cm)
1.4
1.2
1
.8
.6
.4
0
20
40
60
80
100
Return rate (%)

TABLE 1.

Modelled Calibration change for different return levels.

Return Level (No. of Photons)	Peak mm	Mean mm	LEHM mm
1	0	0	0
2	1	0	1
3	1	2	4
4	2	3	3
5	3	3	4
6	4	4	6
7	5	5	7
8	5	6	7
9	5	6	8
10	5	7	8
50	15	18	12

LAGEOS CoM Corrections for different return levels.

Return Level (No. of Photons)	Peak mm	Mean mm	LEHM mm
1	246	240	250
2	249	241	249
3	252	241	249
4	251	242	250
5	252	243	250
6	254	243	248
7	254	243	247
8	255	242	248
9	255	243	248
10	257	244	248
50	250	249	250

Figure 2.

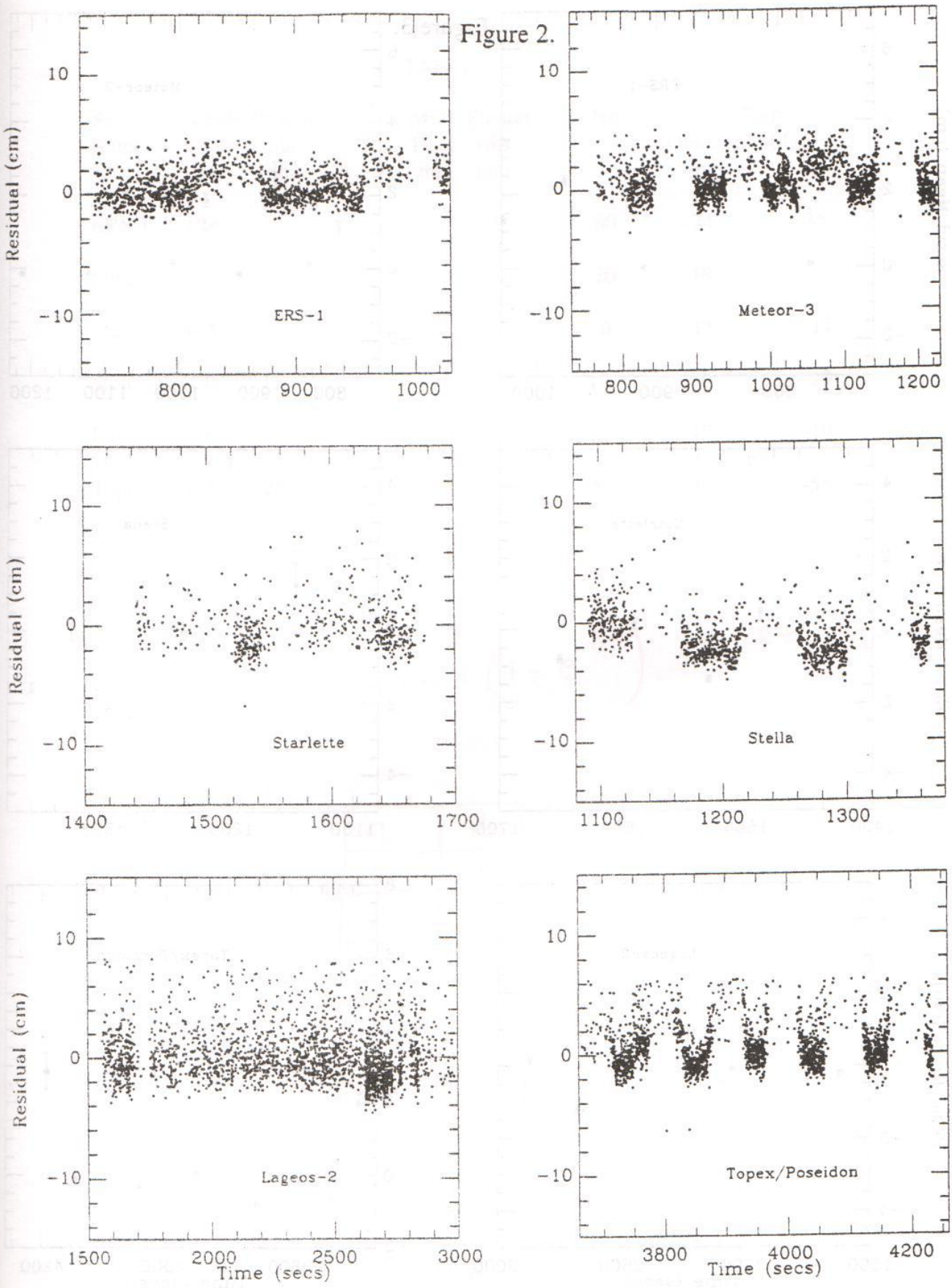
Residual (cm)
10
0
-10
ERS-1
800
900
1000
Meteor-3
1100
1200
Starlette
1400
1500
1600
1700
Stella
1300
Lageos-2
2000
2500
3000
Time (secs)
Topex/Poseidon
3800
4000
4200

Figure 3.

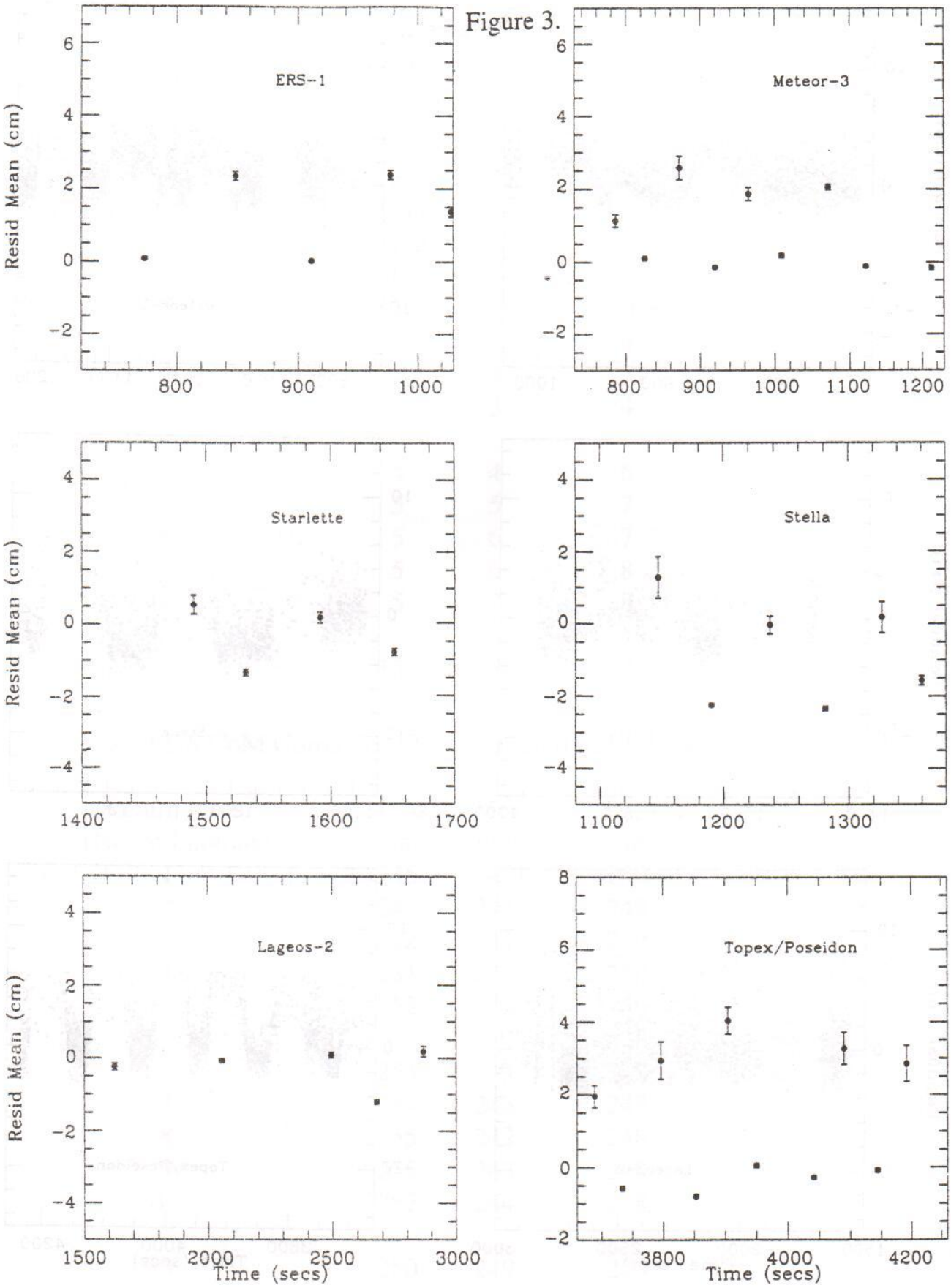
ERS-1
Meteor-3
Starlette
Stella
Lageos-2
Topex/Poseidon
Resid Mean (cm)
Time (secs)

TABLE 2

Sat Name	Single-Photon Peak mm	Single-Photon rms mm	Multi-Photon Peak mm	Multi-Photon rms mm	Np	Step Observed mm	Step Modelled mm
ERS-1	+24	11	0	9	80	-24	-35
Meteor	+18	14	0	11	20	-18	-
Star	+ 5	19	-10	14	6	-15	-11
Stell	0	12	-20	13	12	-20	-20
Lag-2	0	16	-12	15	5	-12	-10
Topex	+35	25	0	10	100	-35	-55

$$R = 100 \times \left(1 - e^{-(qn)}\right)$$

R = return rate
n = no. of photons
q = quantum efficiency

For $q = 0.2$

n	R
1	18
2	33
3	45
4	55
5	63
6	70
8	80
10	86
15	95
20	98

Properties of Avalanche Photo Diodes

U. Schreiber, W. Maier
Forschungseinrichtung Satellitengeodäsie
Fundamentalstation Wettzell
D-93444 Kötzting
Germany

K. H. Haufe
Institut für Angewandte Geodäsie
Aussenstelle Wettzell
D-93444 Kötzting
Germany

B. Kriegel
Silicon Sensor GmbH
Ostendstrasse 1
D-12459 Berlin

Abstract

At the Wettzell Laser Ranging System the usefulness of various types of avalanche photo diodes (APD) operated in the Geiger mode has been under investigation since 1989. Their application in laser ranging is analysed and compared to the performance of microchannelplates and photomultipliers. From measurements of local targets at various levels of intensity, a significant offset from the expected range was obtained. The possible cause for this timewalk effect is discussed in this paper.

1. Introduction

One of the most remarkable properties of avalanche photo diodes in general is their high sensitivity for light detection in the single photon domain, which is far beyond that of photomultipliers, particularly in the red wavelength band. Moreover, these diodes do not require high voltages to be operated. Another good feature is, that unlike photomultipliers they can not be destroyed by excessive light exposure. However, there are drawbacks to be considered as well. APDs for ranging applications usually have a small photosensitive surface area. This makes the focussing of the aperture of the ranging telescope onto the chip difficult. Another problem is, that the behaviour of the various types of detectors is significantly different with respect to a precise timing of the detected laser pulse. Under normal conditions the photocurrent of a photomultiplier is proportional to the intensity of the incident signal. This is not the case for an APD operated in the Geiger mode. A

diode always shows a characteristic output signal shape. This is caused by the process of an avalanche breakdown. There is no change in shape or amplitude with the amount of input light.

2. Timing the propagation of light with an MCP and APD

When a MCP is used as a detector in a laser ranging system, variations of the amplitude of the output signal must be compensated, so that they do not cause a jitter in switching the ranging timer. This is achieved by using a constant fraction discriminator. By triggering at the half of the maximum voltage from the rising edge of the detected pulse, the jitter in timing is minimised. However, care must be taken, to adjust the discriminator properly, in order to be safe from systematic walk offs. Figure 1 shows a diagram, where the dependency of the detection of the time of flight of a laser pulse is plotted over the variation of the intensity. From the measurements it can be concluded, that the influence of the received signal strength can be neglected for the given setup. When the same experiment is carried out for an avalanche photo diode an entirely different behaviour can be seen. After some stability in the low light level regime, a dramatic walk off towards shorter ranges can be observed. The offset finally becomes as large as 1 ns. This can be seen in figure 2. Putting together the observed effects, one can find the following summary.

- Below a certain detection threshold, the distribution of the values of range measurements are following the expected statistics, including laser pulse width and jitter of the timing devices and the detectors.
- The return rate itself is proportional to the introduced light intensity. The shape of the obtained histogram is that of a Gaussian.
- Above this detection threshold the previously mentioned timewalk effects can be observed. With increasing amplitude of light, a progressive narrowing of the distribution of the ranges is found as well as an worsening asymmetry of the shape of the histogram. Towards shorter ranges, the slope becomes steeper, while it develops a 'tail' in the direction of longer ranges.

3. Modelling the observations

There have been continued discussions, concerning the idea, that an avalanche diode acts like a fast switch. The observed timewalk reflects the fact, that the duration of the incident laser pulse needs to be considered [1, 2] in the search for a source of the bias. This discussion is assuming one single retroreflector, so that the target geometry in the following can be neglected. At a very low light level, the photon which is causing an avalanche statistically originates from the center of the pulse, where the probability for detection is at a maximum. At higher intensities, a photon from the beginning of the laser pulse already has a high probability to trigger the avalanche. That means, that the observed timewalk is a representation of the laser's pulse shape. In other words, one is "walking" down the slope of the laser pulse, as the light intensity is increased. However this approach fails to

account for all the observations. It is misleading in that it produces unrealistic broad laser pulses too. Therefore some refinements to this model are neccessary.

Now let us consider a given threshold for the detection, which is fixed and located, where the normalised probability of detection becomes 1. As long as the input signal stays well below this threshold, one obtains a symmetric Gaussian shaped distribution of the range measurements. The probability of detection is proportional to the pulse amplitude and no bias is observed. This relation is plotted in figure 3. For amplitudes high above this threshold, the situation becomes different. When the signal exceeds the threshold and assuming, that no avalanche has been generated, then the probability of starting an avalanche in the next moment is again decreasing. In analogy to other processes in physics, such as the decay of an electric field at the boundary to some dielectric material, it is assumed, that the probability of detection also follows an exponential decay function. In figure 4 this behaviour is sketched. The shaded area shows the form of the histogram, that can be expected. It illustrates the observed asymmetry, the increasing sharpness of the measurements (when the intensity is so high, that the domain of the steepest increase in the Gaussian is reached) and it also accounts for a timewalk.

Taking the laser pulse to be of the shape of a Gaussian

$$I_s = I_0 e^{-a^2 \Delta t^2} \tag{1}$$

and solving for an offset Δt from the middle of the curve, one yields

$$\Delta t = \sqrt{\frac{ln \frac{I_0}{I_s}}{a^2}}, \tag{2}$$

or in a more general form

$$\Delta t = -\frac{1}{a}\sqrt{ln(sx)}, \tag{3}$$

where x is introduced, to allow for an adjustment along the horizontal intensity axis. Tuning the parameters s, x and a to the data and calculating theoretical curves for some laser pulses of different length, one obtains figure 5. As can be expected by this approach, there is a strong dependence between pulse width and timewalk. This conclusion however, must be regarded with caution, as we now show.

4. Experimantal Data

Data from five different photo diodes have been taken or was made available [3, 4]. Figure 6 shows a diagram of the same scale as figure 5. Obviously one can group the data into two different detector families. The detectors having less systematic walk off are all SPADs [5]. The other family are diodes such as the RCA 30902s and SSO AD-220 (Silicon Sensor). Different lasers have been used in either detector family for the measurements. This however contradicts the theoretical concept of section 3. Therefore one may conclude, that the

applied pulse width does not have the relevance which may be expected by looking at the problem and which has been considered in the previous section.

There are significant differences in the design of the diodes, which strongly suggest that the reason for the observed timewalk is related to a process within the semiconductor structure. The diode is essentially consisting of two layers relevant for the simplified understanding here. One is the absorption layer, the other the avalanche region. In the absorption layer, a incoming photon is absorbed by creating an electron- hole- pair. Assuming, that no recombination takes place, this pair is entering the avalanche region. In the Geiger mode the electric field in this layer is so large, that the accelerated electrons (holes) are generating secondary electrons (holes) by collision. This is called the multiplication process. A rapid growth of the current is the result. One has to keep in mind, that shortly after entering the avalanche region, electrons are soon moving at their maximum drift velocity. The multiplication process is fast, but not instantaneous. In fact it is dependent on many parameters, such as intensity and wavelength of exposed light intensity and of course to the temperature, composition and structure of the semiconductor chip. The level of the bias voltage, the amplitude of the Geiger pulse and the the external electronic circuit are also of importance. Therefore it is suggested, that the cause of the observed light intensity dependent timewalk is due to a shortening of the avalanche growing process by the injection of more than one photoelectron (hole) into the avalanche region. This process can be very complicated, because on one hand multiple avalanche sources are speeding up the growth, while on the other hand a growing avalanche causes depolarisation inside the avalanche region. This weakens the electric field and therefore the electron acceleration is decreased.

Looking at the observed properties in chapter 2 again, the threshold would then be the level of intensity, where the multiplication factor no longer is constant due to additional avalanche sources. The skewness of the "high intensity" histogram could be interpreted as a probability of recording an event on a low multiplication factor compared to one, caused by a high factor. The sharp rise of the histogram towards shorter ranges reflects the fact, that the multiplication factor can not become infinite.

Figure 7 illustrates another example of a variation in the avalanche growing process. The residual plot shows a LAGEOS pass, tracked simultaneously on two frequencies ($\lambda_1 = 0.532\mu m$ and $\lambda_2 = 1.06\mu m$), using the same avalanche diode as a detector. The elevation angle dependent spacing between the two tracks of residuals is due to dispersion in the atmosphere. However, to adjust the measurement to the atmospheric model, a constant offset value of as much as $200ps$ needs to be inserted.

5. Conclusions

Starting with some experience gained by using avalanche diodes, a theoretical understanding of observed effects has been attempted. The initial model looked at the probability of starting an avalanche with respect to the length of the laser pulse. Unlike other models, it could also account for the observed asymmetry of range histograms at high laser intensities. But it failed to predict the right amount of the observed timewalk.

By grouping all available data from various diodes together, a systematic offset between diodes of different structure became evident. Finally the multipication process of the

avalanche buildup was identified as the cause for the bias. There is also a bias between simultaneous range measurements on two different frequencies for the same reason.

References

[1] R. Neubert, "Modelling Bias Effects of APDs", *Oral presentation from a meeting about the characteristics of APDs*, held in Graz, March (1994)

[2] G. Appleby, "Satellite Signature Effects and APD Characteristics",*Oral presentation from a meeting about the characteristics of APDs*, held in Graz, March (1994)

[3] L. Grunwaldt, R. Neubert, Li Ya, "Operational Characteristics Of Commercial Silicon Avalanche Photodiodes For Use As Laser Radar Receivers", *Proceedings Of 7th International Workshop on Laser Ranging Instrumentation*, (1989)

[4] G. Appleby, private communications (1993)

[5] I. Prochazka, K. Hamal, B. Sopko, "Photodiode Based Detektor Package For Centimeter Satellite Ranging", *Proceedings Of 7th International Workshop on Laser Ranging Instrumentation*, (1989)

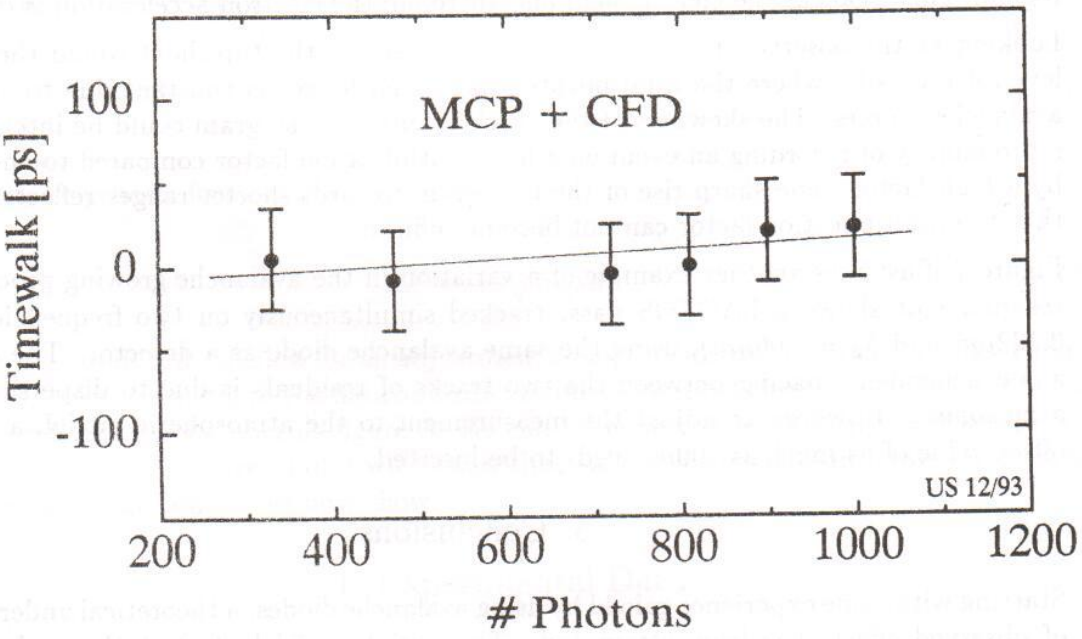

Figure 1: The diagram shows the dependency of the recorded time of flight along a constant path. The intensity of the laser pulse was varied over a critical region. The detector is a microchannel plate (MCP). A constant fraction discriminator is used to compensate changes in the laser amplitude

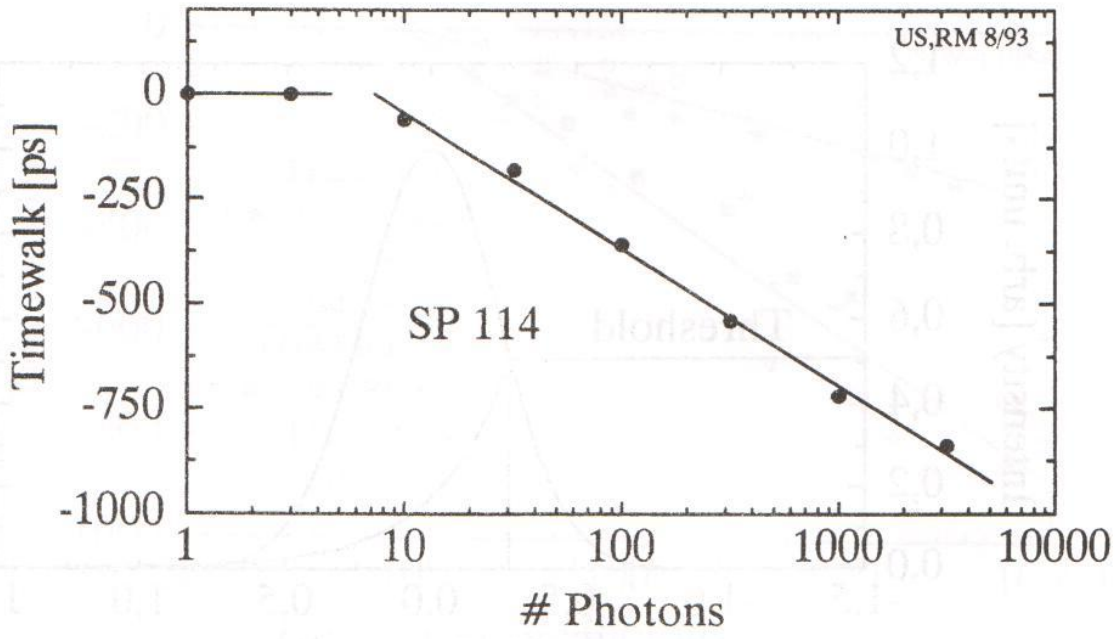

Figure 2: The dependency of the recorded time of flight of a laser pulse over a constant path. The intensity of the laser pulse was varied over a broad region. The detector is an avalanche diode

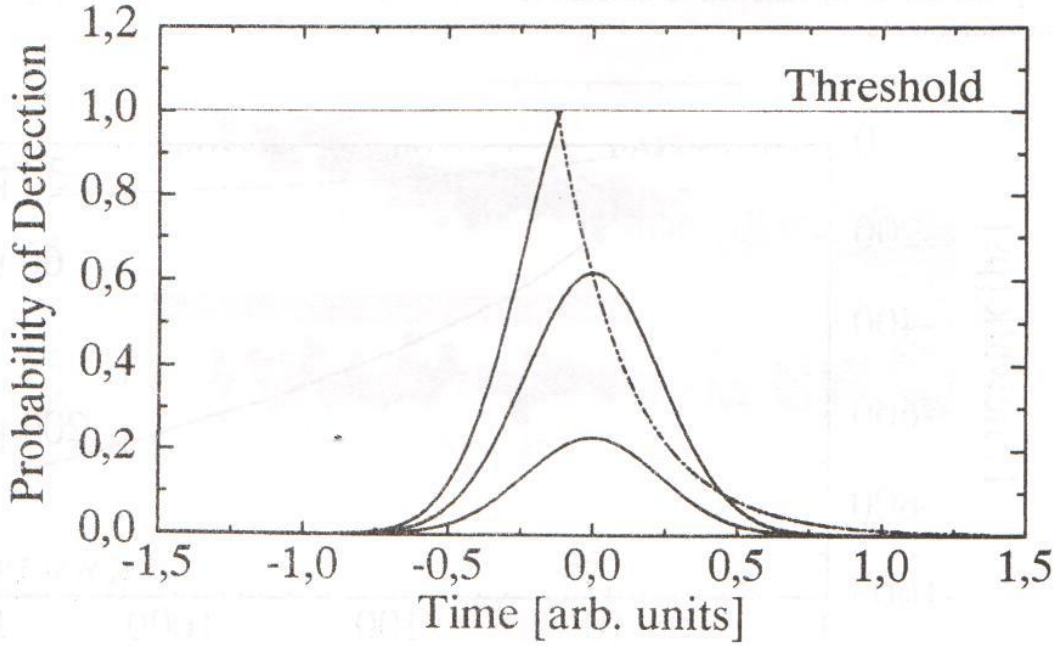

Figure 3: An illustration of the distribution of repeated range measurements for two characteristic situations. For pulse amplitudes well below the detection threshold no bias is observed. The data rate is directly proportional to the light intensity. For pulses exceeding the treshold an asymmetry in the shape of the histogram is obtained, as well as a bias for the range

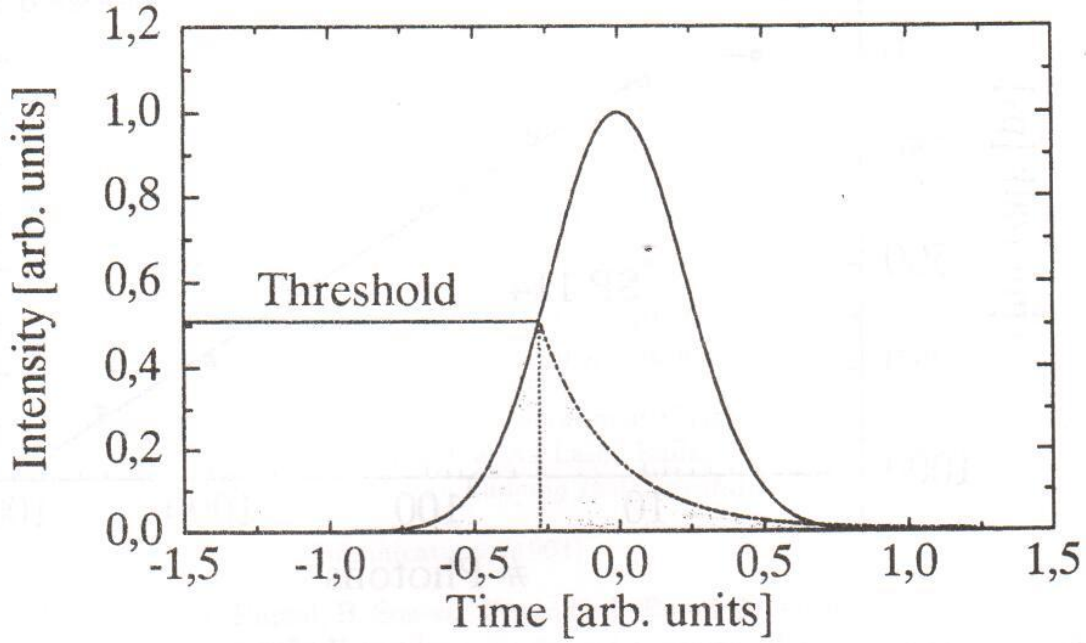

Figure 4: The shape of the modeled histogram for pulses at intensities high above the detection threshold. The falling edge of the histogram (shaded area) is represented by an exponential decay function to account for the observed skewness in the histograms of real measurements

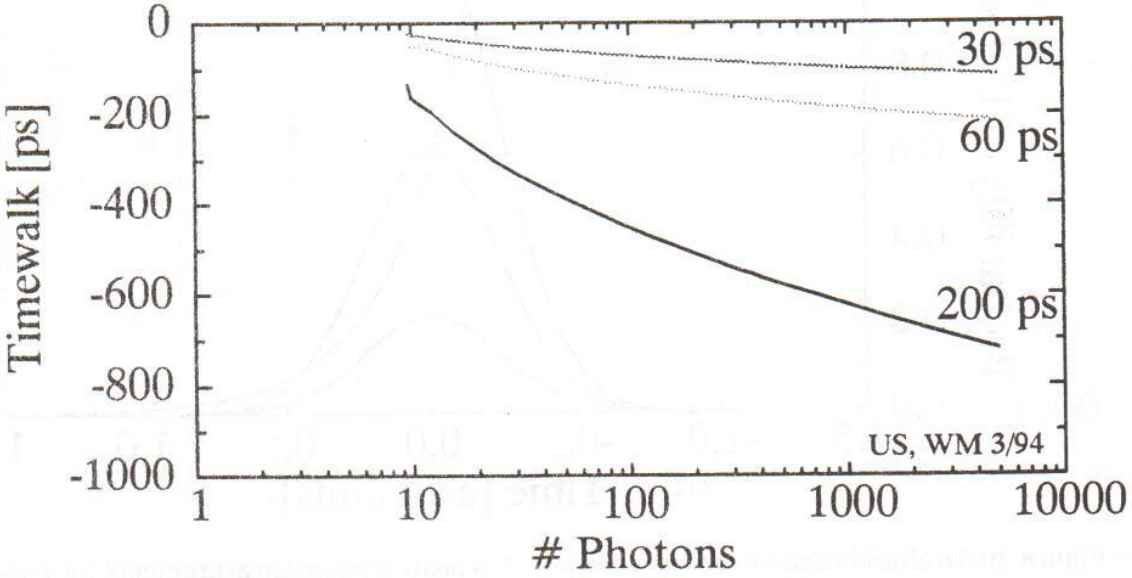

Figure 5: The calculated timewalk for some laser pulses of different length, according to the proposed model

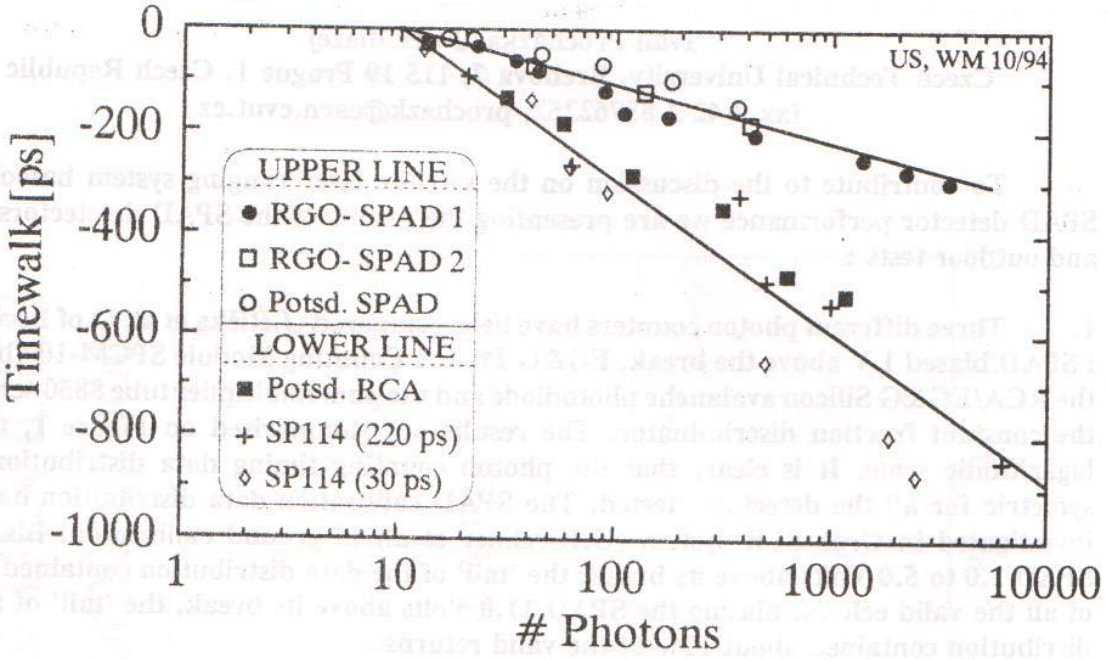

Figure 6: The measured timewalk for some avalanche photo diodes of different structure and with different lasers. One can see, that the obtained bias is depending on the type of diode, rather than the pulse width of the used laser

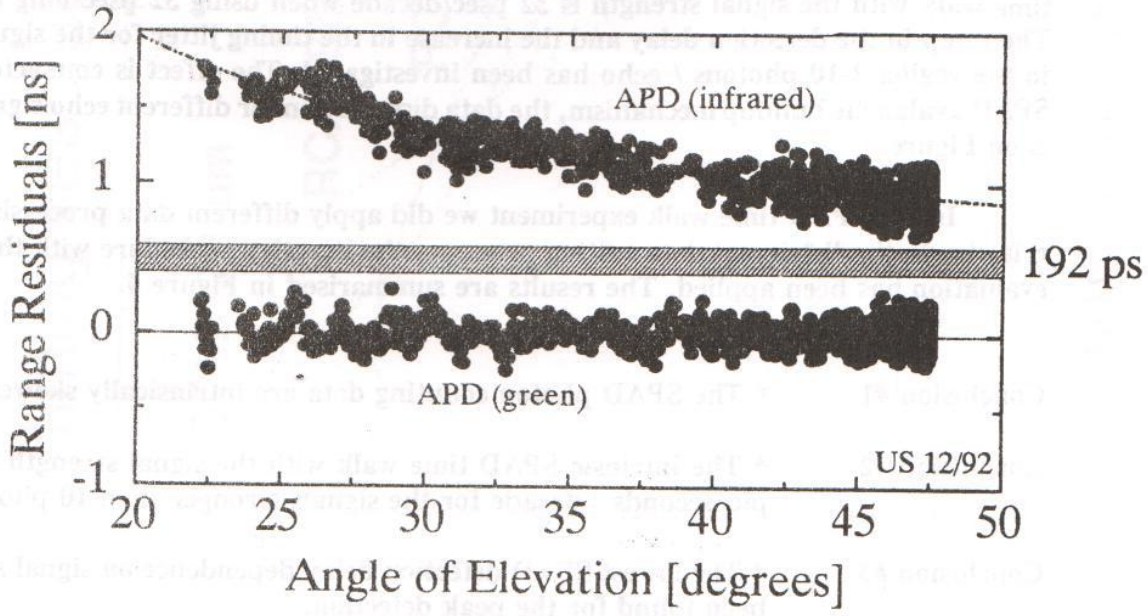

Figure 7: The residual plot of a satellite pass (LAGEOS), tracked simultaneously on two frequencies ($\lambda_1 = 0.532\mu m$ and $\lambda_2 = 1.06\mu m$. The difference in range is due to atmospheric dispersion. However there is a constant deficit of 200 ps in this seperation. This illustrates the frequency dependence of the multiplication process in the avalanche diode.

SPAD FOR LASER RANGING
Comments on detector effects

Ivan Procházka, Josef Blažej
Czech Technical University, Brehova 7, 115 19 Prague 1, Czech Republic
fax +42 2 85762252, prochazk@earn.cvut.cz

To contribute to the discussion on the satellite laser ranging system based on the SPAD detector performance we are presenting the results of the SPAD detetectors indoor and outdoor tests :

1. Three different photon counters have been compared (J.Říčka et al, U.of Bern, 1991) : SPAD biased 1 V above the break, EG&G Photon Counting Module SPCM-100 based on the RCA/EG&G Silicon avalanche photodiode and the photomultiplier tube 8850 series with the constant fraction discriminator. The results are summarised on Figure 1, note the logarithmic scale. It is clear, that the photon counting timing data distribution is not symetric for all the detectors tested. The SPAD calibration data distribution have been investigated in Graz SLR system (G.Kirchner et al) in ground calibration. Biasing the SPAD 1.0 to 5.0 Volts above its break, the 'tail' of the data distribution contained 22-23% of all the valid echoes, biasing the SPAD 11.0 Volts above its break, the 'tail' of the data disribution contained about 12% of the valid returns.

2. Exploiting the Hamamatsu picosecond laser diode pulser as a signal source and the Time to Amplitude Converter (TAC) and the Pulse Height Analyser PC card as a timing system, we have been investigating the SPAD time walk with the echo signal strength. The results are summarised on Figure 2, raw data (peak detection) are displayed. The SPAD time walk with the signal strength is 32 psec/decade when using 32 psec long laser pulse. The jump in the detection delay and the increase in the timing jitter for the signal strength in the region 2-10 photons / echo has been investigated. The effect is connected with the SPAD avalanche buildup mechanism, the data distribution for different echo signal strength is on Figure 3.

3. In the SPAD time walk experiment we did apply different data processing / editing criteria. In the 'k*sigma' data editing processes the iterative procedure with the sigma re-evaluation has been applied. The results are summarised in Figure 4.

Conclusion #1	* The SPAD photon counting data are intrinsically skewed.
Conclusion #2	* The intrinsic SPAD time walk with the signal strength is below 32 picoseconds / decade for the signals stronger than 10 photons/echo.
Conclusion #3	* The lowest SPAD detection delay dependence on signal strength has been found for the peak detection.

PHOTON COUNTING DEVICES
timing resolution comparison

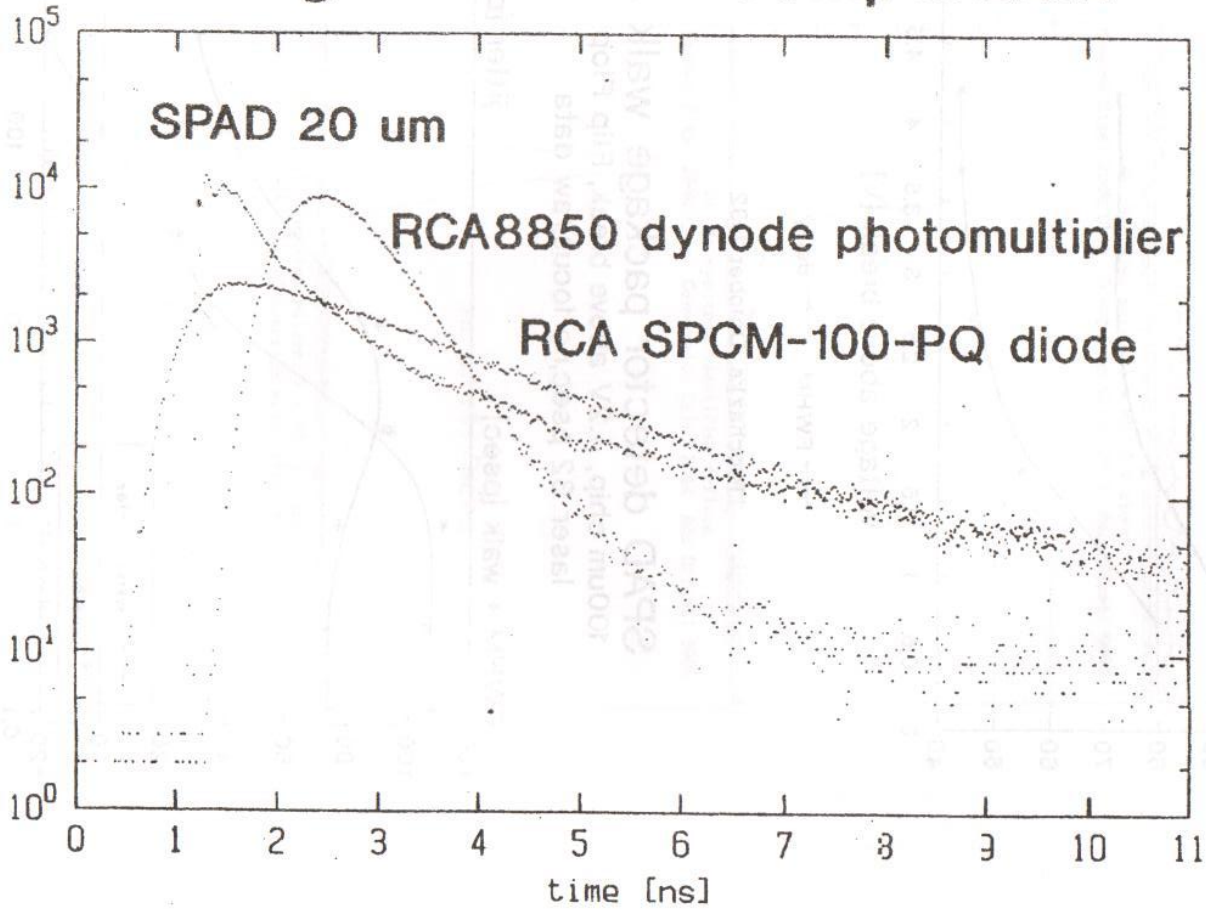

J.Ricka,M.Hoebel,I.Prochazka, U of Bern, May 1991

Figure 1

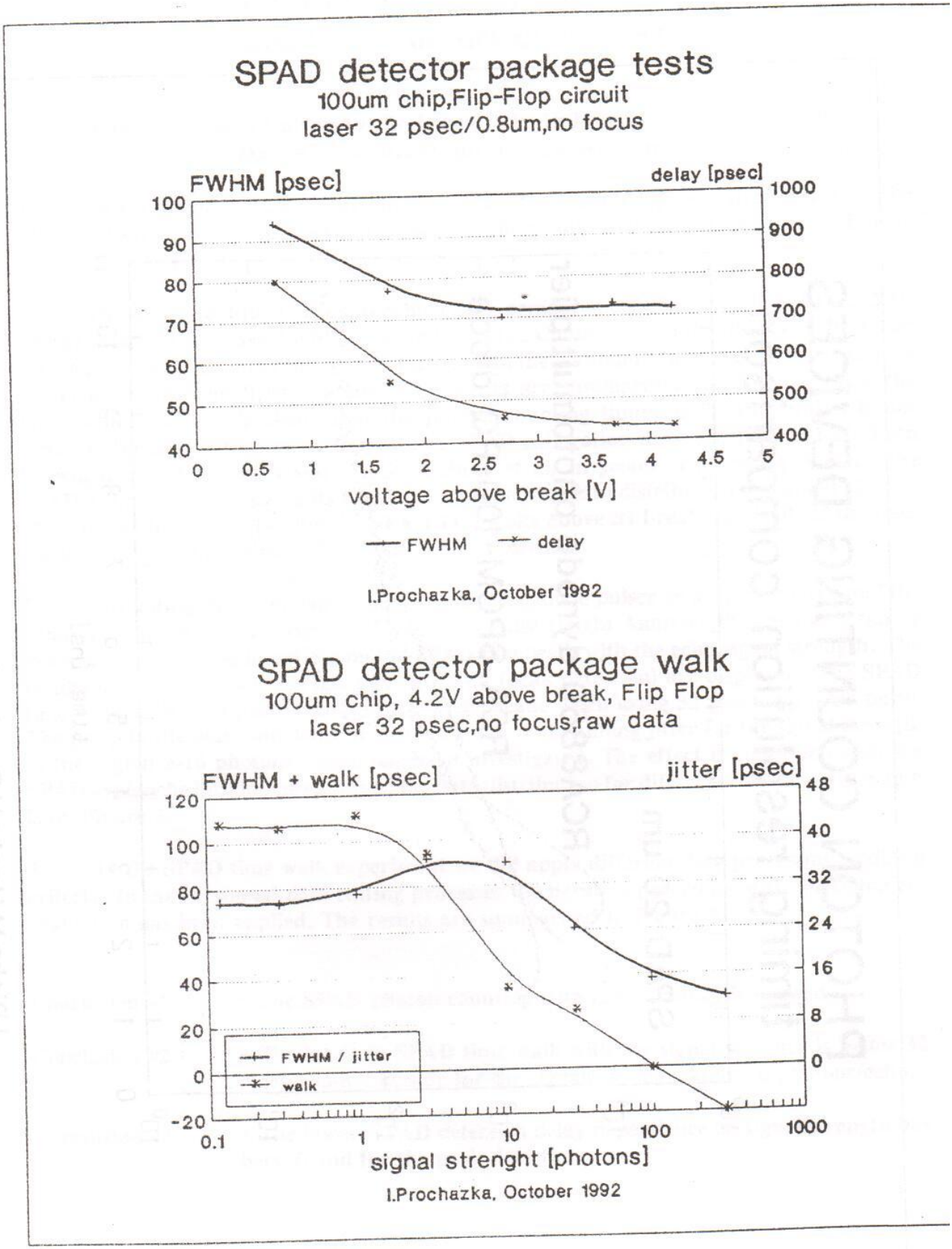
SPAD detector package tests
100um chip,Flip-Flop circuit
laser 32 psec/0.8um,no focus
FWHM [psec]
delay [psec]
100
90
80
70
60
50
40
1000
900
800
700
600
500
400
0
0.5
1
1.5
2
2.5
3
3.5
4
4.5
5
voltage above break [V]
FWHM
delay
I.Prochazka, October 1992
SPAD detector package walk
100um chip, 4.2V above break, Flip Flop
laser 32 psec,no focus,raw data
FWHM + walk [psec]
jitter [psec]
120
100
80
60
40
20
0
-20
48
40
32
24
16
8
0
FWHM / jitter
walk
0.1
1
10
100
1000
signal strenght [photons]
I.Prochazka, October 1992

Figure 2

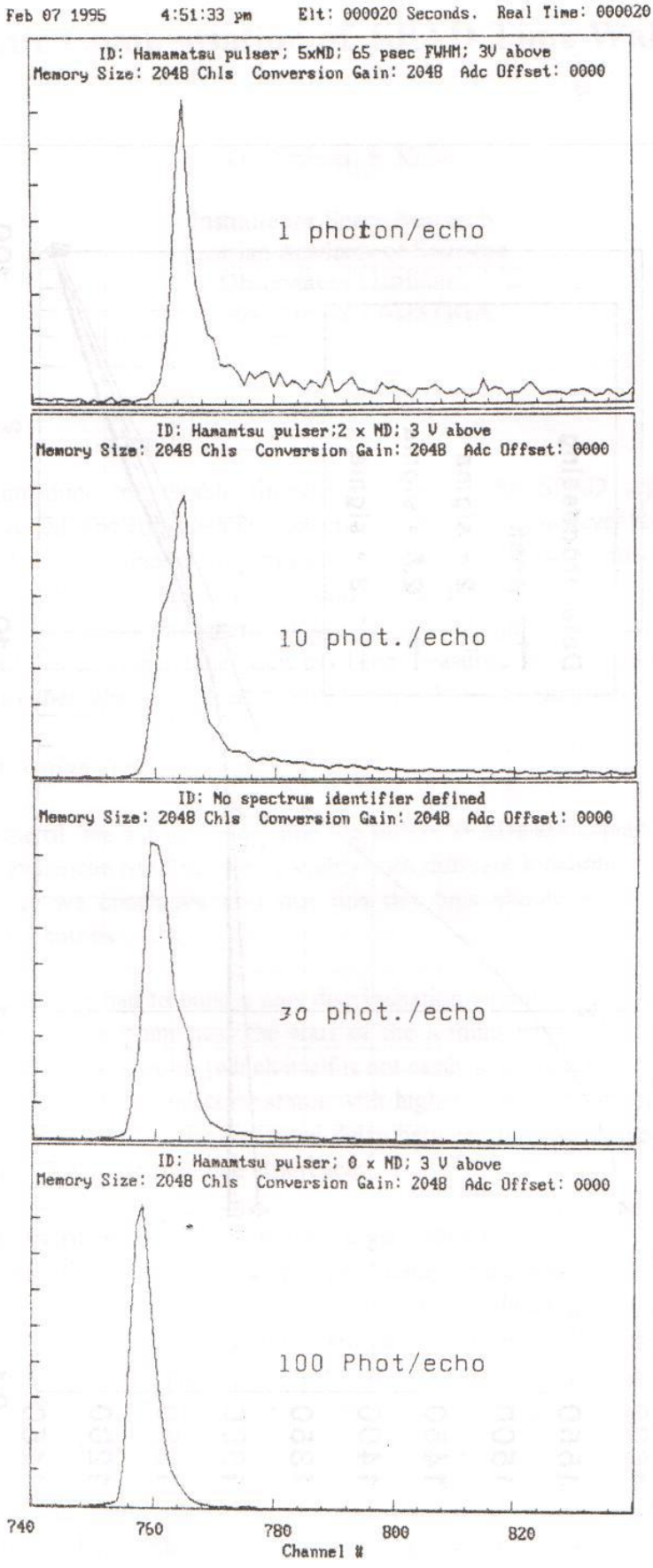
Feb 07 1995 4:51:33 pm Elt: 000020 Seconds. Real Time: 000020
ID: Hamamatsu pulser; 5xND; 65 psec FWHM; 3V above
Memory Size: 2048 Chls Conversion Gain: 2048 Adc Offset: 0000
1 photon/echo
ID: Hamamtsu pulser;2 x ND; 3 V above
Memory Size: 2048 Chls Conversion Gain: 2048 Adc Offset: 0000
10 phot./echo
ID: No spectrum identifier defined
Memory Size: 2048 Chls Conversion Gain: 2048 Adc Offset: 0000
30 phot./echo
ID: Hamamtsu pulser; 0 x ND; 3 V above
Memory Size: 2048 Chls Conversion Gain: 2048 Adc Offset: 0000
100 Phot/echo
740
760
780
800
820
Channel #

Figure 3

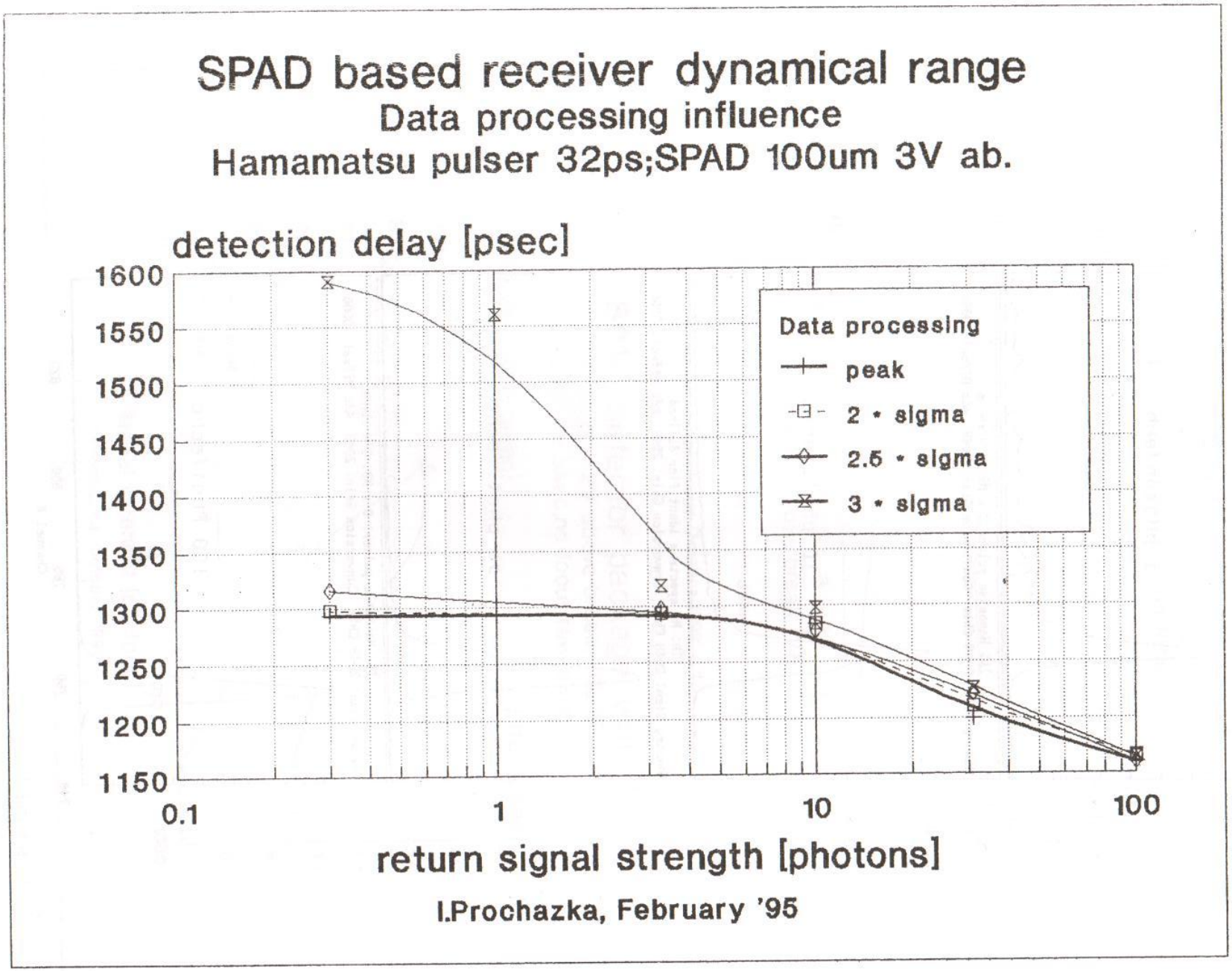
SPAD based receiver dynamical range
Data processing influence
Hamamatsu pulser 32ps;SPAD 100um 3V ab.
detection delay [psec]
1600
1550
1500
1450
1400
1350
1300
1250
1200
1150
0.1
1
10
100
Data processing
peak
2 * sigma
2.5 * sigma
3 * sigma
return signal strength [photons]
I.Prochazka, February '95

Figure 4

Automatic Compensation of SPAD Time Walk Effects

G. Kirchner, F. Koidl

Institute for Space Research
Austrian Academy of Sciences
Observatory Lustbühel
A-8042 GRAZ / AUSTRIA

1.0 Introduction

SPADs introduce measurable timewalk effects if the SPAD input energy is not sufficiently controlled, and considerably exceeds the Single-Photon-Level [1]; this effect mainly depends on SPAD type, amount of input energy, and laser pulse width; for the Graz SLR system (Czech SPAD, 35-ps-laser, few mJ only in SemiTrain) the worst case time walk can reach up to e.g. 12 mm (80 ps) from ERS-1 (with too high input energy); ranging to the calibration target, even higher time walk has been measured, due to higher received energy available. In this experiment, we tested received energy levels causing time walks up to 200 ps.

2.0 Measuring Avalanche Rise Time Differences

In [2], some of the avalanche dynamics in silicon SPADs are explained; as a result, it is shown that the avalanche rise time varies slighty with different locations of the avalanche seed point; in addition, we concluded also that this rise time should vary again with different numbers of input photons.

To verify this, we had to build a new discrimination circuit; usually, a fast comparator is used to trigger on some point near the start of the leading edge (about 10% of maximum amplitude) of the avalanche pulse (which itself is not easily accessible); to measure any changes in rise time, we added a second comparator with higher threshold (about 90% of maximum amplitude). Any differences in the measured delay between the two comparators thus should be proportional to avalanche rise time differences.

With this discriminator, series of test target calibrations were measured; energy was varied from Single Photon Level, to a level producing a time walk of up to 200 ps (fig.1a); received energy was estimated using SemiTrain presence (indicating SPE-Level, right part) or Pre-Pulse presence (indicating strong signal, left part; produced by Pockels Cell leakage in the laser, which has a specified contrast ratio of ≥500:1). After removing SemiTrain, Pre-Pulses and noise, a time walk of -170 ps is clearly visible (Fig. 1b); the granularity is caused by the 20-ps-resolution of the HP5370A counter.

Using a second counter, we measured also the delays between the two comparators; it was found that this delay changed by roughly 20 ps within this energy range, indicating a corresponding change of SPAD rise time.

3.0 Time Walk Compensation

Assuming a linear connection between rise time changes and time walk effect, we tried to use this rise time changes directly in the discriminator for adjustable, automatic time walk compensation; a few different ideas for such circuits were implemented and tested (and all of them are still in test phase!); these circuits all deliver a single output pulse, which is fully time walk compensated, and where the compensation can be adjusted to or near „Zero Time Walk".

First test calibrations, with only roughly adjusted time walk compensation circuits, using same parameters as in Fig. 1, showed a remaining time walk of only +19 ps (Fig. 2a, 2b), indicating a slight over-compensation; „Zero" time walk should be obtainable with better adjustment or an easier adjustable new discriminator circuit (which is in development now).

Just to demonstrate adjustability, another measurement was recorded with high over-compensation of time walk (Fig. 3a, 3b), resulting in a +470 ps time walk (compare the „real" time walk of -170 ps!).

4.0 Conclusion

Our first tests are promising; we expect that it should be possible to build and to adjust a discriminator circuit which should automatically compensate - at least to a large amount - any time walk effects which also produce a change in the avalanche rise time; however, some cautious remarks should be noted:

- All circuits are still in test phase; none of them is used in routine operation up to now;
- Adjustment of time walk compensation is critical and time consuming;
- 1 ps of rise time change is „translated" into 10 ps shift of avalanche pulse timing;
- Any jitter in rise time change detection therefore is also „translated" into a tenfold timing jitter;
- This scheme intrinsically contains potential error sources, and requires careful design and tests of ciruits;

Finally, it reminds us somehow on the Constant Fraction Discriminators - which we stopped operating in 1989 (and we were quite happy to do that!) - and their critical adjustments; maybe that just the scale of the adjustments has changed now to the 1-ps-level ...

References:

[1] Determination of Satellite Signatures and Time Walk Effects in Graz. G. Kirchner, F. Koidl; 9th International Workshop on Laser Ranging Instrumentation, Canberra, 1994; Proceedings.

[2] Tracking Capabilities of SPADs for Laser Ranging. Cova et al.; 8th International Workshop on Laser Ranging Instrumentation, Annapolis, 1992

SPAD TIME WALK: Target Calibrations

NO COMPENSATION

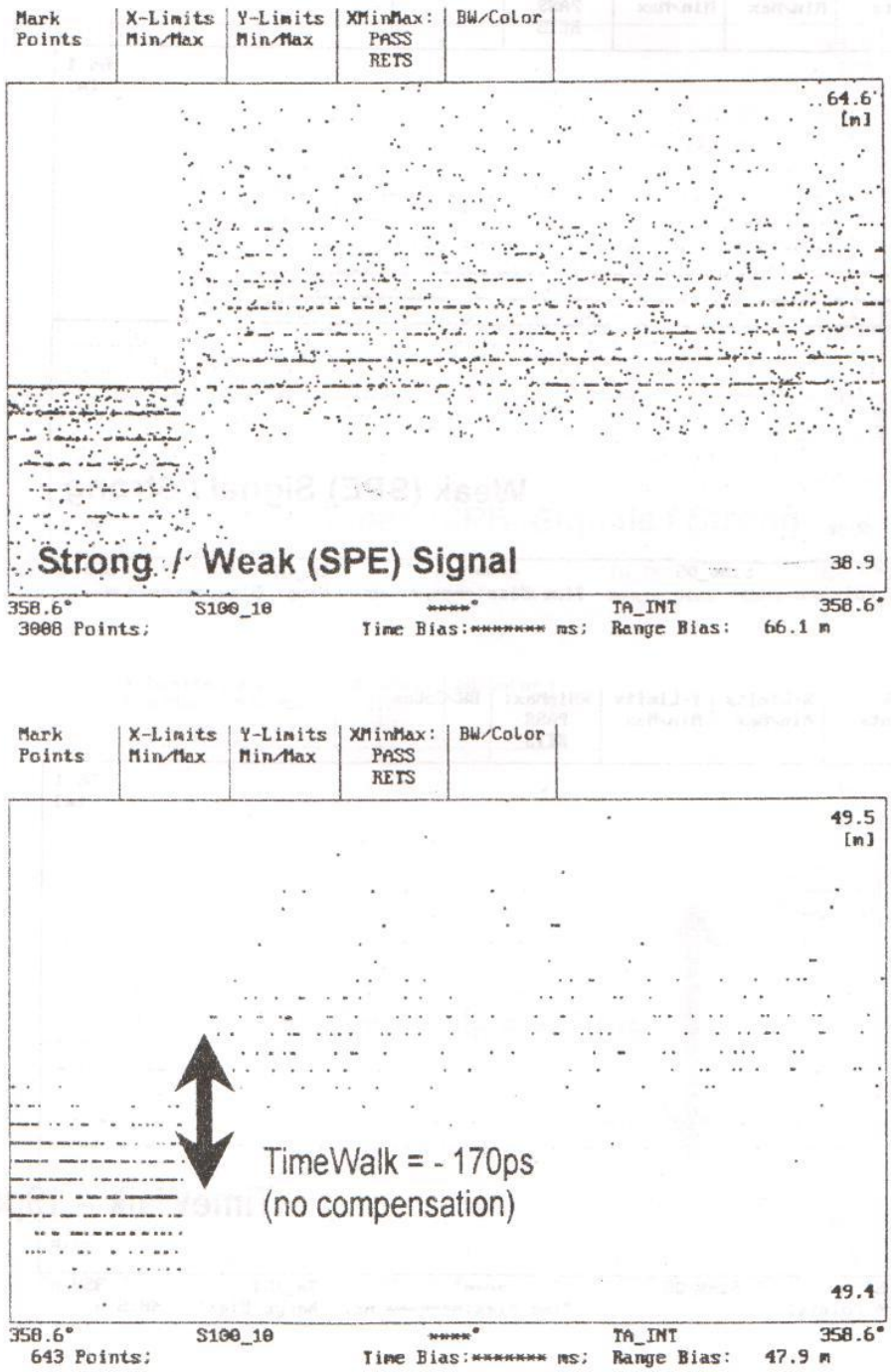

Fig.1: NO Compensation; -170 ps time walk from target

SPAD TIME WALK: Target Calibrations

WITH COMPENSATION

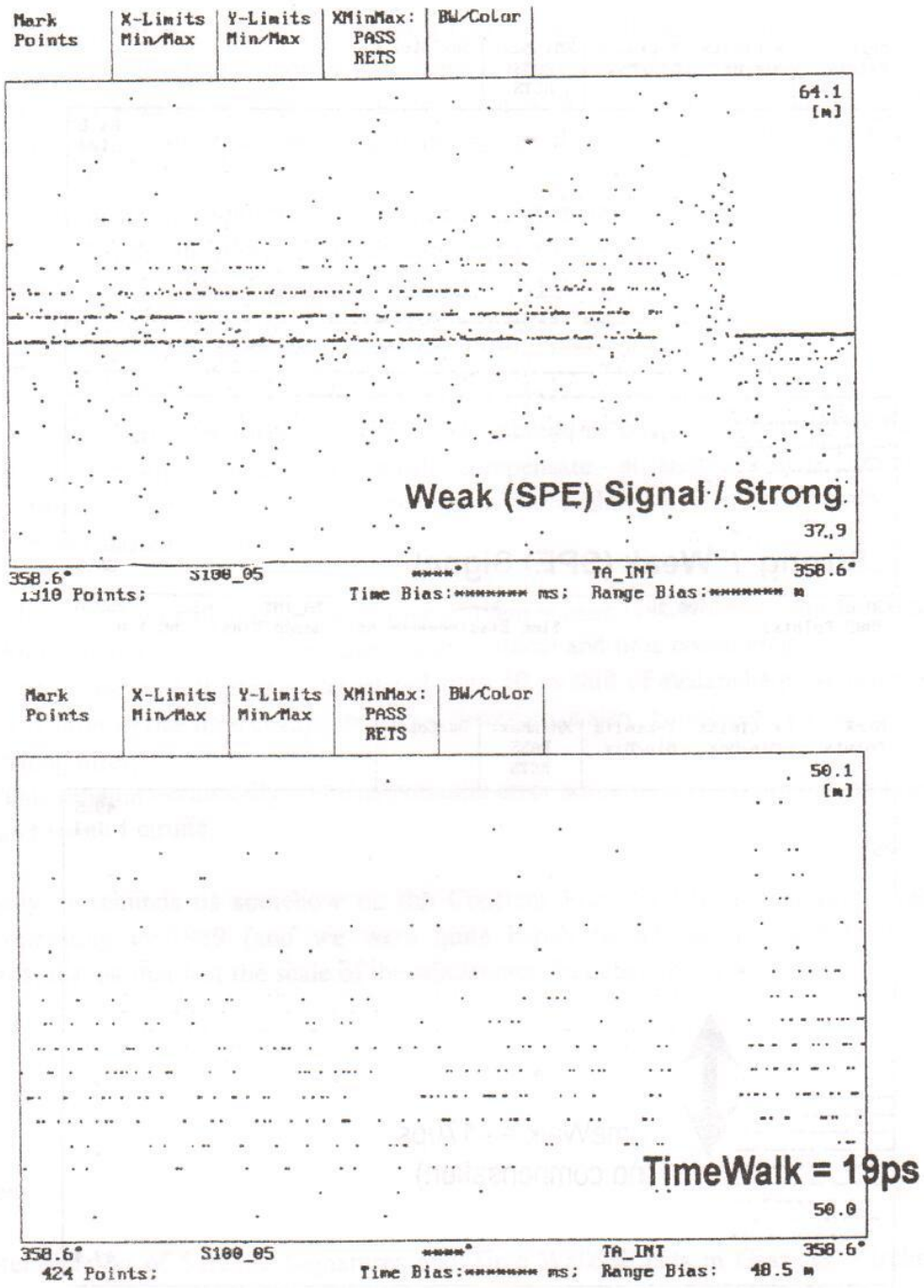

Fig.2: WITH Compensation; +19 ps time walk remaining

SPAD TIME WALK: Target Calibrations

Over - Compensation

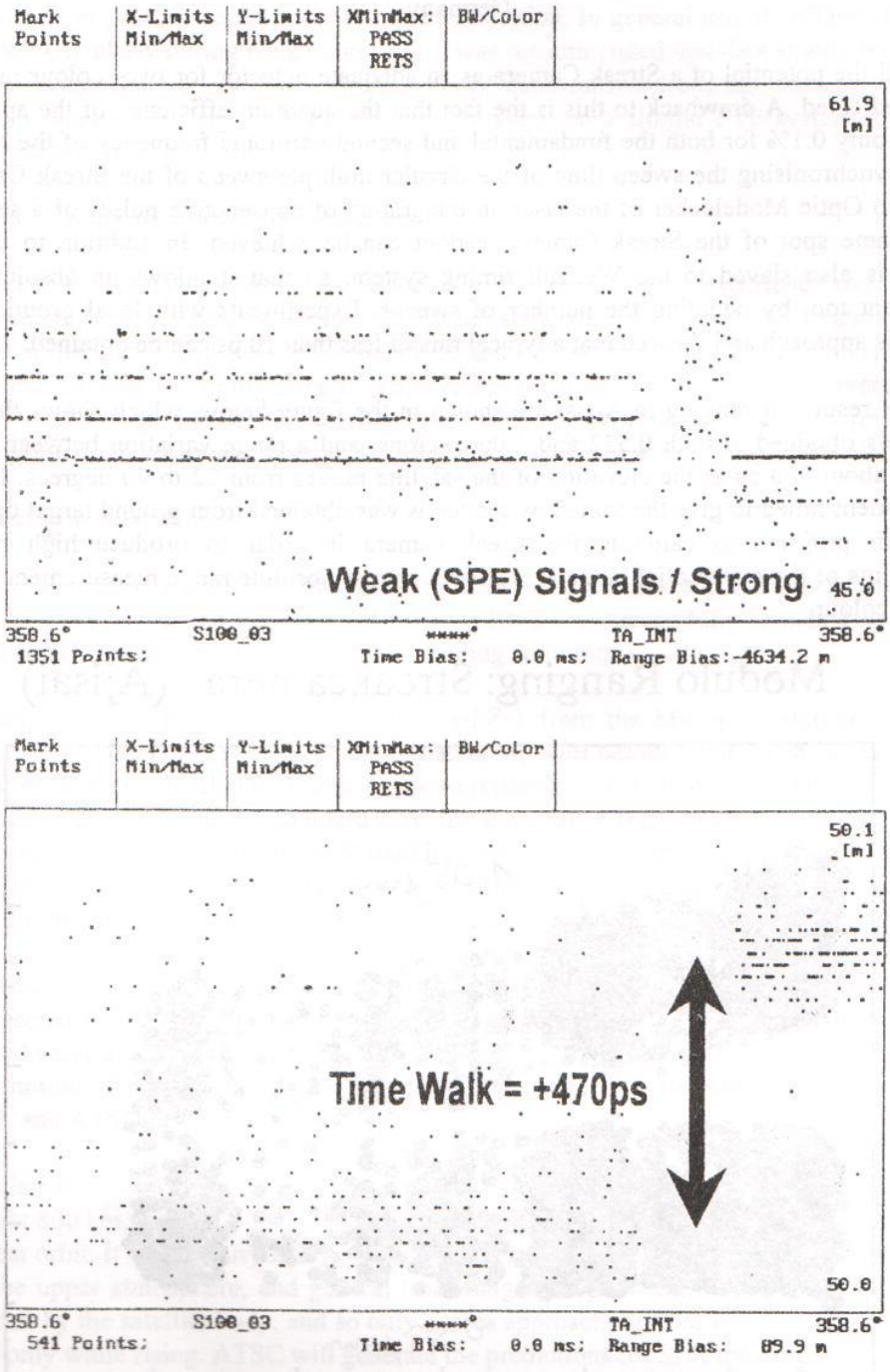

Fig.3: OVER-Compensation; +470 ps time walk from target

Two colour ranging to Ajisai using a Streak Camera detector

Stephan Riepl
Forschungseinrichtung Satellitengeodäsie
Fundamentalstation Wettzell
D-93444 Kötzting
Germany

At Wettzell the potential of a Streak Camera as an adequate detector for two- colour ranging is being investigated. A drawback to this is the fact that the quantum efficiency of the applied S1 cathode is only 0.1% for both the fundamental and second harmonic frequency of the Nd:YAG laser. By synchronising the sweep time of the circular multiple sweep of the Streak Camera to the Acousto Optic Modelocker of the laser an integration of consecutive pulses of a semi train onto the same spot of the Streak Camera readout can be achieved. In addition to that, this frequency is also slaved to the Wettzell timing system, so that it allows an absolute range measurement too, by counting the number of sweeps. Experiments with local ground targets verified this approach and showed that a typical rms of less than 10 ps can be obtained.

Some early results of ranging to Ajisai are shown in the figure below, which shows the strong return levels obtained at both 0.532 and 1.06 microns, and a range variation between the two colours of about 800 ps as the elevation of the satellite moves from 22 to 70 degrees. However this experiment failed to give the same low scatter as was obtained from ground target operation. Work is in progress to calibrate the streak camera in order to produce high precision measurements of the differential range as well as a precise absolute range measurement for each individual colour.

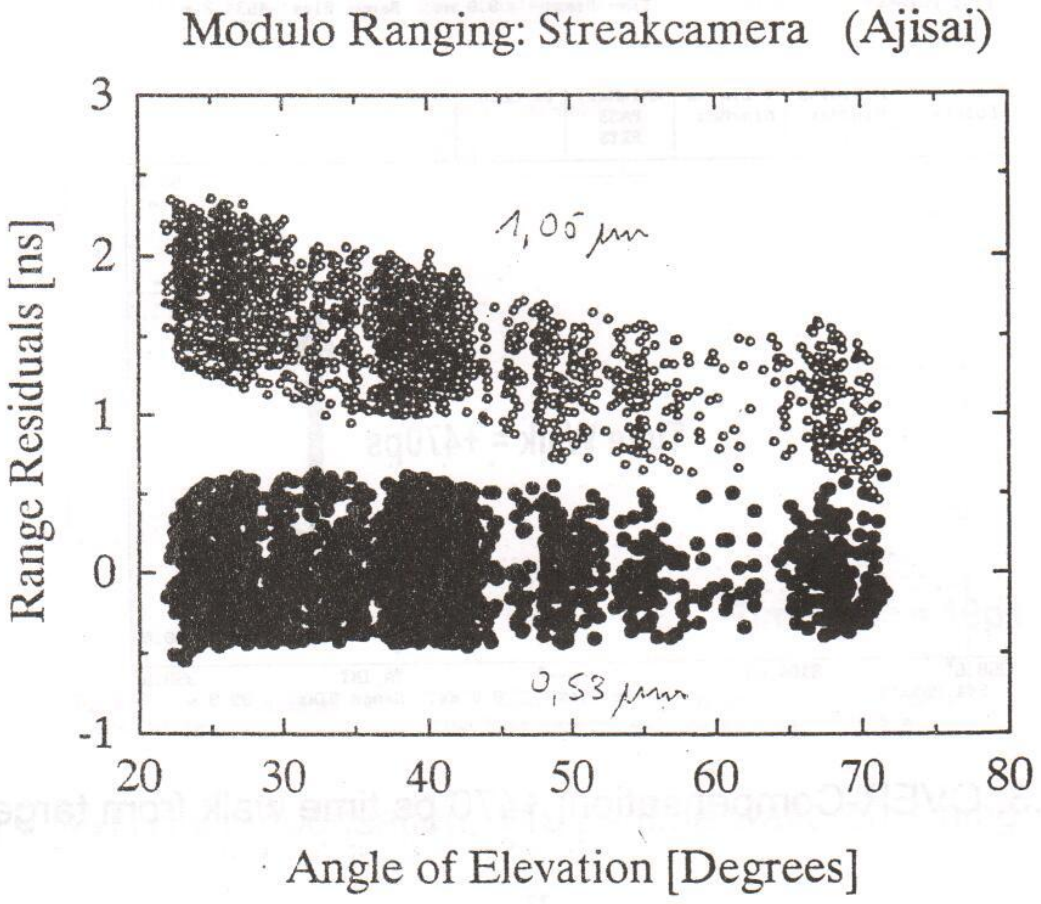

Report on the formal session at the EUROLAS meeting.

Report from the Eurolas Data Centre (EDC)

Seemueller reported that the EDC is expanding its FTP capability to facilitate data transfer to the EDC and to provide access to station documentation. In general use of INTERNET can be very slow, particularly during peak hours, and it was recommended that data should be sent during off peak hours. There continue to be problems of data transfer from the Russian stations to EDC. Bianco mentioned that at Matera they are working on a similar FTP system to access system documentation.

Report from quick-look analysis centre

Noomen reviewed the DUT data processing system and their experience over the past year. Items planned for enhancement of their analysis system are: improved treatment of the earth rotation parameters, increased frequency of analysis, more refined force models (JGM-3, ocean loading, etc.), and working directly with normal equations instead of direct inversion. At present the standard quick look analysis using 10 day arcs obtains typically 2 to 3 cm rms of fit, and can detect range biases greater than about 8 cm and time biases greater than about 40 microsec.

Status of new satellites

Massmann gave a report on the status of tracking of ERS-1 and Meteor-3, and plans for the launch and commissioning phase of ERS-2. (ERS-2 was successfully launched on 21st April, and SLR tracking has commenced and is proceeding smoothly.)

Koenig reported plans for the launch of GFZ-1 from the Mir space-station, and plans for a campaign of angular position measurements of Mir before the launch. Chen described the Fourier series model that they plan to use to represent the daily error of the IRV orbit due to the lack of a drag term in the standard IRV force model. (GFZ-1 was successfully launched from Mir on 19th April, and initial SLR tracking coverage was very good. However when the passes moved into daytime tracking was lost, and not regained until the passes moved into night again, but during the scond passage through daytime the SLR tracking has been much more successful.)

Towsley (NRL) reported on the tether mission planned for mid 1996, consisting of two satellites connected by a 4 km tether, in order to study the dynamics of tethered systems. Each satellite would carry a retro-reflector. Additional terms would be needed to the IRVs in order to allow for the motion of either satellite about the common centre of mass. These would be considered by NRL and ATSC.

Sinclair reported on the plans for ADEOS, to be launched by the Japanese in February 1996, at height 800 km, inclination 98.6°, sun-synchronous (descending node at 10.30 local time), 41-day repeat orbit. It would carry a large open-structure retro-reflector, for use for pollution monitoring of the upper atmosphere, and general laser ranging experiments. The reflector would be partly hidden by the satellite body, and so only passes approaching from left of centre could be tracked, and only while rising. ATSC will generate the predictions for SLR tracking.

Proposal for the revision of full rate data deliveries

Seemueller reported on the proposal from NASA for the revision of full-rate data deliveries, which would require stations to send to the data centre one full-rate data file each day for each satellite, instead of the monthly files of data sent at present. This was accepted by the SLR stations present without enthusiasm but without demur. However this proposal is not regarded with any enthusiasm at all by the EDC, as it will involve a significant increase of effort and expense to handle the much increased number of files. Also NASA, as part of its cost reduction program, is considering the reduction and possibly the deletion of full-rate data activities, except for specialised requirements. Hence it is clear that this proposal is not acceptable as it stands and needs further consideration.

Interaction of global SLR networks

The potential reduction of NASA SLR activity had raised alarm within Eurolas and the Western Pacific Laser Tracking Network (WPLTN). Pearlman reported that a proposal to reduce personnel requirements and yet maintain almost all of the NASA station operations was being given favourable consideration by NASA. WPLTN had raised with Eurolas the question of whether these two networks could take on some of the burden of non-tracking activites at present carried out by NASA (e.g., predictions, data centre activity). It was agreed that there were some possibilities.

Status of INTAS proposal

The European Community is providing some funding to countries of the Former Soviet Union via the International Association for the Promotion of Cooperation with the Scientists from the Independent States of the former Soviet Union (INTAS). A Eurolas proposal for the partial support of some SLR stations in the FSU has been accepted by INTAS. The project will provide a modest level of support for the stations at Maidanak and Katsively, and will typically be sufficient for the purchase of a time interval counter, a GPS-time receiver, and a PC. It is expected that the project will get underway in August-September 1995, and run for two years.

Discussion of NASA proposal for revision of the Q/L normal point format

This session at the Eurolas meeting continued the discussion of the proposal presented by Van Husson at the Laser Ranging Instrumentation Workshop in Canberra (Nov 94) for a revision of the data format for station-formed normal points. The discussion at Canberra had run out of time.

The reasons why revision is considered necessary are:

1. To provide additional information on the statistical distribution of the raw data, in order to compensate for not having the full-rate data
2. To make provision for 2-colour ranging
3. To include extra information in order to permit correction for satellite signature
4. To accommodate wavelengths greater than 1 micrometre
5. To clarify the descriptions given in the present format of a few of the data quantities.
6. To give more information on the characteristics of the station during calibration ranging to a terrestrial target.

One of the main objectives in the design of the format was to maintain compatibility with the present format, so that with only minimal changes existing software could use both the old format and the new format. The new format should contain new information for the analyst who wishes to use it, but there should be no necessity to use the new information, as the present items in the format would remain unchanged.

A concensus viewpoint was reached by this Eurolas meeting of the desirability of these objectives and how they could be achieved, and subsequently a draft layout and specification of the format has been compiled by Sinclair, for examination by WPLTN and NASA, and eventual consideration by CSTG.

SLR Tracking to ERS−1, ERS−2 and METEOR−3/7

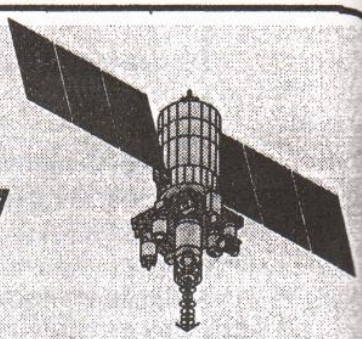

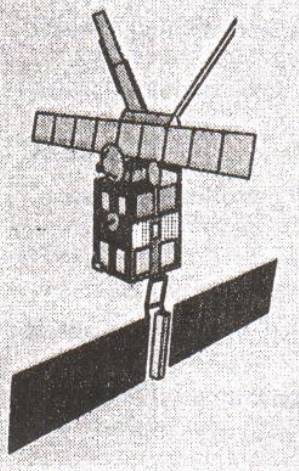

F.−H. Massmann

GeoForschungsZentrum Potsdam, Dept. 1,
German Processing and Archiving Facility (D−PAF),
Münchnerstr. 20, D−82230 Oberpfaffenhofen, Germany

GFZ
D−PAF

GEO FORSCHUNGS ZENTRUM POTSDAM

Status ERS−1, Meteor−3/7

- Both satellites are in an extremely good condition
- SLR tracking to both satellites is good
- Quality of orbit predictions is excellent
- Sometimes communication problems with China, Japan
- Still only 4 stations on the Southern hemisphere (out of about 25)

GFZ
D−PAF

Future ERS−1, Meteor−3/7

- Meteor−3 operations will continue,
  −> SLR tracking still necessary
- ERS−1
  - These days manoeuvre into 35d repeat orbit
  - After launch of ERS−2 intensive SLR tracking necessary (for three months) for ERS−2 RA cross calibration
  - (as of today) ERS−1 will be switched off after ERS−2 Commissioning Phase and stored in orbit
    −> no further SLR tracking required

Status ERS−2

- **Orbit:** 35d repeat cycle (as for ERS−1)
  one day offset to ERS−1
- **Launch date:** mid April 1995 (depending on todays Ariane launch)
  −> conflict with GFZ−1
- **Phases:**
  - Early Operations Phase: two days
  - First Payload Switch−on and Verification Phase: two weeks
  - Commissioning Phase: three months
  - Routine Operations: three years
- **GFZ/D−PAF:** same support as for ERS−1
  (IRVs, time bias functions, reports)

GEO FORSCHUNGS ZENTRUM POTSDAM

Acquired SLR Passes per Week (Q/L, ONP)

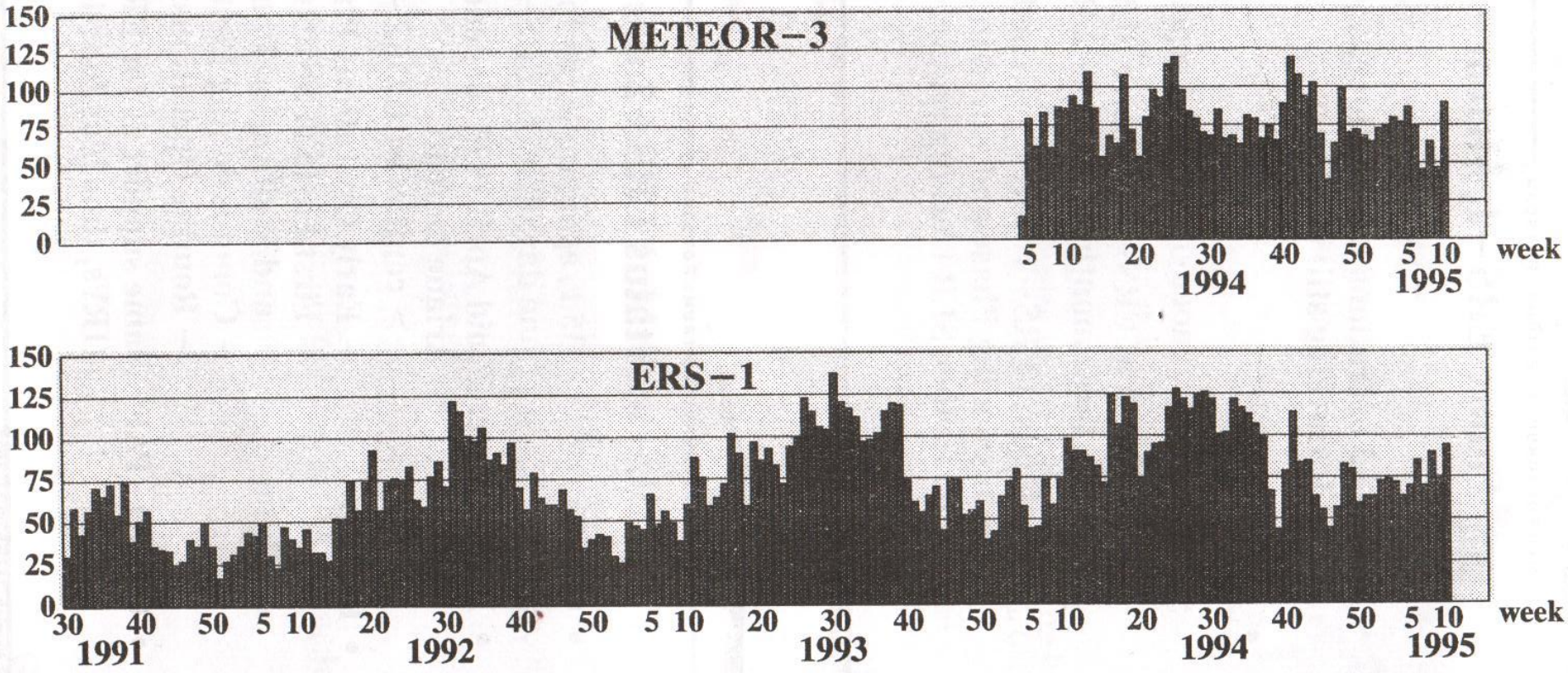

GFZ
D–PAF

Drag Function for GFZ−1 IRVs

Z. Chen R. Koenig

GeoForschungsZentrum Potsdam (GFZ)

German Processing and Archiving Facility for ERS (D−PAF)

D−82230 Oberpfaffenhofen, Germany

Introduction

Tuning of IRVs is a means to account for the missing drag model in the integration program at satellite tracking stations. For satellites at certain altitudes, e.g. ERS−1, Meteor−3, the tuning accuracy is sufficient for effective pointing. At the low altitudes of GFZ−1 the tuning process along does not provide the accuracy required, a drag function for GFZ−1 in support for tuned IRVs has been designed.

Drag Functions

1. Daily parabolic function: $y = a + b*t + c*t*t$ $\quad 0 < t \leq 1$
2. Mean parabolic function for the whole prediction period: $y = a + b*dt + c*dt*dt$ $\quad 0 < dt \leq 1$
3. Fourier function for the whole prediction period: $y = a + b*\sum_{k=1}^{kmax}(-1)^k \cos kx/k^2 + c*\sum_{k=1}^{kmax}(-1)^k \sin kx/k$, $x = 2\pi(t-0.5)$ $\quad 0 < t \leq N$

Function	Advantage(s)	Short Coming(s)
Daily parabolic function	simple function	required for each IRV, change of validity
Mean parabolic function	valid for the whole period	time axis has leaps
Fourier function	valid for the whole period, easy to use	(negligible) more computation time

Accuracy Comparisons			
	Function	σ_0 [ms]	V_{max} [ms]
pred_950214	Daily parabolic function	3.8 − 5.8	11 − 16
	Mean parabolic function	7.6	24
	Fourier function	7.6	23
pred_950223	Daily parabolic function	4.1 − 6.2	12−18
	Mean parabolic function	8.0	37
	Fourier function	8.0	34

Fourier Fitting Results

1. For low solar and geomagnetic activity:

$$drag(X) = B\sum_{k=1}^{k_{max}} (-1)^k \frac{\cos kX}{k^2} + C\sum_{k=1}^{k_{max}} (-1)^k \frac{\sin kX}{k}$$

Prediction Set	Max. Degree	B[ms]	C[ms]	σ_0[ms]	v_{max}[ms]
Pred_950214	3	35.4	1.1	7.8	27.
	6	35.4	1.1	7.6	23.
	10	35.4	1.1	7.6	24.
Pred_950223	3	45.3	1.6	8.4	34.
	6	45.3	1.6	8.0	34.
	10	45.3	1.5	8.0	36.
Pred_950306	3	76.6	2.4	9.5	49.
	6	76.6	2.4	8.6	39.
	10	76.6	2.4	8.4	35.

Recommendation: kmax = 6

2. For high solar and geomagnetic activity:
Recommendation: If the solar flux is high and the geomagnetic activity varies largely, application of more than one drag functions for one prediction period could become necessary. In addition, higher expansion degree should be used to improve the fitting results.

Conclusions

For GFZ−1 tracking a Drag Function to improve the accuracy of tuned IRVs is necessary.

The Fourier Function seems to be the best choice.

In case of low solar and geomagnetic activity, the Fourier drag function provides an accuracy of better than 10 ms.

In case of high solar and geomagnetic activity variations, more than one Fourier drag function could become necessary.

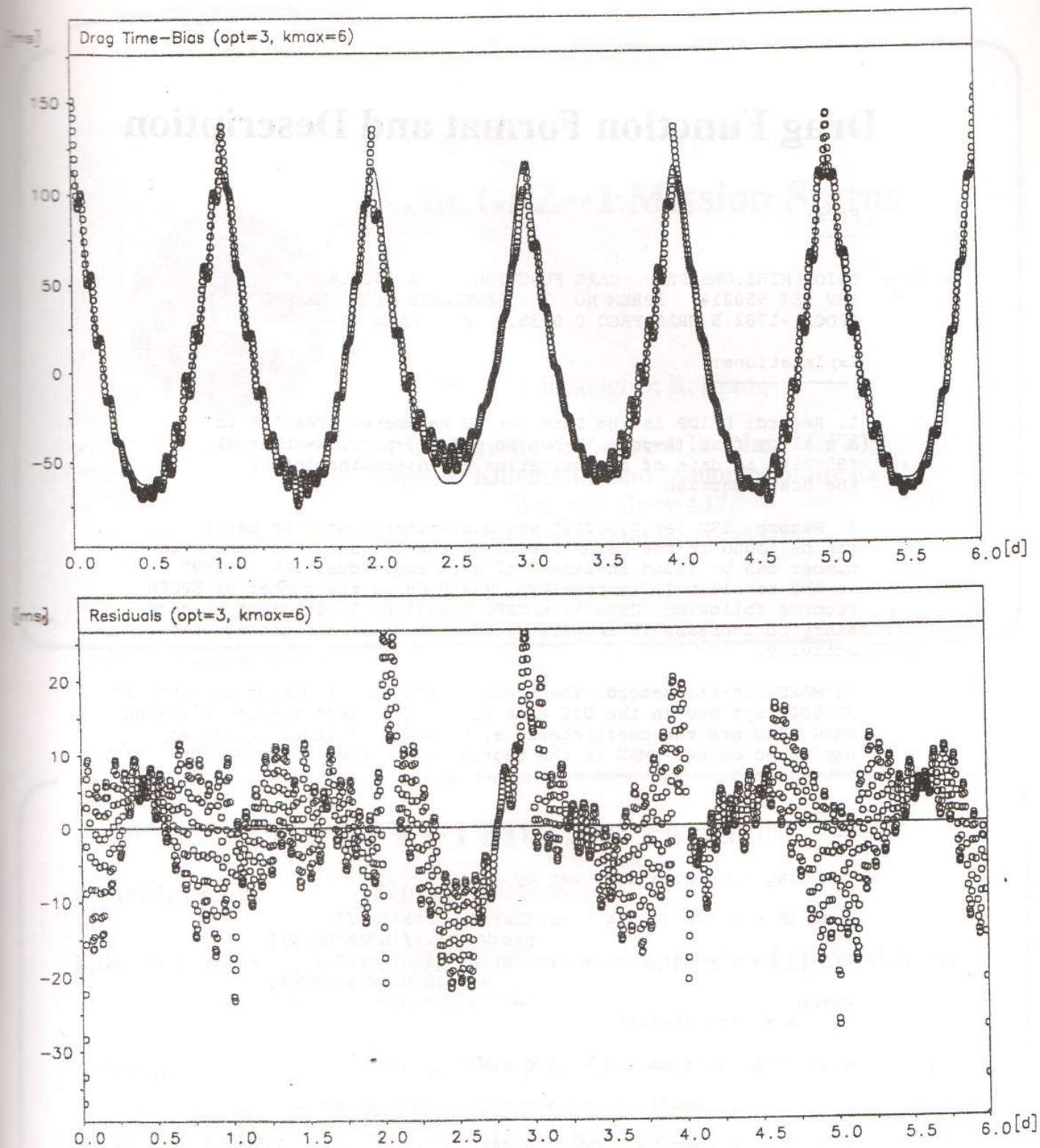

Mir. Along-track differences of IRV orbit from precise orbit, expressed as time bias.

(i) Before fitting a drag function

(ii) After fitting a drag function

Drag Function Format and Description

Form:

```
DSIDP MIR1.ORB.PRD   DRAG FUNCTION     A 950216
IRV SET 950214   EPHEM NO  7   SATELLITE 9999  MAXEPOCH  1
EPOCH -1782.5 DRAG FRCO 0.0 35.0  0.1  NMAX  3
```

Explanations:
---

1. Record: DSIDP is the Data Set ID Parameter. The "A" is a quality flag (A=good, B=not so good, C=poor, X=unknown). "950216" is date of determination and dissemination of the drag function.

2. Record: IRV set "950214" was disseminated at that date; can be found in the DSIDP record of the IRV set. The ephemeris number can be found in line 3 of each individual IRV. "9999" is the satellit ID in the IRVs. MAXEPOCH is the number of EPOCH records following. Usually MAXEPOCH will be 1. It might be necessary to increase it in periods of high solar and geomagnetic activity.

3(+MAXEPOCH-1). Record: The EPOCH of the drag function is given in JD2000 days and in the UTC time scale. The coefficients following DRAG FRCO are the coefficients a, b and c of the drag TBF as explained below. NMAX is the degree of the Fourier expansion recommended.

Usage:

The drag time bias is given by

```
drag TB = a + b*[-cosx + cos(2x)/4 - cos(3x)/9 ...
                       +- cos(NMAX*x)/(NMAX*NMAX)]
          + c*[-sinx + sin(2x)/2 - sin(3x)/3 ...
                            +- sin(NMAX*x)/NMAX]
```

where

$$x = 2*pi*(t-0.5)$$

with drag TB in ms and t in d since epoch.

In above the coefficients are a=0.0, b=35.0, c=0.1

In order to compute a drag TB for February 16th, 1995,

```
 0:00 UTC = -1780.50 JD2000 = 49693 MJD  drag TB =  48 ms
 6:00 UTC = -1780.25                     drag TB =  -9 ms
12:00 UTC = -1780.00                     drag TB = -30 ms
18:00 UTC = -1779.75                     drag TB =  -9 ms
24:00 UTC = -1779.50                     drag TB =  48 ms
```

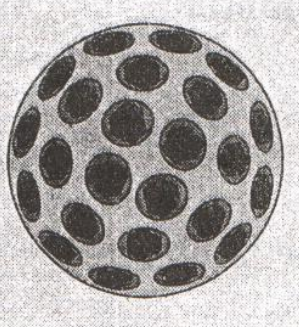

The GFZ–1 Mission Status

Ch. Reigber, R. König

GeoForschungsZentrum Potsdam (GFZ),
Dept. 1: Kinematics and Dynamics of the Earth,
Telegrafenberg A17,
14473 Potsdam, Germany

GFZ
D–PAF

Thei

The GFZ–1 Mission: Partners

Coordination	Kayser–Threde
Fabrication	RNIIKP (Russian institute of space device engineering)
Transport	RKK Energia (Russian space cooperation)
SLR Tracking	International SLR network
Radar Tracking	US Space Com (Accuracy 10–20 km) Russian anti–satellite radar (??) FGAN Bonn (??)
Data, voice, video	GSOC, ZUP

GFZ
D–PAF

The GFZ–1 Mission

Purpose:	**Improvement of gravity model** **Interest in atmospheric studies coming up**
Launch:	**April 5th: PROGRESS cargo to MIR** **April 19th: ejection from MIR** **April 22nd: 1st backup ejection date** **April 24th: 2nd backup ejection date**
Basic characteristics	**Diameter 215 mm** **Mass 20.5 kg** **CoM 58.2 mm**
Orbit	**Initial altitude 398 km** **Inclination 51.6 deg**

GFZ–1 Altitude Decay

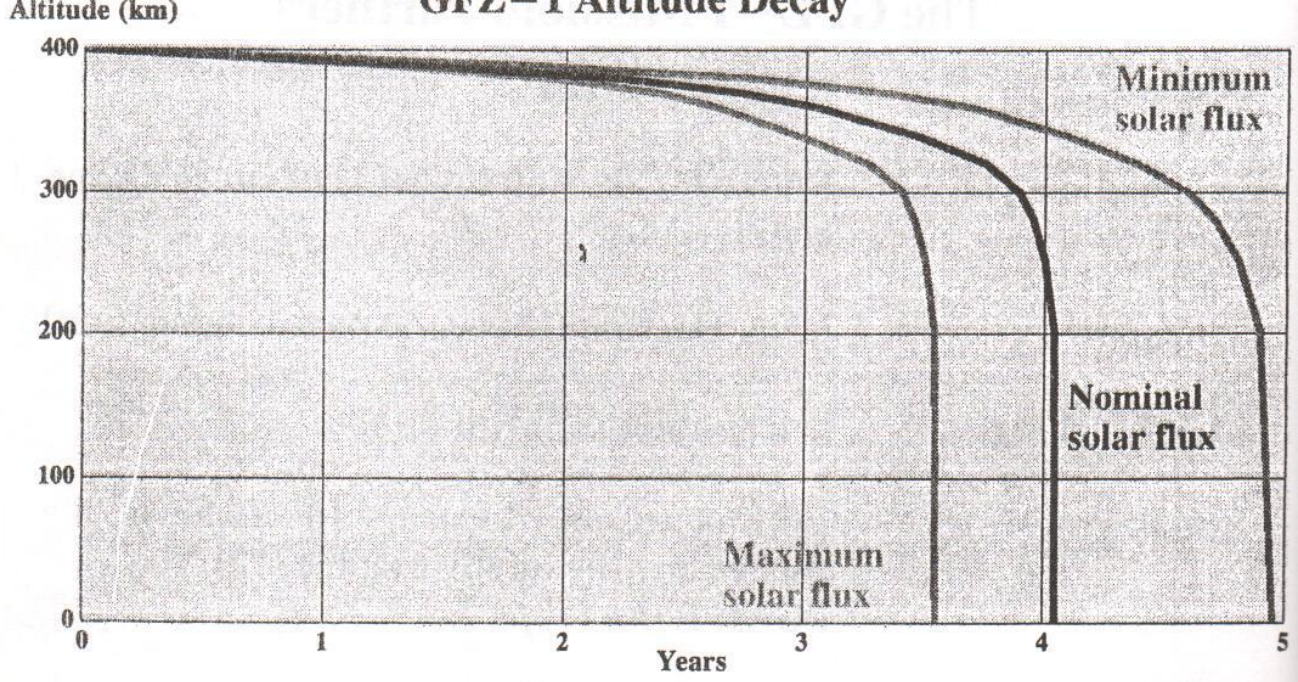

LIST OF PARTICIPANTS

Graham Appleby
Royal Greenwich Observatory
Madingley Road
Cambridge UK CB3 0EZ
United Kingdom
0044-1223 374737
0044-1223 374700
gma@ast.cam.ac.uk

Aldo Banni
Astronomical Observatory of Cagliari
Loc. Poggio dei Pini, strada 54
I-09012 Capoterra, Cagliari
Italien
0039-70-725246
0039-70-725425
banni@astca1.ca.astro.it od.
banni@vaxca2.unica.it

Francois Barlier
CERGA/GRGS, Observatoire de la Cote d'Azur
Avenue Nicolas Copernic
F-06130 Grasse
France
0033-93-365849
0033-93-368963
barlier@ocar01.obs-azur.fr

Richard Biancale
GRGS/CNES
18, av. Edouard-Belin
F-31055 Toulouse-Cedex
France
0033-61-33 29 78
0033-61-25 30 98
biancale@mfh.cnes.fr

Guiseppe Bianco
Agenzia Spaziale Italiana
Centro di Geodesia Spaziale
P.O. Box 155
I-75100 Matera
Italia
0039-835-339001
0039-835-339005
laser@asimt0.mt.asi.it od.
bianco@hp755.mt.asi.it

Zongping Chen
GeoForschungsZentrum Potsdam, (GFZ)
GFZ/DPAF c/o DLR
Postfach 11 16
82230 Wessling/Oberpfaffenhofen
Muenchner Str. 20
82234 Wessling
Deutschland
0049-8153-28-1391
0049-8153-28-1207
chen@dfd.dlr.de

Hermann Drewes
Deutsches Geodaetisches Forschungsinstitut, Abt.I
Marstallplatz 8
D-80539 Muenchen
Deutschland
0049-89-23031-106
0049-89-23031-240
mailer@dgfi.badw-muenchen.de

Dieter Egger
Technische Universitaet Muenchen,
Institut fuer Astronomische und Physikalische Geodaesie
Postfach
80290 Muenchen
Deutschland
0049-89-2105-3190
0049-89-2105-3178
dieter@alpha.fesg.tu-muenchen.de

The GFZ–1 Mission

Purpose:	Improvement of gravity model Interest in atmospheric studies coming up
Launch:	April 5th: PROGRESS cargo to MIR April 19th: ejection from MIR April 22nd: 1st backup ejection date April 24th: 2nd backup ejection date
Basic characteristics	Diameter 215 mm Mass 20.5 kg CoM 58.2 mm
Orbit	Initial altitude 398 km Inclination 51.6 deg

GFZ–1 Altitude Decay

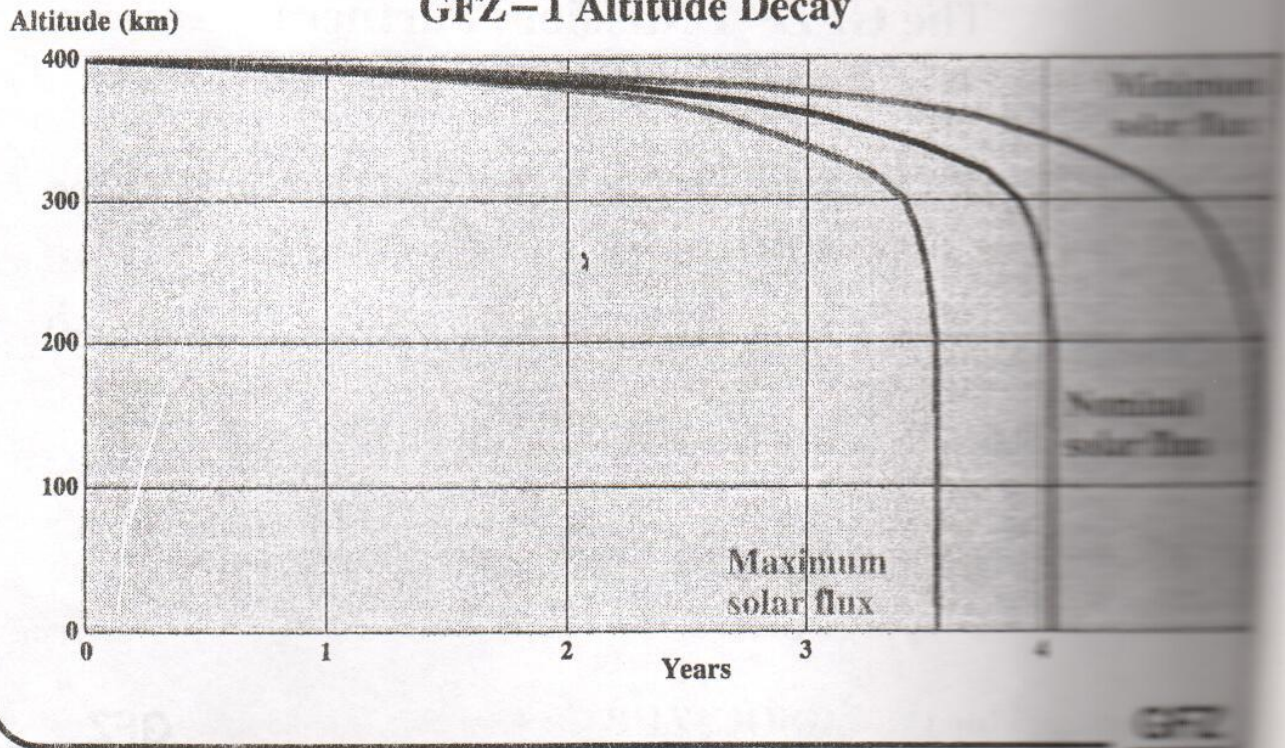

GEO FORSCHUNGS ZENTRUM POTSDAM

The GFZ–1 Mission

Purpose:	**Improvement of gravity model** **Interest in atmospheric studies coming up**
Launch:	**April 5th: PROGRESS cargo to MIR** **April 19th: ejection from MIR** **April 22nd: 1st backup ejection date** **April 24th: 2nd backup ejection date**
Basic characteristics	**Diameter 215 mm** **Mass 20.5 kg** **CoM 58.2 mm**
Orbit	**Initial altitude 398 km** **Inclination 51.6 deg**

GFZ
D–PAF

GFZ-1_Eurola

GEO FORSCHUNGS ZENTRUM POTSDAM

GFZ–1 Altitude Decay

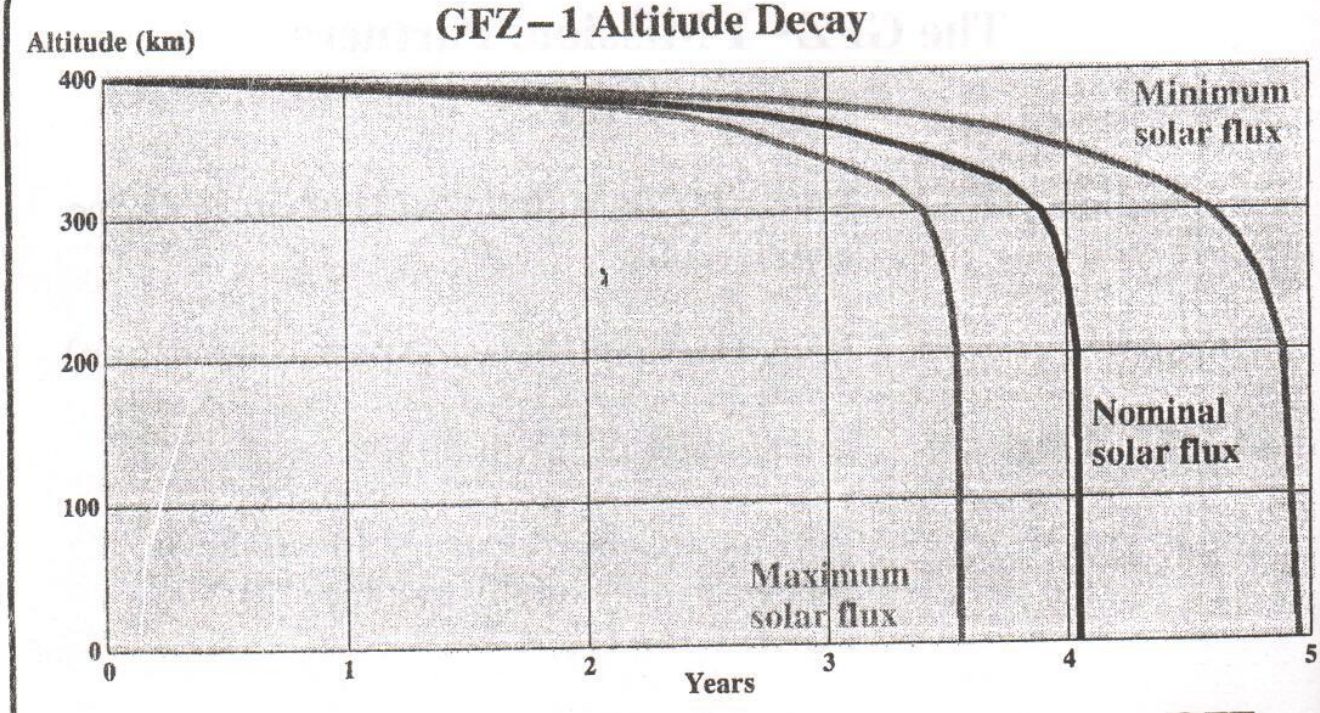

GFZ
D–PAF

Ludwig Grunwaldt
GeoForschungsZentrum Potsdam
Bereich 15
Postfach 60 07 51
14407 Potsdam
Haus 17, Telegrafenberg A17
14473 Potsdam
Deutschland
0049-331-288-1153
0049-331-288-1111
grun@gfz-potsdam.de

Werner Gurtner
Universitaet Bern
Astronomisches Institut
Sidlerstr. 5
CH-3012 Bern
Schweiz
0041-31-631-8591
0041-31-631 38 69
gurtner@aiub.unibe.ch od.
laser@aiub.unibe.ch

S. Van Husson
Allied Signal Tech Services Corp./SLR
Goddard Corporate Park, 7515 Mission Dr.
Lanham, MD 20706/USA
001-301-805-3981
001-301-805-3974
Bitnet: bfec@cddis1 or
tcp/ip:bfec@cddis.gsfc.nasa.gov

Georg Kirchner
Institut fuer Weltraumforschung
Abt. Satellitengeodaesie
Lustbuehelstr. 46
A-8042 Graz
Oesterreich
0043-316-472231
0043-316-462678
kirchner@flubiw01.tu-graz.ac.at

Rolf Koenig
GeoForschungsZentrum Potsdam
GFZ/DPAF c/o DLR
Postfach 11 16
82230 Wessling
Muenchner Str. 20
82234 Wessling
Deutschland
0049-8153-28-1353
0049-8153-28-1207
koenigr@dfd.dlr.de

Kasimir Lapushka
University of Latvia
Astronomical Observatory
Boulevard Rainis 19
LV-1586 Riga
Lettland
00371-2-611984
00371-78-20180
lapushka@astr2.lu.lv od.
slrs1884@astr2.lu.lv

Huangjia Li
GeoForschungsZentrum Potsdam, (GFZ)
GFZ/DPAF c/o DLR
Postfach 11 16
82230 Wessling/Oberpfaffenhofen
Muenchner Str. 20
82234 Wessling
Deutschland
0049-8153-28-1351
0049-8153-28-1207
pprmail@dfd.dlr.de

Franz-Heinrich Massmann
GeoForschungsZentrum Potsdam (GFZ)
GFZ/DPAF c/o DLR Oberpfaffenhofen
Postfach 11 16
82230 Wessling
Muenchner Str. 20
82234 Wessling
Deutschland
0049-8153-28-1206
0049-8153-28-1207
fhm@dfd.dlr.de

Alan Murdoch
NASA SLR
7515 Mission Drive
Lanham, MD 20706
USA
001-301-805-3993
ltnam@cdslr1.atsc.allied.com

Leonardo Mureddu
Stazione Astronomico Geodetica di Cagliari
Via Ospedale 72
I-09100 Cagliari
Italia
0039-70-725246
0039-70-725425
mureddu@astca1.ca.astro.it

Reinhard Neubert
GeoForschungsZentrum Potsdam, Ber.15
Postfach 60 07 51
14407 Potsdam
Haus 17, Telegrafenberg A17
14473 Potsdam/Deutschland
0049-331-288-1153/1156
0049-331-288-1127
neub@gfz.potsdam.de

Ron Noomen
Delft University of Technology
Faculty of Aerospace Engineering
Kluyverweg 1
NL-2629 HS Delft/Niederlande
0031-15-78 5377
0031-15-78 3444
ron.noomen@lr.tudelft.nl

Antonin Novotny
Czech. Technical University,
Faculty of Nuclear Science & Physical Engineering
Dept. of Phys. Electronics
Brehova 7
115 19 Prague 1
The Czech Republic
0042-2-857 62244
0042-2-857 62252
novotny@troja.fjfi.cvut.cz
tjean@earn.cvut.cz

Matti V. Paunonen
Metsaehovi Observatory
Finnish Geodetic Institute
Ilmalankatu 1A
SF00240 Helsinki
Finnland
00358-0-264 994
00358-0-264 995
geodeet@csc.fi

Michael R. Pearlman
Smithsonian Astrophysical Observatory
60 Garden Street
Cambridge, MA 02138
U.S.A.
001-617-495-7481
001-617-495-7105
mpearlman@cfa.harvard.edu

Amey R. Peltzer
Naval Research Laboratory
Code 8123
4555 Overlook Avenue SW
Washington, DC 20375
USA
001-202-767-3982
001-202-767-6611
peltzer@nrlfs1.nrl.navy.mil
peltzer@nrlvax.nrl.navy.mil

Francois Pierron
Grasse Laser Station
Observatoire du Calern Caussol
SLR Station Grasse
F-06460 Saint Vallier de Thiey
France
0033-93-405420
0033-93-092614
pierron@slr.obs-azur.fr od.
pierron@rossini.obs-azur.fr

Jorge del Pino
Estacion de Rastreo de Satelites Santiago de Cuba
Academia de Ciencias des Cuba / A.C.C.
km 5 1/2 Carretera de Siboney
Ctro.Nacion.de Investig.Sismologicas
CENAIS, calle 17 e/ 4 y 6, no.61
Santiago 90400
Cuba
0053-226-41623
0053-226-41579
cenais@ceniai.cu

Ivan Prochazka
Czech. Technical University,
Faculty of Nuclear Science & Physical Engineering
Dept. of Phys. Electronics
Brehova 7
115 19 Prague 1
The Czech Republic
0042-2-857 62246
0042-2-857 62252
prochazk@troja.fjfi.cvut.cz

Stephan Riepl
Technische Universitaet Muenchen
Fundamentalstation Wettzell
93444 Koetzting/Bayer. Wald
Deutschland
0049-9941-603-201
0049-9941-603 222
riepl@wettzell.ifag.de

Stanislaw Schillak
Polish Academy of Sciences,
Space Research Center,
AOS Astronomical Latitute Observatory
Borowiec, ul. Drapalka 4
62-035 Kornik
Poland
0048-61-170187
0048-61-170219
aoslas@pozn1v.tup.edu.pl

Wolfgang Schlueter
IfAG Fundamentalstation Wettzell
Institut fuer Angewandte Geodaesie
93444 Koetzting
Deutschland
0049-9941-603 107
0049-9941-603 222
schlueter@wettzell.ifag.de

Ulrich Schreiber
IfAG Fundamentalstation Wettzell
Technische Universitaet Muenchen
93444 Koetzting
Deutschland
0049-9941-603 113
0049-9941-603 222
schreiber@wettzell.ifag.de

Wolfgang Seemueller
Deutsches Geodaetisches
Forschungsinstitut, Abt.I
Marstallplatz 8
D-80539 Muenchen
Deutschland
0049-89-23031-109
0049-89-23031-240
edc@dgfi.badw-muenchen.de

Andrew Sinclair
Royal Greenwich Observatory
Madingley Road
Cambridge CB3 0EZ
United Kingdom
0044-1223-374-741
0044-1223-374-700
ats@ast.cam.ac.uk

Peter Sperber
Fundamentalstation Wettzell
Institut fuer Angewandte Geodaesie
93444 Koetzting/Bayer. Wald
Deutschland
0089-9941-603-207
0089-9941-603 222
sperber@wettzell.ifag.de

Robert H. Towsley
Naval Research Laboratory
455 Overlook Avenue SW
Washington DC 20375
USA
001-202-767-1747
001-202-767-6611
towsley@nrlfs1.nrl.navy.mil

Erik Vermaat
Delft University of Technology
Kootwijk Observatory for Satellite Geodesy
Fac. of Geodetic Engineering
P.O.Box 5030
NL-2600 GA Delft
Niederlande
0031-15-78 1679
0031-15-78 3711
evermaat@geo.tudelft.nl

Peter Wilson
GeoForschungsZentrum
Postfach 60 07 51
14407 Potsdam
Telegrafenberg A 17
14473 Potsdam
Deutschland
0049-331-288-1172
0049-331-288-1111
wilson@gfz-potsdam.de

Roger Wood
Royal Greenwich Observatory
Herstmonceux Castle
Hailsham
E. Sussex, BN 27 1RP
United Kingdom
0044-1323-833888
0044-1323-833929

Youris Zhagar
University of Latvia
Astronomical Observatory
SLR Group Riga-2
19, Boulevard Rainis
LV-1586 Riga
Latvia (Lettland)
00371 -2 -223149
-614113
00371-78 -20180
yzh@mii.lu.lv or yzh@cclu.lv